ISSN 1881-7831 Online ISSN 1881-784X

DD&T

Drug Discoveries & Therapeutics

Volume 5 • Number 5 • 2011

IRCA BSSA

IACMHR

www.ddtjournal.com

DD&T
Drug Discoveries & Therapeutics

ISSN: 1881-7831
Online ISSN: 1881-784X
CODEN: DDTRBX
Issues/Year: 6
Language: English
Publisher: IACMHR Co., Ltd.

Drug Discoveries & Therapeutics is one of a series of peer-reviewed journals of the International Research and Cooperation Association for Bio & Socio-Sciences Advancement (IRCA-BSSA) Group and is published bimonthly by the International Advancement Center for Medicine & Health Research Co., Ltd. (IACMHR Co., Ltd.) and supported by the IRCA-BSSA and Shandong University China-Japan Cooperation Center for Drug Discovery & Screening (SDU-DDSC).

Drug Discoveries & Therapeutics publishes contributions in all fields of pharmaceutical and therapeutic research such as medicinal chemistry, pharmacology, pharmaceutical analysis, pharmaceutics, pharmaceutical administration, and experimental and clinical studies of effects, mechanisms, or uses of various treatments. Studies in drug-related fields such as biology, biochemistry, physiology, microbiology, and immunology are also within the scope of this journal.

Drug Discoveries & Therapeutics publishes Original Articles, Brief Reports, Reviews, Policy Forum articles, Case Reports, News, and Letters on all aspects of the field of pharmaceutical research. All contributions should seek to promote international collaboration in pharmaceutical science.

Editorial Board

Editorial Office

Pearl City Koishikawa 603,
2-4-5 Kasuga, Bunkyo-ku,
Tokyo 112-0003, Japan
Tel: 03-5840-9697
Fax: 03-5840-9698
E-mail: office@ddtjournal.com

Drug Discoveries & Therapeutics

Editorial and Head Office

Pearl City Koishikawa 603, 2-4-5 Kasuga, Bunkyo-ku,
Tokyo 112-0003, Japan

Tel: +81-3-5840-9697, Fax: +81-3-5840-9698
E-mail: office@ddtjournal.com
URL: www.ddtjournal.com

CONTENTS

Volume 5, Number 5, 2011

Reviews

Original Articles

Review

DOI: 10.5582/ddt.2011.v5.5.202

Targeting apoptosis pathways in cancer with magnolol and honokiol, bioactive constituents of the bark of *Magnolia officinalis*

Huanli Xu[1,2], Wei Tang[2], Guanhua Du[1,*], Norihiro Kokudo[2]

[1] *National Center for Pharmaceutical Screening, Institute of Materia Medica, Chinese Academy of Medical Science and Peking Union Medical College, Beijing, China;*
[2] *Hepato-Biliary-Pancreatic Surgery Division, Department of Surgery, Graduate School of Medicine, the University of Tokyo, Tokyo, Japan.*

ABSTRACT: Magnolol and honokiol, main active compounds from the bark of *Magnolia officinalis*, have been found to have various pharmacological actions, including anti-oxidative, anti-inflammatory, anti-tumor, and anti-microbial properties, without appreciable toxicity. Recently, the anti-tumor activity of magnolol and honokiol has been extensively investigated. Magnolol and honokiol were found to possess anti-tumor activity by targeting the apoptosis pathways, which have been considered as targets for cancer therapies. This review will focus on the mechanisms by which magnolol and honokiol act on apoptosis pathways in cancer that have been characterized thus far, including the death receptor-mediated pathway, mitochondria-mediated pathway, caspase-mediated common pathway, and regulation of apoptosis-related proteins. These breakthrough findings may have important implications for targeted cancer therapy and modern applications of traditional Chinese medicine.

Keywords: Anti-tumor activity, apoptosis pathways, honokiol, magnolol, *Magnolia officinalis*

1. Introduction

Apoptosis is a normal physiological process that plays an important role in many normal functions ranging from embryonic development to adult tissue homeostasis (*1*). Defects in apoptosis are common phenomena in many types of cancer and are also the critical step in tumorigenesis and resistance to therapy (*2*). Thus, apoptotic pathways have been considered as targets for cancer therapies (*3*).

Traditional Chinese medicine (TCM) has held and still holds an important position in primary health care in China and has recently been recognized by Western countries as a fertile source of novel lead molecules as part of modern drug discovery. Although TCM has been used for thousands of years in China, its mechanisms of healing at the molecular level are still largely unknown. To better understand the therapeutic action of TCM, considerable efforts have been made to identify the principal constituents of TCM and to unravel the molecular mechanisms behind the efficacy observed (*4*). Over the last two decades, more and more bioactive compounds have been identified from TCM herbs. Magnolol and honokiol, main active compounds from the bark of *Magnolia officinalis* (Cortex Magnoliae Officinalis), have been found to possess anti-tumor activity by inducing apoptosis in cancer (*5*). This review will focus on the mechanisms by which magnolol and honokiol act on apoptosis pathways in cancer that have been characterized thus far. Due to space limitations, only key studies are cited.

2. Magnolol and honokiol

The Chinese herb *Magnolia officinalis* is widely used as a folk remedy for gastrointestinal disorders, cough, anxiety, and allergic diseases as an oriental medicine in South Korea, China, and Japan (*6*). Magnolia bark is rich in two biphenol compounds, magnolol (5,5'-diallyi-2,2'-dihydroxybiphenyl, $C_{18}H_{18}O_2$) and honokiol (3,5'-diallyl-4,2'-dihydroxybiphenyl, $C_{18}H_{18}O_2$), that have been extensively investigated (*7,8*). The structures of magnolol and honokiol are shown in Figure 1. The magnolol content of magnolia bark is generally in the range of 2-10 percent, while honokiol tends to occur naturally at 1-5 percent in dried magnolia bark (*9*). The potent activity of honokiol and magnolol appears to be due to the presence of hydroxyl and allylic groups on a biphenolic moiety (*10*).

**Address correspondence to:*
Dr. Guanhua Du, National Center for Pharmaceutical Screening, Institute of Materia Medica, Chinese Academy of Medical Science and Peking Union Medical College, 1 XianNongTan Street, Beijing 100050, China.
e-mail: dugh@imm.ac.cn

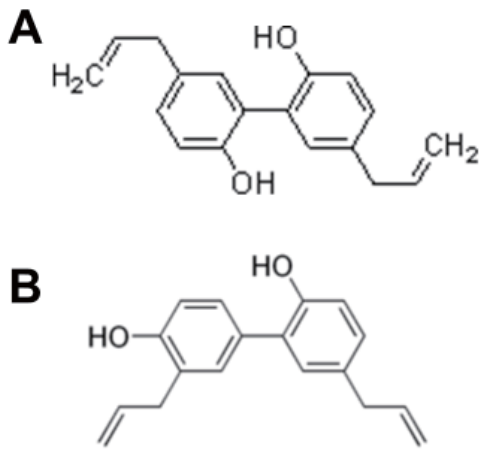

Figure 1. The chemical structures of (A) magnolol and (B) honokiol.

Magnolol, a hydroxylated biphenyl compound isolated from the stem bark of *Magnolia officinalis*, is commonly used to treat acute pain, cough, anxiety, and gastrointestinal disorders in East Asia (*11*). Various pharmacological actions have been reported for magnolol, including anti-inflammatory activity, antimicrobial activity (*12*), antiperoxidative activity (*13*), anti-coagulatory activity, anti-oxidant activity (*14*), neuroprotective activity (*15*), antitumor action (*16-18*), alleviation of inflammatory pain (*19*), and protection of cortical neuronal cells from chemical hypoxia (*20*).

Honokiol, a magnolol isomer, differs in the relative arrangement of one of its hydroxyl groups with respect to allyl groups in the phenolic ring (*21*) and is the most important bioactive constituent within magnolia bark studied thus far. Honokiol has also been found to have a variety of pharmacological action, such as anti-inflammatory action (*22*), antithrombotic activity (*23*), anti-arrhythmic activity (*24*), neuroprotective activity (*15*), antioxidative action (*25*), and anxiolytic action (*26*). Numerous animal studies have also demonstrated that honokiol acts as an anti-stress agent and a potent suppressor of oxidative damage and cancer (*27*).

Recently, magnolol and honokiol have been reported to have antitumor action by inhibiting proliferation, inducing apoptosis and differentiation, countering metastasis, suppressing angiogenesis, and reversing multidrug resistance (*10,28,29*). Numerous signaling pathways have been implicated in the regulation of apoptosis by magnolol and honokiol (*30*).

3. Targeting apoptosis pathways in cancer with magnolol and honokiol

Apoptosis occurs through two main pathways (*31,32*). The first, referred to as the extrinsic or death receptor pathway, involves ligation of death receptors (*e.g.* Fas (CD95), tumor necrosis factor receptors (TNFR), and TNF-related apoptosis-inducing ligand (TRAIL) receptors) with their ligands resulting in a sequential activation of caspase-8 and -3. The second pathway is the intrinsic or mitochondrial pathway in which intrinsic death stimuli (*e.g.* reactive oxygen species (ROS), DNA-damaging reagents, and Ca^{2+} mobilizing stimuli), directly or indirectly activate the mitochondrial pathway, resulting in the release of cytochrome *c* and the formation of the apoptosome complex consisting of cytochrome *c*, Apaf-1, and caspase-9 (Figure 2). Caspase-9 is activated at the apoptosome and in turn activates caspase-3. Between the death receptor and the mitochondrial signaling pathways, the pro-apoptotic protein Bid serves as a cross-talker upon cleavage by activated caspase-8 by inducing the translocation of the pro-apoptotic proteins Bax and/or Bak to the mitochondrial membrane (*33*). Both pathways converge to a final common pathway involved in the activation of a cascade of proteases called caspases that cleave regulatory and structural molecules, culminating in the deaths of cells (Figure 2). Although understanding of the detailed signaling pathways that trigger apoptosis is incomplete, this process is controlled by a number of complex proteins that are activated by various triggers and arranged in sequential signaling modules. In the receptor-mediated pathway, FLICE-inhibitory protein (c-FLIP) and XIAP negatively regulate the activity of caspase-8 and caspase-3, respectively (*31,32*). In the mitochondria pathway, apoptosis is largely controlled by the pro-apoptotic proteins, *e.g.* Bax, Bak, Bid, and Smac, and the anti-apoptotic proteins, *e.g.* Bcl-2, Bcl-xL, Mcl-1, and XIAP (*3*).

Many studies have shown that magnolol and honokiol induce the apoptosis of various tumor cells. Magnolol induces the apoptosis of many human cancer cell lines, including lung squamous cancer CH-27 cells, HL-60 cells, colon cancer COLO 205 cells, and liver cancer HepG2 cells (*34-38*), but does not induce the apoptosis of bovine aorta endothelial BAE cells (*38*) or polymorphonuclear and mononuclear leukocytes (*35*). Honokiol induces the apoptosis of human lymphoid leukemia Molt 4B cells, CH27 cells, B-CLL cells, and RKO cells in a time- and dose-dependent manner (*5,34,39,40*). In addition, honokiol has a more obvious apoptosis-inducing effect on B-CLL cells than on normal mononuclear leukocytes (*40*). *In vivo*, honokiol was highly effective against SVR angiosarcoma (*41*) and breast cancer in nude mice (*42*) and in a human A549 lung cancer xenograft model (*43*) with the increased induction of apoptosis.

This review will focus on the mechanisms by which magnolol and honokiol act on apoptosis pathways in cancer that have been characterized thus far, including the death receptor-mediated pathway, mitochondria-mediated pathway, caspase-mediated common pathway, and regulation of apoptosis-related proteins.

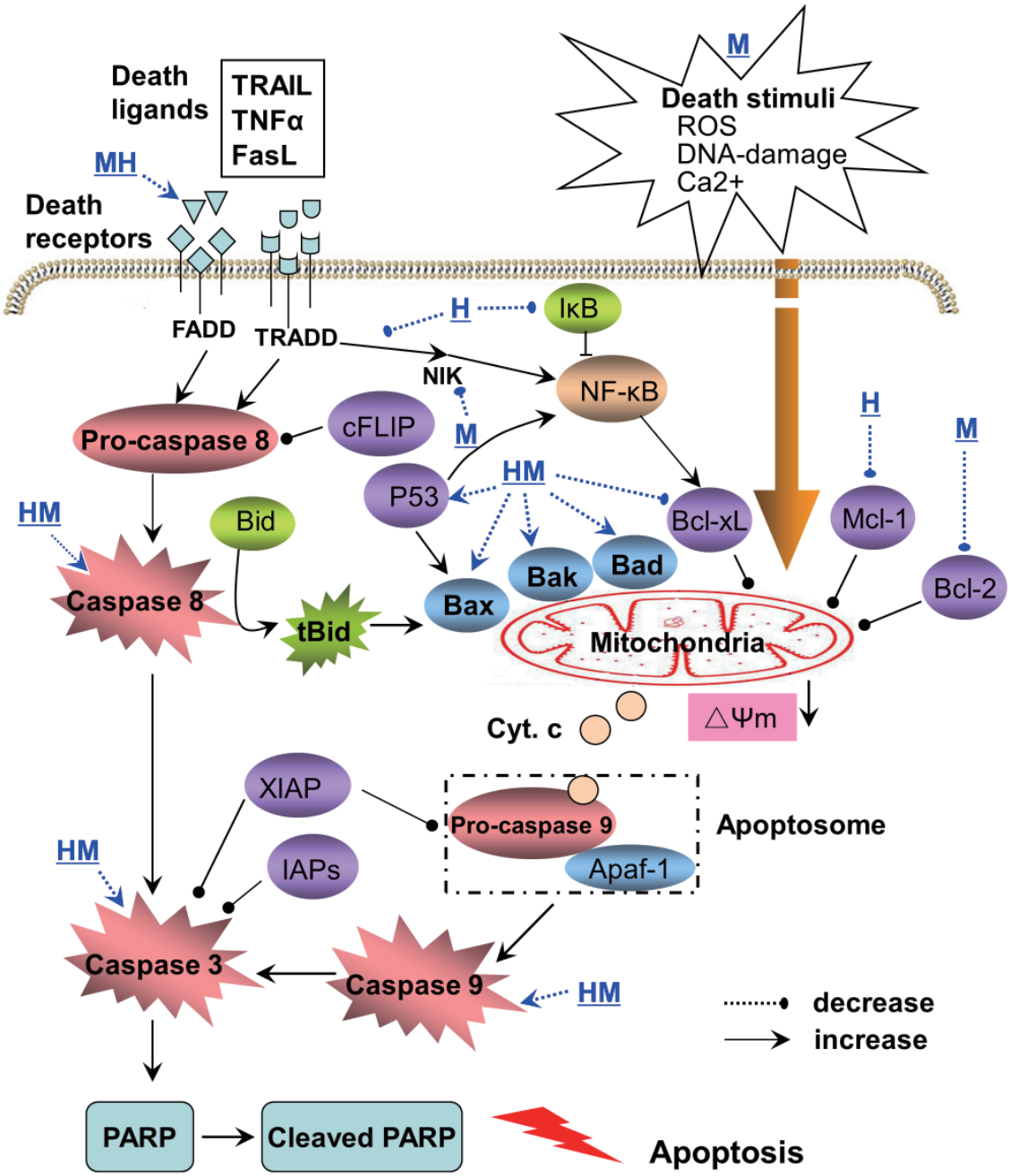

Figure 2. Effects of magnolol (M) and honokiol (H) on extrinsic (also called receptor-mediated) and intrinsic (also called mitochondria-mediated) apoptosis pathways in cancer. The extrinsic pathway involves ligation of death receptors with their ligands, resulting in a sequential activation of caspase-8 and -3. Intrinsic death stimuli, *e.g.* ROS, DNA-damaging reagents, or Ca^{2+} mobilization directly or indirectly activates the mitochondrial pathway by inducing release of cytochrome *c* and formation of the apoptosome, which consists of Apaf-1 and caspase-9. Caspase-9 is activated at the apoptosome and in turn activates pro-caspase-3.

3.1. *Targeting cancer cells by death receptor-mediated apoptosis*

Fas, TRAIL, and TNF receptors are highly specific physiological mediators of the extrinsic signaling pathway of apoptosis. Cross-linking of death receptors either with their natural ligands (*e.g.* FasL, TRAIL, and TNF-α) or with agonistic antibodies (such as anti-APO-1) induces a sequential activation of caspase-8 and -3, which cleaves target proteins and leads to apoptosis (*44*). Activation of the death receptor-mediated apoptotic pathway is primarily inhibited by cellular c-FLIP, which inhibits caspase-8 activation by preventing recruitment of caspase-8 to the death-inducing signaling complex. In some cells, the activation of caspase 8 may be the only requirement for death to ensue, while in other cell types caspase 8 interacts with the intrinsic apoptotic pathway by cleaving Bid (a proapoptotic member of the Bcl-2 family), leading to the subsequent release of cytochrome *c* (*45*).

Studies have shown that activation of the Fas-mediated pathway did not always result in magnolol-induced apoptosis. In response to magnolol administration, Fas was activated and cytochrome *c* was translocated from mitochondria to the cytoplasm through elevation of the cytosolic free Ca^{2+} concentration and downregulation of Bcl-2. Caspase-8 was activated by Fas activation, whereas caspase-9 was activated by cytochrome *c* release (*46*). Pretreating cells with ZB4 (which disrupts the Fas response mechanism) also decreased subsequent magnolol-induced caspase-8 activation and reduced the occurrence of apoptosis (*46*). Whether magnolol activates Fas directly or it promotes the action of a Fas ligand that in turn activates Fas remains to be determined.

Honokiol down-regulated c-FLIP in cancer cells, resulting in sensitization of cancer cells to both TRAIL-mediated and Fas ligand-mediated apoptosis (*47*). Honokiol alone moderately inhibited the growth of human lung cancer cells; when combined with TRAIL, however, honokiol had a greater impact on decreasing cell survival and inducing apoptosis than did TRAIL alone, indicating that honokiol cooperates with TRAIL to enhance apoptosis. This was also true for Fas-induced apoptosis when it was combined with a Fas ligand or an agonistic anti-Fas antibody. Of several apoptosis-associated proteins tested, c-FLIP was the only one that was rapidly down-regulated by honokiol in all of the cell lines tested (*47*). These results indicate that c-FLIP down-regulation is a key step in honokiol's modulation of death receptor-induced apoptosis.

3.2. *Targeting cancer cells by mitochondria-mediated apoptosis*

The effects of magnolol on the intrinsic pathway of apoptosis have been examined in many cell lines, including human leukemia U937 cells (*48*), human hepatoma Hep G2 and colon cancer COLO 205 cells (*46*), and rat vascular smooth muscle cells (VSMCs) (*49*). Magnolol increased caspase-3 and caspase-9 activity significantly and reduced the mitochondrial potential ($\Delta\Psi m$) in these cells. Treatment with magnolol was found to partly inhibit growth by inducing apoptosis in cultured human leukemia U937 cells and apoptosis was found to be induced *via* the sequential ordering of molecular events. Thus, magnolol-induced apoptosis is mediated *via* the intrinsic pathway with release of AIF from mitochondria in U937 cells (*48*). Lin SY, *et al*. showed that treatment with magnolol induced apoptosis by increasing translocation of cytochrome *c* from mitochondria to cytosol and activation of caspase-3, -8, and -9 in cultured Hep G2 and COLO 205 cell lines (*46*). In addition, Huang SH, *et al*. showed that magnolol initiated apoptosis *via* cytochrome *c*/caspase-3/PARP/AIF and PTEN/Akt/caspase-9/PARP pathways and necrosis *via* PARP activation (*50*).

Similar results were found in honokiol-treated cells. Honokiol treatment caused the release of mitochondrial cytochrome *c* to cytosol and sequential activation of caspases in human squamous lung cancer CH27 cells (*51*). Honokiol also induced release of mitochondrial proapoptotic protein AIF to the cytosol in human multiple myeloma (MM) cells (*52*). The current review has mainly focused on induction of mitochondria-mediated apoptosis *via* reactive oxygen species (ROS)-mediated and Ca^{2+}-mediated mechanisms of magnolol and honokiol.

3.2.1. *ROS-mediated mechanisms*

ROS, including free radicals such as superoxide ($\bullet O_2^-$), hydroxyl radicals (•OH), and the non-radical H_2O_2, are generated through multiple sources in the cells (*53*). Tumors, and particularly those in advanced stages, produce elevated levels of ROS and have an altered redox status. ROS and mitochondria play an important role in apoptosis induction under both physiological and pathological conditions (*54*). Interestingly, mitochondria are both sources and targets of ROS. Cytochrome *c* release from mitochondria, which triggers caspase activation, appears to be largely mediated by direct or indirect ROS action (*55*). High levels of ROS may cause the oxidative damage of various cellular components and finally result in cell apoptosis.

Magnolol has been shown to attenuate oxidized low-density lipoprotein (oxLDL)-induced ROS generation, subsequently reducing nuclear factor-kappaB (NF-κB) activation (*56*). Magnolol also inhibited UV-induced mutations by scavenging •OH generated by UV irradiation (*57*). The attenuation of ROS by magnolol has been proposed as a reason for its inhibitory effect on neutrophil adherence to the extracellular matrix during injury (*58*).

Honokiol was also found to be a potent scavenger of hydroxyl radicals, which is likely due to its allyl groups (*22,59*). The ortho allyl group may potentially form a six-member ring after absorption of a hydroxyl group. This may account for its superior antioxidant activity when compared to magnolol, which has two allyl groups with hydroxyl groups in the *para* position and thus cannot form a six-member ring. Honokiol-induced apoptosis has been closely associated with ROS production. Inhibition of reactive oxygen-driven tumors by honokiol is due to its involvement in the NADPH oxidase (NOX) pathway (*22*). This inhibition was first demonstrated in neutrophils (*22*) and later in hepatocytes (*60*) and human umbilical vein endothelial cells (HUVECs) (*22*). A possible chemical mechanism for this involves a peroxide intermediate followed by the phenolic hydroxyl group attacking the peroxide carbon chain, yielding a pentose or hexose ring and water.

3.2.2. *Ca^{2+}-mediated mechanisms*

Ca^{2+} signals are known to play an important role in the regulation of cell death and survival (*61*). One known Ca^{2+}-regulated Bcl-2-associated pro-apoptotic protein is Bad. In non-apoptotic cells, Bad is phosphorylated and sequestered by the cytosolic protein 14-3-3, avoiding its hetero-dimerization with Bcl-2 and Bcl-xL at the mitochondrial membrane. In the presence of an apoptotic stimulus (*e.g.* Ca^{2+}), Bad is dephosphorylated by Ca^{2+}/calmodulin-dependent phosphatase calcineurin, leading to dissociation from its inhibitor 14-3-3 and promoting apoptosis (*62*). Since mitochondria are the major organelles that take up Ca^{2+}, Ca^{2+} over-loading of the mitochondria may also directly lead to release of cytochrome *c* as part of a stress response.

Lin SY, *et al*. showed that treatment with 100 μM of magnolol increased cytosolic free Ca^{2+}, resulting in induced apoptosis in cultured human Hep G2 and COLO 205 cell lines but not in human untransformed gingival fibroblasts and human umbilical vein endothelial cells (*46*). In rat neutrophils, magnolol increased $[Ca^{2+}]_i$ by stimulating Ca^{2+} release from internal stores and Ca^{2+} influx across the plasma membrane in a concentration-dependent manner *via* the inositol trisphosphate signalling pathway (*63*). Magnolol relaxed vascular smooth muscle by releasing endothelium-derived relaxing factor (EDRF) and by inhibiting calcium influx through voltage-gated calcium channels (*64*). Magnolol also increased the probability of these channels opening in a concentration-dependent manner, independent of internal Ca^{2+}, in tracheal smooth muscle cells (*65*).

3.3. *Targeting cancer cells by caspase-mediated apoptosis*

The caspases are a family of proteins that are one of the main executors of the apoptotic process. As of November 2009, twelve caspases have been identified in humans (*66*). There are two types of apoptotic caspases: initiator (apical) caspases (caspase-2, -8, -9, and -10) and effector (executioner) caspases (caspase-3, -6, and -7). Initiator caspases cleave inactive pro-forms of effector caspases, thereby activating them. Effector caspases in turn cleave other protein substrates within the cell, triggering the apoptotic process.

Activation of caspase-3, -8, -9, and -2, and the proteolytic cleavage of poly(adenosine diphosphate-ribose) polymerase (PARP) were noted during apoptosis induced by magnolol (*46*). Pretreatment with Z-Val-Ala-Asp-fluoromethyl ketone (Z-VAD-FMK), a pan-caspase inhibitor, markedly inhibited magnolol-induced cell death but did not prevent cytosolic cytochrome *c* accumulation. Apoptosis may be partially attenuated by caspase-3 and -2 inhibitors. These results indicate that magnolol-induced apoptotic signaling was carried out through mitochondrial alterations to caspase-9 and that the downstream effector caspases were then activated sequentially (*35*).

Honokiol-induced apoptosis is characterized by the activation of caspase-3, -8, and -9 and cleavage of PARP (*48*). Honokiol induced caspase-dependent cell death in all of the B-CLL cells examined and was more toxic toward B-CLL cells than to normal mononuclear cells, suggesting that malignant cells were more susceptible. Although activation of caspase-3, -8, and -9 is triggered by honokiol, the pan-caspase inhibitor Z-VAD-FMK does not abrogate honokiol-induced apoptosis (*52*). Importantly, honokiol treatment induces the release of an executioner of caspase-independent apoptosis, AIF, from mitochondria. Honokiol also induced apoptosis in the SU-DHL4 cell line, which has low levels of caspase-3 and -8 (*52*). These results suggest that honokiol induced apoptosis *via* both caspase-dependent and -independent pathways.

3.4. *Targeting cancer cells by regulating apoptosis-related proteins*

Treatment with magnolol significantly increased the expression of Bad and Bcl-x(S) proteins, whereas it decreased the expression of Bcl-x(L) (*67*). Magnolol treatment also caused a decrease in Ser(136) phosphorylation of Bad, which is a downstream target of Akt, and translocation of Bax to the mitochondrial membrane. Similar results were observed in the human colon cancer HCT116Bax(+/-) cell line but not in the HCT116Bax(-/-) cell line. In addition, apoptotic cell death due to magnolol was found to be associated with significant inhibition of pEGFR, pPI3K, and pAkt (*67*).

Honokiol-induced apoptosis correlated with induction of Bax, Bak, and Bad and a decrease in Bcl-xL and Mcl-1 protein levels. Transient transfection of PC-3 cells with Bak- and Bax-targeted siRNAs and Bcl-xL plasmid conferred partial yet significant protection against honokiol-induced apoptosis (*68*). Another study showed that honokiol caused cleavage of Mcl-1 and downregulation of XIAP while Bad was markedly upregulated; Bid, p-Bad, Bak, Bax, Bcl-2, and Bcl-xL were unchanged (*52*). Honokiol also induced release of mitochondrial proapoptotic protein AIF to the cytosol and prevented phosphorylation of Akt, Stat-3, and Erk2, again implying an upstream target of action (*52,69*).

The effects of magnolol and honokiol on two important apoptosis-related proteins, p53 and NF-κB, have been summarized below.

3.4.1. *p53*

Loss of function of the *p53* tumor suppressor gene is a frequent and important event in the genesis or progression of many human malignancies. In many tumor cells, wild-type p53 is thought to participate

in apoptosis in response to DNA damage (*70*). P53 may transactivate apoptotic regulators, such as Bcl-2 (*49,71-74*) and Bax (*75-77*). Recent studies have shown that p53 plays a role in apoptosis by the mitochondria-mediated apoptotic pathway (*74,78*). Activation of p53 upregulates Bax, increases the ratio of Bax:Bcl-2, and releases cytochrome *c* and other polypeptides from the intermembrane space of mitochondria into the cytoplasm (*76*). p53-dependent apoptosis was activated by the Bax/mitochondrial/caspase-9 pathway.

Honokiol has been found to prevent the growth of MDA-MB-231 breast cancer cells in murine xenografts (*79*). An interesting finding is that MDA-MB-231 cells display mutant p53 and mutant K-ras, which is preferentially observed in the triple-negative breast cancer phenotype (*79,80*). In the same study, honokiol had less activity on the MCF7 breast cancer cell line, which exhibited wild-type p53 and loss of p16ink4a. Given that SVR cells have defects in p53 signaling because of expression of SV40 large T and that MDA-MB-231 cells also express mutant p53, tumors that have defects in p53 signaling may be targets of honokiol. Similarly, honokiol caused apoptosis in other solid-tumor cell lines that feature mutant p53 and ras activation, including lung and bladder cell lines (*81*). Thus, honokiol appears to have distinct activity against tumors with mutant p53, through its inhibition of ras-phospholipase D activation, and tumors with wild-type p53, through its induction of cyclophilin D. However, Wang T, *et al*. showed that honokiol induced RKO cell apoptosis by activating the caspase cascade *via* a p53-indepenent pathway (*82*). Hahm ER, *et al*. also showed that exposure of human prostate cancer cells (PC-3, LNCaP, and C4-2) to honokiol resulted in apoptotic DNA fragmentation in a concentration- and time-dependent manner, irrespective of their androgen responsiveness or p53 status (*68*).

3.4.2. *NF-κB*

The NF-κB pathway is one of the most important cellular signal transduction pathways involved in immunity, inflammation, proliferation, and defense against apoptosis (*83*). NF-κB is generally considered to be a survival factor that activates expression of various anti-apoptotic genes, *e.g*. Bcl-2, Bcl-xL, Mcl-1 and c-FLIP, that block apoptosis (*83,84*). The classic form of NF-κB is the p65/p50 heterodimer that contains the transcriptional activation domain and is sequestered in the cytoplasm as an inactive complex by IκB. Acute stimuli such as TNF-α, LPS or PMA lead to the activation of IκB kinases (IKK), which in turn phosphorylate Ser32 and Ser36 within the *N*-terminal response domain of IκB. Phosphorylated IκB undergoes ubiquitination-dependent proteolysis and the release of IκB unmasks the nuclear localization signal and results in the translocation of NF-κB to the nucleus, followed by the activation of specific target genes.

Both magnolol and honokiol have been shown to inhibit the NF-κB signaling pathway. In a previous study, magnolol was shown to reduce the nuclear NF-κB content in TNF-α-stimulated endothelial cells (*85*). However, their mechanisms of action are poorly understood. Chen YH, *et al*. demonstrated that magnolol suppressed IKK activity, stabilized cytoplasmic IκBα, and subsequently reduced the nuclear translocation and phosphorylation of the p65 subunit of NF-κB (*86*). Magnolol also inhibited NF-κB-dependent reporter gene expression induced by TNF-α and it inhibited over-expression of NIK, IKK, and the p65 subunit while it enhanced TNF-α-mediated apoptosis. In human U937 promonocytes cells, magnolol inhibited the TNF-α-stimulated phosphorylation and degradation of the cytosolic NF-κB inhibitor IκBα and did so in a dose-dependent manner (*87*). In addition, magnolol differentially down-regulated the expression of NF-κB-regulated inflammatory gene products, *e.g.* MMP-9, IL-8, MCP-1, MIP-1α, and TNF-α. The involvement of IKK was further verified in a HeLa cell NF-κB-dependent luciferase reporter system (*87*).

Honokiol affected NF-κB signaling, but not through a direct effect on NF-κB DNA binding (*88*). Honokiol inhibited TNF-induced NF-κB activation and IkBα phosphorylation and degradation through its inhibition of the activation of IκBα kinase and Akt. Honokiol also inhibited NF-κB-dependent reporter gene expression induced by TNFR1, TRADD, TRAF, NIK, and IKKβ (*88*). Consistent with honokiol's effect on NF-κB, honokiol decreased levels of NF-κB target genes, including IAP1, IAP2, Bcl-xL, Bcl-2, cFLIP, TRAF1, and survivin (*88*). NF-κB and NF-κB-regulated gene expression inhibited by honokiol can thus enhance apoptosis. Honokiol also down-regulated NF-κB activation in an *in vivo* mouse dorsal skin model. Another study showed that honokiol blocked the production of TNF-α, MCP-1, interleukin-8, and ICAM-1 and was found to act at the level of IKK or upstream of IKK, indicating a possible mechanism of its anti-tumor action (*89*).

4. Summary

In recent years, various biologically active constituents have been isolated from TCM and have been found to have varied activity in experimental studies. Honokiol and magnolol have been found to have anti-oxidative, anti-inflammatory, anti-tumor, and anti-microbial properties in preclinical models. Their safety during long-term administration, combined with their cost and future therapeutic potential, makes them ideal therapeutic agents (*90*). In addition, magnolol and honokiol are small molecular weight natural products that are orally bioavailable and able to cross the blood-brain barrier. Clinical trials are needed to fully realize

the potential of honokiol and magnolol as effective antitumor drugs. Honokiol and magnolol analogues with improved pharmacokinetic and pharmacodynamics will also encourage further advances.

Many studies have shown that both magnolol and honokiol induce apoptosis of many types of cancer cells, though those studies describe different mechanisms of action. Moreover, investigation of how they specifically induce apoptosis in cancers and spare normal cells will provide new clues to help identify more efficient drugs and to develop apoptosis-targeting therapies.

References

1. Kasibhatla S, Tseng B. Why target apoptosis in cancer treatment. Mol Cancer Ther. 2003; 2:573-580.
2. Kaufmann SH, Earnshaw WC. Induction of apoptosis by cancer chemotherapy. Exp Cell Res. 2000; 256:42-49.
3. Ghobrial IM, Witzig TE, Adjei AA. Targeting apoptosis pathways in cancer therapy. C.A. Cancer J Clin. 2005; 55:178-194.
4. Hsiao WL, Liu L. The role of traditional Chinese herbal medicines in cancer therapy – from TCM theory to mechanistic insights. Planta Med. 2010; 76:1118-1131.
5. Chen F, Wang T, Wu YF, Gu Y, Xu XL, Zheng S, Hu X. Honokiol: A potent chemotherapy candidate for human colorectal carcinoma. World J Gastroenterol. 2004; 10:3459-3463.
6. Maruyama Y, Kuribara H, Morita M, Yuzurihara M, Weintraub ST. Identification of magnolol and honokiol as anxiolytic agents in extracts of saiboku-to, an oriental herbal medicine. J Nat Prod. 1998; 61:135-138.
7. Shen CC, Ni CL, Shen YC, Huang YL, Kuo CH, Wu TS, Chen CC. Phenolic constituents from the stem bark of Magnolia officinalis. J Nat Prod. 2009; 72:168-171.
8. Watanabe K, Watanabe H, GotoY, Yamaguchi M, Yamamoto N, Hagino K. Pharmacological properties of magnolol and honokiol extracted from Magnolia officinalis: Central depressant effects. Planta Med. 1983; 49:103-108.
9. Cheng DC, Liu JW. Quantitative analysis of magnolol and honokiol in the bark of Magnolia officinalis Rehd et Wils and Magnolia rostrata WW Smith. Acta Pharmaceutica Sinica. 1982; 17:360-364.
10. Amblard F, Govindarajan B, Lefkove B, Rapp KL, Detorio M, Arbiser JL, Schinazi RF. Synthesis, cytotoxicity, and antiviral activities of new neolignans related to honokiol and magnolol. Bioorg Med Chem Lett. 2007; 17:4428-4431.
11. Jeong SI, Kim YS, Lee MY, Kang JK, Lee S, Choi BK, Jung KY. Regulation of contractile activity by magnolol in the rat isolated gastrointestinal tracts. Pharmacol Res. 2009; 59:183-188.
12. Park J, Lee J, Jung E, Kim K, Park B, Jung K, Park E, Kim J, Park D. *In vitro* antibacterial and anti-inflammatory effects of honokiol and magnolol against Propionibacterium sp. Eur J Pharmacol. 2004; 496:189-195.
13. Haraguchi H, Ishikawa H, Shirataki N, Fukuda A. Antiperoxidative activity of neolignans from Magnolia obovata. J Pharm Pharmacol. 1997; 49:209-212.
14. Tsai YC, Cheng PY, Kung CW, Peng YJ, Ke TH, Wang JJ, Yen MH. Beneficial effects of magnolol in a rodent model of endotoxin shock. Eur J Pharmacol. 2010; 641:67-73.
15. Lin YR, Chen HH, Ko CH, Chan MH. Neuroprotective activity of honokiol and magnolol in cerebellar granule cell damage. Eur J Pharmacol. 2006; 537:64-69.
16. Kuo DH, Lai YS, Lo CY, Cheng AC, Wu H, Pan MH. Inhibitory effect of magnolol on TPA-induced skin inflammation and tumor promotion in mice. J Agric Food Chem. 2010; 58:5777-5783.
17. Konoshima T, Kozuka M, Tokuda H, Nishino H, Iwashima A, Haruna M, Ito K, Tanabe M. Studies on inhibitors of skin tumor promotion, IX. Neolignans from Magnolia officinalis. J Nat Prod. 1991; 54:816-822.
18. Lee SJ, Cho YH, Park K, Kim EJ, Jung KH, Park SS, Kim WJ, Moon SK. Magnolol elicits activation of the extracellular signal-regulated kinase pathway by inducing p27KIP1-mediated G2/M-phase cell cycle arrest in human urinary bladder cancer 5637 cells. Biochem Pharmacol. 2008; 75:2289-2300.
19. Lin YR, Chen HH, Ko CH, Chan MH. Effects of honokiol and magnolol on acute and inflammatory pain models in mice. Life Sci. 2007; 81:1071-1078.
20. Lee MM, Hseih MT, Kuo JS, Yeh FT, Huang HM. Magnolol protects cortical neuronal cells from chemical hypoxia in rats. Neuroreport. 1998; 9:3451-3456.
21. Li H, Wang X, Hu Y. Distinct photoacidity of honokiol from magnolol. J Fluoresc. 2011; 21:265-273.
22. Liou KT, Shen YC, Chen CF, Tsao CM, Tsai SK. The anti-inflammatory effect of honokiol on neutrophils: Mechanisms in the inhibition of reactive oxygen species production. Eur J Pharmacol. 2003; 475:19-27.
23. Teng CM, Chen CC, Ko FN, Lee LG, Huang TF, Chen YP, Hsu HY. Two antiplatelet agents from Magnolia officinalis. Thromb Res. 1988; 50:757-765.
24. Liou KT, Lin SM, Huang SS, Chih CL, Tsai SK. Honokiol ameliorates cerebral infarction from ischemia-reperfusion injury in rats. Planta Med. 2003; 69:130-134.
25. Lo YC, Teng CM, Chen CF, Chen CC, Hong CY. Magnolol and honokiol isolated from Magnolia officinalis protect rat heart mitochondria against lipid peroxidation. Biochem Pharmacol. 1994; 47:549-553.
26. Kuribara H, Kishi E, Hattori N, Yuzurihara M, Maruyama Y. Application of the elevated plus-maze test in mice for evaluation of the content of honokiol in water extracts of magnolia. Phytother Res. 1999; 13:593-596.
27. Kim BH, Cho JY. Anti-inflammatory effect of honokiol is mediated by PI3K/Akt pathway suppression. Acta Pharmacol Sin. 2008; 29:113-122.
28. Hwang ES, Park KK. Magnolol suppresses metastasis *via* inhibition of invasion, migration, and matrix metalloproteinase-2/-9 activities in PC-3 human prostate carcinoma cells. Biosci Biotechnol Biochem. 2010; 74:961-967.
29. Luo H, Zhong Q, Chen LJ, Qi XR, Fu AF, Yang HS, Yang F, Lin HG, Wei YQ, Zhao X. Liposomal honokiol, a promising agent for treatment of cisplatin-resistant human ovarian cancer. J Cancer Res Clin Oncol. 2008; 134:937-945.
30. You Q, Li M, Jiao G. Magnolol induces apoptosis *via* activation of both mitochondrial and death receptor pathways in A375-S2 cells. Arch Pharm Res. 2009; 32:1789-1794.
31. Johnstone RW, Frew AJ, Smyth MJ. The TRAIL apoptotic pathway in cancer onset, progression and

therapy. Nat Rev Cancer. 2008; 8:782-798.
32. Li-Weber M. Targeting apoptosis pathways in cancer by Chinese medicine. Cancer Lett. 2010.
33. Billen LP, Shamas-Din A, Andrews DW. Bid: A Bax-like BH3 protein. Oncogene. 2008; 27:S93-104.
34. Yang SE, Hsieh MT, Tsai TH, Hsu SL. Effector mechanism of magnolol-induced apoptosis in human lung squamous carcinoma CH27 cells. Br J Pharmacol. 2003; 138:193-201.
35. Zhong WB, Wang CY, Ho KJ, Lu FJ, Chang TC, Lee WS. Magnolol induces apoptosis in human leukemia cells *via* cytochrome *c* release and caspase activation. Anticancer Drugs. 2003; 14:211-217.
36. Lin SY, Liu JD, Chang HC, Yeh SD, Lin CH, Lee WS. Magnolol suppresses proliferation of cultured human colon and liver cancer cells by inhibiting DNA synthesis and activating apoptosis. J Cell Biochem. 2002; 84:532-544.
37. Syu WJ, Shen CC, Lu JJ, Lee GH, Sun CM. Antimicrobial and cytotoxic activities of neolignans from Magnolia officinalis. Chem Biodivers. 2004; 1:530-537.
38. Ikeda K, Nagase H. Magnolol has the ability to induce apoptosis in tumor cells. Biol Pharm Bull. 2002; 25:1546-1549.
39. Hibasami H, Achiwa Y, Katsuzaki H, Imai K, Yoshioka K, Nakanishi K, Ishii Y, Hasegawa M, Komiya T. Honokiol induces apoptosis in human lymphoid leukemia Molt 4B cells. Int J Mol Med. 1998; 2:671-673.
40. Battle TE, Arbiser J, Frank DA. The natural product honokiol induces caspase-dependent apoptosis in B-cell chronic lymphocytic leukemia (B-CLL) cells. Blood. 2005; 106:690-697.
41. Bai X, Cerimele F, Ushio-Fukai M, *et al*. Honokiol, a small molecular weight natural product, inhibits angiogenesis *in vitro* and tumor growth *in vivo*. J Biol Chem. 2003; 278:35501-35507.
42. Wolf I, O'Kelly J, Wakimoto N, Nguyen A, Amblard F, Karlan BY, Arbiser JL, Koeffler HP. Honokiol, a natural biphenyl, inhibits *in vitro* and *in vivo* growth of breast cancer through induction of apoptosis and cell cycle arrest. Int J Oncol. 2007; 30:1529-1537.
43. Jiang QQ, Fan LY, Yang GL, Guo WH, Hou WL, Chen LJ, Wei YQ. Improved therapeutic effectiveness by combining liposomal honokiol with cisplatin in lung cancer model. BMC Cancer. 2008; 8:242.
44. Krammer PH. CD95's deadly mission in the immune system. Nature. 2000; 407:789-795.
45. Wajant H. The Fas signaling pathway: more than a paradigm. Science. 2002; 296:1635-1636.
46. Lin SY, Chang YT, Liu JD, Yu CH, Ho YS, Lee YH, Lee WS. Molecular mechanisms of apoptosis induced by magnolol in colon and liver cancer cells. Mol Carcinog. 2001; 32:73-83.
47. Raja SM, Chen S, Yue P, Acker TM, Lefkove B, Arbiser JL, Khuri FR, Sun SY. The natural product honokiol preferentially inhibits cellular FLICE-inhibitory protein and augments death receptor-induced apoptosis. Mol Cancer Ther. 2008; 7:2212-2223.
48. Ikai T, Akao Y, Nakagawa Y, Ohguchi K, Sakai Y, Nozawa Y. Magnolol-induced apoptosis is mediated *via* the intrinsic pathway with release of AIF from mitochondria in U937 cells. Biol Pharm Bull. 2006; 29:2498-2501.
49. Chen JH, Wu CC, Hsiao G, Yen MH. Magnolol induces apoptosis in vascular smooth muscle. Naunyn Schmiedebergs Arch Pharmacol. 2003; 368:127-133.
50. Huang SH, Chen Y, Tung PY, Wu JC, Chen KH, Wu JM, Wang SM. Mechanisms for the magnolol-induced cell death of CGTH W-2 thyroid carcinoma cells. J Cell Biochem. 2007; 101:1011-1022.
51. Yang SE, Hsieh MT, Tsai TH, Hsu SL. Down-modulation of Bcl-XL, release of cytochrome *c* and sequential activation of caspases during honokiol-induced apoptosis in human squamous lung cancer CH27 cells. Biochem Pharmacol. 2002; 63:1641-1651.
52. Ishitsuka K, Hideshima T, Hamasaki M, *et al*. Honokiol overcomes conventional drug resistance in human multiple myeloma by induction of caspase-dependent and -independent apoptosis. Blood. 2005; 106:1794-1800.
53. Schumacker PT. Reactive oxygen species in cancer cells: Live by the sword, die by the sword. Cancer Cell. 2006; 10:175-176.
54. Turrens JF. Mitochondrial formation of reactive oxygen species. J Physiol. 2003; 552:335-344.
55. Simon HU, Haj-Yehia A, Levi-Schaffer F. Role of reactive oxygen species (ROS) in apoptosis induction. Apoptosis. 2000; 5:415-418.
56. Ou HC, Chou FP, Sheu WH, Hsu SL, Lee WJ. Protective effects of magnolol against oxidized LDL-induced apoptosis in endothelial cells. Arch Toxicol. 2007; 81:421-432.
57. Fujita S, Taira J. Biphenyl compounds are hydroxyl radical scavengers: Their effective inhibition for UV-induced mutation in Salmonella typhimurium TA102. Free Radic Biol Med. 1994; 17:273-277.
58. Shen YC, Sung YJ, Chen CF. Magnolol inhibits Mac-1 (CD11b/CD18)-dependent neutrophil adhesion: Relationship with its antioxidant effect. Eur J Pharmacol. 1998; 343:79-86.
59. Park EJ, Zhao YZ, Na M, Bae K, Kim YH, Lee BH, Sohn DH. Protective effects of honokiol and magnolol on tertiary butyl hydroperoxide- or D-galactosamine-induced toxicity in rat primary hepatocytes. Planta Med. 2003; 69:33-37.
60. Park EJ, Kim SY, Zhao YZ, Sohn DH. Honokiol reduces oxidative stress, c-jun-NH_2-terminal kinase phosphorylation and protects against glycochenodeoxycholic acid-induced apoptosis in primary cultured rat hepatocytes. Planta Med. 2006; 72:661-664.
61. Roderick HL, Cook SJ. Ca^{2+} signalling checkpoints in cancer: Remodelling Ca^{2+} for cancer cell proliferation and survival. Nat Rev Cancer. 2008; 8:361-375.
62. Wang HG, Pathan N, Ethell IM, *et al*. Ca^{2+}-induced apoptosis through calcineurin dephosphorylation of BAD. Science. 1999; 284:339-343.
63. Wang JP, Chen CC. Magnolol induces cytosolic-free Ca^{2+} elevation in rat neutrophils primarily *via* inositol trisphosphate signalling pathway. Eur J Pharmacol. 1998; 352:329-334.
64. Teng CM, Yu SM, Chen CC, Huang YL, Huang TF. EDRF-release and Ca^{+}(+)-channel blockade by magnolol, an antiplatelet agent isolated from Chinese herb Magnolia officinalis, in rat thoracic aorta. Life Sci. 1990; 47:1153-1161.
65. Wu SN, Chen CC, Li HF, Lo YK, Chen SA, Chiang HT. Stimulation of the BK(Ca) channel in cultured smooth muscle cells of human trachea by magnolol. Thorax. 2002; 57:67-74.
66. Yeretssian G, Doiron K, Shao W, Leavitt BR, Hayden MR, Nicholson DW, Saleh M. Gender differences

in expression of the human caspase-12 long variant determines susceptibility to Listeria monocytogenes infection. Proc Natl Acad Sci U S A. 2009; 106:9016-9020.
67. Lee DH, Szczepanski MJ, Lee YJ. Magnolol induces apoptosis *via* inhibiting the EGFR/PI3K/Akt signaling pathway in human prostate cancer cells. J Cell Biochem. 2009; 106:1113-1122.
68. Hahm ER, Arlotti JA, Marynowski SW, Singh SV. Honokiol, a constituent of oriental medicinal herb magnolia officinalis, inhibits growth of PC-3 xenografts *in vivo* in association with apoptosis induction. Clin Cancer Res. 2008; 14:1248-1257.
69. Funa NS, Reddy K, Bhandarkar S, Kurenova EV, Yang L, Cance WG, Welsh M, Arbiser JL. Shb gene knockdown increases the susceptibility of SVR endothelial tumor cells to apoptotic stimuli *in vitro* and *in vivo*. J Invest Dermatol. 2008; 128:710-716.
70. Bellamy CO. p53 and apoptosis. Br Med Bull. 1997; 53:522-538.
71. Haldar S, Negrini M, Monne M, Sabbioni S, Croce CM. Down-regulation of bcl-2 by p53 in breast cancer cells. Cancer Res. 1994; 54:2095-2097.
72. Beham A, Marin MC, Fernandez A, Herrmann J, Brisbay S, Tari AM, Lopez-Berestein G, Lozano G, Sarkiss M, McDonnell TJ. Bcl-2 inhibits p53 nuclear import following DNA damage. Oncogene. 1997; 15:2767-2772.
73. Marin MC, Hsu B, Meyn RE, Donehower LA, el-Naggar AK, McDonnell TJ. Evidence that p53 and bcl-2 are regulators of a common cell death pathway important for *in vivo* lymphomagenesis. Oncogene. 1994; 9:3107-3112.
74. Walia V, Kakar S, Elble R. Micromanagement of the mitochondrial apoptotic pathway by p53. Front Biosci. 2011; 16:749-758.
75. Miyashita T, Krajewski S, Krajewska M, Wang HG, Lin HK, Liebermann DA, Hoffman B, Reed JC. Tumor suppressor p53 is a regulator of bcl-2 and bax gene expression *in vitro* and *in vivo*. Oncogene. 1994; 9:1799-1805.
76. Selvakumaran M, Lin HK, Miyashita T, Wang HG, Krajewski S, Reed JC, Hoffman B, Liebermann D. Immediate early up-regulation of bax expression by p53 but not TGF beta 1: A paradigm for distinct apoptotic pathways. Oncogene. 1994; 9:1791-1798.
77. Qiu P, Guan H, Dong P, Li S, Ho CT, Pan MH, McClements DJ, Xiao H. The p53-, Bax- and p21-dependent inhibition of colon cancer cell growth by 5-hydroxy polymethoxyflavones. Mol Nutr Food Res. 2011; 55: 613-622.
78. Trinh DL, Elwi AN, Kim SW. Direct interaction between p53 and Tid1 proteins affects p53 mitochondrial localization and apoptosisy as a target for cancer therapy. Oncotarget. 2010; 1:396-404.
79. Hui L, Zheng Y, Yan Y, Bargonetti J, Foster DA. Mutant p53 in MDA-MB-231 breast cancer cells is stabilized by elevated phospholipase D activity and contributes to survival signals generated by phospholipase D. Oncogene. 2006; 25:7305-7310.
80. Zhong M, Shen Y, Zheng Y, Joseph T, Jackson D, Foster DA. Phospholipase D prevents apoptosis in v-Src-transformed rat fibroblasts and MDA-MB-231 breast cancer cells. Biochem Biophys Res Commun. 2003; 302:615-619.
81. Garcia A, Zheng Y, Zhao C, Toschi A, Fan J, Shraibman N, Brown HA, Bar-Sagi D, Foster DA, Arbiser JL. Honokiol suppresses survival signals mediated by Ras-dependent phospholipase D activity in human cancer cells. Clin Cancer Res. 2008; 14:4267-4274.
82. Wang T, Chen F, Chen Z, Wu YF, Xu XL, Zheng S, Hu X. Honokiol induces apoptosis through p53-independent pathway in human colorectal cell line RKO. World J Gastroenterol. 2004; 10:2205-2208.
83. Dutta J, Fan Y, Gupta N, Fan G, Gelinas, C. Current insights into the regulation of programmed cell death by NF-kappaB. Oncogene. 2006; 25:6800-6816.
84. Jost PJ, Ruland J. Aberrant NF-kappaB signaling in lymphoma: Mechanisms, consequences, and therapeutic implications. Blood. 2007; 109:2700-2707.
85. Chen YL, Lin KF, Shiao MS, Chen YT, Hong CY, Lin SJ. Magnolol, a potent antioxidant from Magnolia officinalis, attenuates intimal thickening and MCP-1 expression after balloon injury of the aorta in cholesterol-fed rabbits. Basic Res Cardiol. 2001; 96:353-363.
86. Chen YH, Lin SJ, Chen JW, Ku HH, Chen YL. Magnolol attenuates VCAM-1 expression *in vitro* in TNF-alpha-treated human aortic endothelial cells and *in vivo* in the aorta of cholesterol-fed rabbits. Br J Pharmacol. 2002; 135:37-47.
87. Tse AK, Wan CK, Zhu GY, Shen XL, Cheung HY, Yang M, Fong WF. Magnolol suppresses NF-kappaB activation and NF-kappaB regulated gene expression through inhibition of IkappaB kinase activation. Mol Immunol. 2007; 4:2647-2658.
88. Ahn KS, Sethi G, Shishodia S, Sung B, Arbiser JL, Aggarwal BB. Honokiol potentiates apoptosis, suppresses osteoclastogenesis, and inhibits invasion through modulation of nuclear factor-kappaB activation pathway. Mol Cancer Res. 2006; 4:621-633.
89. Tse AK, Wan CK, Shen XL, Yang M, Fong WF. Honokiol inhibits TNF-alpha-stimulated NF-kappaB activation and NF-kappaB-regulated gene expression through suppression of IKK activation. Biochem Pharmacol. 2005; 70:1443-1457.
90. Shen JL, Man KM, Huang PH, Chen WC, Chen DC, Cheng YW, Liu PL, Chou MC, Chen YH. Honokiol and magnolol as multifunctional antioxidative molecules for dermatologic disorders. Molecules. 2010; 15:6452-6465.

(Received August 06, 2011; Revised October 01, 2011; Accepted October 09, 2011)

Review

DOI: 10.5582/ddt.2011.v5.5.211

Agents that induce pseudo-allergic reaction

Hong Wang[1,2], Huaishan Wang[1,2], Zhaoping Liu [1,2,*]

[1] *School of Pharmaceutical Sciences, Shandong University, Ji'nan, Shandong, China;*
[2] *Center for New Drugs Evaluation, Shandong University, Ji'nan, Shandong, China.*

ABSTRACT: Pseudo-allergic reactions may result from the activation of inflammatory or anaphylactic mechanisms independent of antigen-specific immune responses. Recent statistics show that pseudo-allergic reactions may represent as high as two thirds of all immediate hypersensitivity reactions, implying a great amount of morbidity and numerous health care costs. In this review, we concentrate on agents mediating pseudo-allergic reactions and evaluate accurately the available information on their modes of action. The agents discussed here are divided into three types: (*i*) Direct mast cell activators, which may activate mast cells in an IgE-independent manner, such as opioid drugs, basic secretagogues and calcium ionophore A23187; (*ii*) Complement activators, including liposomes, radiocontrast media and Cremophor EL, which may activate the complement system by different pathways: the classical pathway, the mannose-binding lectin pathway or the alternative pathway; (*iii*) Nonsteroidal anti-inflammatory drugs, which may inhibit the function of cyclooxygenase-1, resulting in the occurrence of adverse reactions. In addition, nonclinical detection methods of pseudo-allergic reactions are also reviewed in order to supply valuable information for clinical diagnosis.

Keywords: Pseudo-allergic reaction, anaphylaxis, mast cell, complement, nonsteroidal anti-inflammatory drugs

1. Introduction

Hypersensitivity reactions have been classified into four types from I to IV by Coombs and Gell in 1963 (*1*). With further studies of adverse drug reactions, a new type of hypersensitivity reaction has increasingly been recognized (*2*), which is an acute, potentially fatal, systemic hypersensitivity reaction arising *via* a non-IgE-dependent mechanism. The reaction occurs at the first contact with the drug without prior sensitization, and does not increase upon repeated exposure. Because of its similarity to a type I allergy in clinical symptoms (Table 1), it has long been termed a pseudo-allergic reaction. In 2001, the European Academy of Allergology and Clinical Immunology (EAACI) proposed to use the term "nonallergic anaphylaxis" instead of "pseudo-allergic reaction" when immunologic mechanisms cannot be proven (*3*,*4*). However, the reactions discussed here have several causes, including but not limited to complement activation, which belong to antigen-independent immune responses. In addition, the term "pseudo-allergic reaction" was still used in the paper "Guidance for Industry: Immunotoxicology evaluation of investigational new drugs" published by FDA in 2002 (*5*). Therefore, we use the term "pseudo-allergic reaction" here.

Pseudo-allergic reactions can be attributed to the activation of inflammatory or anaphylactic mechanisms unrelated to antigen-specific immune responses (*5*). These reactions may be induced by the following agents: direct mast cell activators, complement activators and nonsteroidal anti-inflammatory drugs. A series of physiological and pathological reactions can be induced by these agents in human bodies resulting in the appearance of symptoms of pseudo-allergic reactions such as nausea, dermatitis, hypotension, anaphylactic shock and even death (Table 1).

It has been indicated that more than 30% of adverse drug reactions are immediate hypersensitivity reactions (*6*), and as high as two thirds of all immediate hypersensitivity reactions may be pseudo-allergic reactions (*7*), implying a great deal of morbidity and numerous health care costs every year (*8*). Owing to the lack of systematic study of the pathogenesis of these reactions, and the dearth of universal agreement on their diagnostic criteria, the epidemiology, pathophysiology, and management of these reactions are greatly inhibited, resulting in a failure to diagnose and treat pseudo-allergic reactions in a consistent manner (*9*). Therefore, the aim of this review is to introduce the possible causes of pseudo-allergic reactions, based on agents of known structures that are capable of mediating the reactions. Nonclinical detection methods of pseudo-allergic reactions are also reviewed and discussed.

**Address correspondence to:*
Dr. Zhaoping Liu, Center for New Drugs Evaluation, Shandong University, 44# Wen Hua Xi Road, Ji'nan, 250012, China.
e-mail: liuzhaoping1958@126.com

Table 1. Symptoms of pseudo-allergic reactions

System	Potential symptoms and signs
Respiratory	Sneezing, coughing, asthma attack, bronchospasm, choking, rhinitis, tachypnea, stridor
Gastrointestinal	Vomiting, nausea, abdominal pain, diarrhea
Cardiovascular	Angioedema, hypertension, angina pectoris, ventricular tachycardia, arrhythmias, cardiac arrest
Neuromuscular	Chills, confusion, muscle pain
Skin and mucosa	Rash, cyanosis, dermatitis, erythema, pruritus, skin eruptions, urticaria, conjunctivitis
Severe adverse reactions	Anaphylactic shock, death

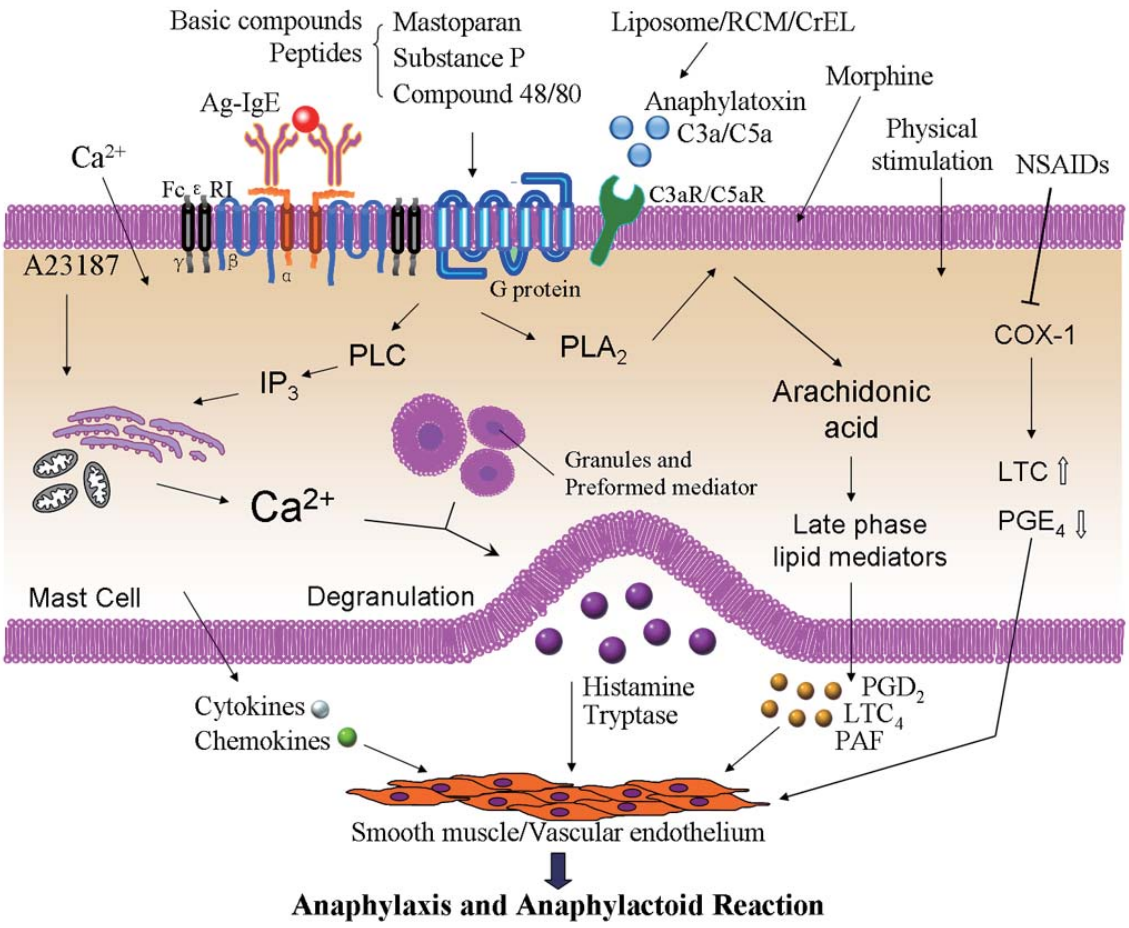

Figure 1. Pathways and mediators of anaphylaxis and pseudo-allergic reaction. Mast cells play a significant role in allergic and pseudo-allergic reactions. Activation of mast cells can be mediated both in an IgE dependent and independent manner, resulting in the release of preformed mediators such as histamine and tryptase, mediators newly synthesed such as PLD_2, LTC_4 and PAF, as well as cytokines and chemokines. G proteins are involved in the activation of mast cells induced by basic compounds and peptides. Mast cells can also be activated *via* the complement activation pathways.

2. Pseudo-allergic reaction caused by direct mast cell activators

Mast cells can be activated *via* several different mechanisms, among which is the classical pathway known as IgE-mediated mast cell activation, which is triggered by the cross-linking of FcεR1 receptors with antigen-specific IgE (*10*). Mast cell activation can also be completed in an IgE-independent manner using commercially available activators, such as opioid drugs, basic secretagogues, and calcium ionophores.

Upon activation, the degranulation reactions of mast cells are induced: (*i*) Performed mediators stored in granules are released, including histamine, tryptase, heparin and serotonin, which are responsible for most of acute effects of mast cells (*11-14*); (*ii*) Lipid-derived mediators are newly synthesized, such as prostaglandin D_2 (PGD_2), leukotriene C_4 (LTC_4) and platelet-activating factor (PAF), which mediate other relatively subacute functions of mast cells (*15-17*); (*iii*) Cytokines and chemokines (*18*) (Figure 1).

2.1. *By opioid drugs*

Opioid drugs have been widely used for the treatment of pain for thousands of years. Since they are such

commonly used drugs, adverse reactions are a concern. For example, morphine, codeine, and meperidine hydrochloride have been reported to induce mild pseudo-allergic reactions *via* the direct activation of mast cells (*19,20*). Moreover, some endogenous opioid peptides such as dynorphin, [D-Ala^2-D-Leu^5] enkephalin, β-endorphin, and morphiceptin have also been demonstrated to induce activation of skin mast cells (*21*).

It has been established that pseudo-allergic reactions caused by opioid drugs result from activation of opioid receptors present on mast cells (*21,22*). Moreover, opioid receptor activation has been proved to be associated with phospholipase C linked transduction mechanisms (*23*). Furthermore, one of the main mechanisms of mast cell degranulation has been shown to be activation of phospholipase C-linked pathways (*24*). As a result, we can assume that activation of mast cells induced by opioid drugs may be attributed to a phospholipase C-linked mechanism.

2.2. *By basic secretagogues*

Mast cells can be activated directly by a lot of polycationic molecules collectively known as the basic secretagogues, including naturally occurring polyamines such as hymenoptera venoms, various amines such as compound 48/80, and positively charged neuropeptides such as substance P (*25*).

Hymenoptera venoms are complicated mixtures of pharmacologically and biochemically active compounds such as peptides, proteins and biogenic amines, which may induce severe pain, local tissue damage and even death. Mastoparan, obtained from wasp venom, is an amidated tetradecapeptide responsible for the activation of mast cells and the release of histamine (*26*). The regulatory mechanism of mastoparans may be associated with the modulation of proteins including phospholipase A2 and phospholipase C (*27,28*). Moreover, some mastoparans are reported to bind G-protein coupled receptors (GPCRs), resulting in activation of mast cells (*29,30*). [Lys^{10}, Leu^{13}] mastoparan, another tetradecapeptide from wasp venom toxin, has been found to have the same mast cell activation role as mastoparan, and it is a much better tool for study of the mechanism of mast cell degranulation and intracellular signal transmission (*26*). What is more, it has been discovered recently that two novel mastoparan peptides (Polybia-MP-II and -III) from the venom of the neotropical social wasp *Polybia paulista* can also trigger activation of mast cells (*31*).

Compound 48/80, a condensation product of phenethylamine cross-linked by formaldehyde, is known as one of the most potent secretagogues of mast cells. It can strongly activate cellular exocytosis, causing a rapid release of allergic mediators such as histamine. As a result, it has been widely used to study the mechanism of anaphylaxis (*32*). Activation of mast cells induced by compound 48/80 is reported to be associated with phospholipase D and heterotrimeric GTP-binding proteins (*33*). Besides, compound 48/80 can activate trimeric G proteins, and mainly those of the Gi or Go categories (*34,35*).

It is well-known that mast cells and basophils are both significant participants in allergic diseases, but the effect of compound 48/80 on basophils is less certain. Degranulation of basophils has been studied both *in vivo* and *in vitro* after exposure to compound 48/80. Shelley and Juhlin observed degranulation of normal human basophil leucocytes in the presence of the compound (*36*), while Haye *et al*. were unable to confirm that result with basophils from eight patients with non-allergic urticaria (*37*). Marks *et al*. failed to demonstrate such *in vivo* degranulation in cockerels and rabbits, either (*38*).

Substance P (SP), an 11-amino acid peptide member of the tachykinin family, plays a significant role in immunological and inflammatory states, and is a mediator of asthma, tissue injury, arthritis, allergy and autoimmune diseases (*39*). Neuropeptide SP has been shown to trigger activation of mast cells and results in selective secretion of abundant mediators, such as cytokines and chemokines (*40*). The mechanism involved may be that SP can directly activate pertussis toxin (PTX)-sensitive G proteins (such as Gi_2 and Gi_3) in mast cells, mobilizating phospholipase Cb that causes exocytosis, and stimulating phosphatidylinositol 3-kinase that induces synthesis and release of arachidonic acid metabolites (*41*). What's more, it has been established that mast cell activation induced by SP proceeds through the neurokinin-1 receptor (NK1R) of G proteins (*42*), which mediates the main biological effects of SP. SP has also been shown to induce NK-1 receptor-independent activation of mast cells, which is associated with activation of the MrgX2 receptor (*43*), a member of the G protein-coupled receptor (GPCR) family (*44*).

2.3. *By calcium*

Calcium is known as a key second messenger in immunologic responses and degranulation processes of mast cells and basophils (*45,46*). The regulation of cytoplasmic calcium levels on mast cell secretory activity requires the introduction of calcium ionophores. For example, calcium ionophore A23187, a mobile-carrier of divalent cations such as Ca^{2+}, Mg^{2+}, and double H^+ (*47,48*), can reduce the level of Ca^{2+} stored in mitochondria or increase the inflow from the extracellular medium (*49,50*), resulting in the elevation of the cytosolic Ca^{2+}, which can induce mast cell exocytosis and release of histamine. The mechanism involved in the role of calcium ionophore A23187 may be based on the two following aspects:

(*i*) The release of Ca^{2+} from internal stores has been reported to be associated with some second messengers, including phospholipase C, phospholipase D, inositol 1,4,5-triphosphate (IP_3), and diacylglycerol (DG) (*51*). (*ii*) Degranulation dependent on the influx of extracular Ca^{2+} may be related to the members of the SNARE (soluble NSF attachment protein receptor) family, such as SNAP-23 (synaptosome-associated protein of 23 kDa), syntaxin, synaptotagmin, and molecules of the VAMPs (vesicle-associate membrane protein) family which regulate the granuleto-granule or granule-to-plasma membrane fusion process (*52*). In addition to Ca^{2+}, Mg^{2+} and Zn^{2+} are also necessary for the activation of mast cells (*53*).

3. Pseudo-allergic reaction caused by complement activators

More than 30 complex components are included in the complement system of the human body, which play significant roles in defense against infection, distinction between innate and adaptive immunity, and repairing injured tissues (*54,55*). Due to imbalance or deficiency of the complement regulating system, diseases may be caused by complement activation, such as complement activation-related pseudo-allergy (CARPA) (*56*). It is suggested that the complement system can be activated by some drugs and excipients, resulting in production of anaphylatoxins such as C3a, C4a, and C5a (*56*). They can bind to the complement receptors C3aR, C4aR, and C5aR, respectively, on the surface of membranes, and stimulate degranulation of serosa mast cells and peripheral blood basophils (*57*). The complement system is activated by three different pathways: the classical pathway, the mannose-binding lectin pathway and the alternative pathway (Figure 2) (*58*), which are different at the stage of C3 component activation in the most significant moment of system activation (*59*).

Known examples of CARPA are caused by liposomes (*60*), radiocontrast media (RCM) such

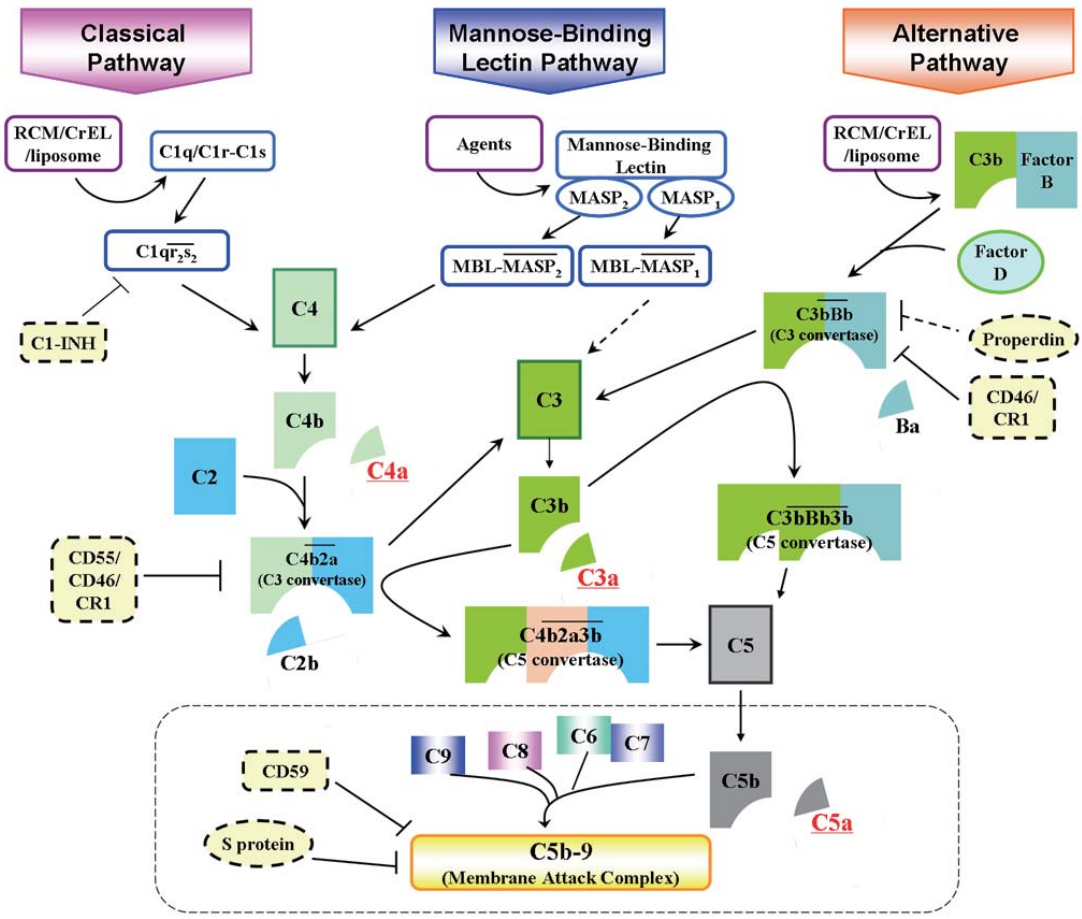

Figure 2. Pathways of complement activation. The complement system can be activated *via* three different pathways: the classical pathway, the mannose-binding lectin pathway and the alternative pathway. All three pathways cleave C3 and form membrane attack complex (MAC) C5b-9 eventually. $C1qr_2s_2$ complex is the promoter of the classical pathway and mannose-binding lectin-$MASP_1$/$MASP_2$ is the promoter of the mannose-binding lectin pathway. Both cleave C4 to C4a and C4b, the latter binding to fragment of C2, forming the C3 convertase of the classical and mannose-binding lectin pathway. Besides, MASP1 could cleave C3 directly. The alternative pathway is started by the forming of C3b-Bb complex (C3 convertase), by which C3 can be hydrolyzed to C3a and C3b, the latter can bind to C3 convertase and C5 convertase is formed. C5 convertase cleaves C5 to C5a and C5b, resulting in the same cause and end effect.

as metrizamide, iohexol, iopamadol, ioversol and ioxaglate (*61,62*), adjuvant amphiphilic emulsifier solvent systems such as Cremophor EL(CrEL) in Taxol (*63*) and so on.

3.1. *By liposomes*

Liposomes are increasingly used for targeted or controlled release of many diagnostic agents and drugs in medicine. To date, marketed liposomal drugs, such as Doxil (Caelyx) (*64*), Abelcet (*65*), AmBisome (*66*), Amphocil (*67*), and DaunoXome (*68*), have been reported to cause CARPA with morbidity rates varying from 3 to 45 percent. Taking Doxil as an example, the reported incidence changes between 0-25%, with the average value of 8% and the median value of 5% (*69*).

It has been shown that different characteristics of liposomes and experimental conditions can result in different pathways or levels of complement activation, leading to the mechanistic study of CARPA caused by liposomes being difficult (*70*). For example, the characteristics of liposomes such as large size, polydispersity, surface charges and high cholesterol (> 45%) content are all shown to promote the incidence of CARPA (*69*). The results published by Chanan-Khan *et al.* have demonstrated that the complement activation caused by some lipsomes is through the mechanism of an increase of Bb, an active fragment of the alternative pathway (*65*). In addition, the activation of complement systems can also be induced in the classical pathway by direct binding of C1q to complement reactive protein-tagged liposomes or the phospholipid bilayer. S protein-bound C terminal complex (SC5b-9), the terminal complement complex, has been shown to be highly sensitive in predicting CARPA in clinical studies. Therefore, the SC5b-9 assay could be a biomarker for clinical diagnosis and laboratory studies (*71*).

3.2. *By RCM*

Radiocontrast media (RCM), which are widely used in diagnostic radiology or radiotherapy, have been reported to cause adverse reactions with an annual incidence rate of about 2.1-12.66% (*72*), and deaths of 1 to 3 per 100,000 administrations (*73*). For example, sodium iothalamate, a kind of RCM, has been found to induce CARPA in dogs as well as other RCMs, such as metrizamide, iothalamate, diatrizoate, acetrizoate, iodipamide, and iopanoate (*74*). What is more, clinical studies showed that 42 patients out of 220 presented pseudo-allergic reactions after RCM injection, with symptoms appearing in 90 sec and disappearing 30 min later (*75*).

Similarly to liposomes, RCM reactions can be influenced by characteristics of the RCM, including osmolarity, charge, iodine number, administration speeds and the recent constitutional features of patients (*76*). Hirshfeld *et al*. compared nonionic, low-osmolality radiocontrast agents with ionic, high-osmolality agents during cardiac catheterization and found the latter ones could induce adverse reactions more easily (*77*). Moreover, it has been shown that adverse reactions induced by ionic contrast materials are in the range of 4% to 12% while those by nonionic contrast materials are 1% to 3% (*62*). Katayama *et al*., in research with over 300,000 contrast administrations, found the prevalence of severe adverse drug reactions was 0.04% for nonionic contrast media and 0.2% for ionic contrast media (*78*).

A report demonstrates that the intravenous infusion of RCM results in the release of vasoactive mediators, such as histamine and serotonin, which may stem from mast cells or basophils. An increase in plasma histamine levels has also been observed after intravenous administration of RCM in dogs (*79*) as well as in humans (*80*). The mechanism involved seems to be mediated by proteins of the alterative pathway, because the synergistic effect would not be shown in serum without the complement components (*81*). To be specific, the mechanism involved in RCM reactions may be associated with production of C3a and C5a, or suppress complement regulatory factors I and H *in vivo* and *in vitro*, leading to activation of the complement system in both the classical and alternative pathways (*61*).

3.3. *By CrEL*

CrEL, a non-ionic detergent, has been widely used as a vehicle for insoluble drugs, including anticancer agents such as paclitaxel (taxol) and immunosuppressants such as cyclosporine (*82*). The drugs mentioned above dissolved in CrEL may cause severe and even life-threatening CARPA, especially taxol (*83*). It has been demonstrated in a clinical study that an equivalent volume mixture of CrEL and taxol has caused a significant increase of the serum levels of SC5b-9 and Bb fragments, end products of complement activation (*63*).

It has been shown that the complement activation induced by CrEL is mainly through the alternative pathway. One possible mechanism is that CrEL could form non-ionic block copolymer surfactants, L101 and L102, both of which can bind to C3 on the surface of cell membranes and result in activation of the complement alternative pathway (*63*). Other studies revealed that microdroplets with varying sizes up to 300 nm could be formed by CrEL interacting with plasma lipoproteins HDL and LDL. These microdroplets can bind to C3bBb, one of C3 convertases, leading to the release of anaphylactoxin C3a or C5a and the occurrence of pseudo-allergic reactions (*84,85*). In addition, Szebeni *et al.* found that taxol could form 8-20 nm spherical structures in aqueous solutions, and

therefore, Taxol or pure CrEL in aqueous solutions might be eliminated *via* 30 kDa cutoff filters and thus activation of the complement system significantly reduced (*84*).

4. Pseudo-allergic reaction caused by nonsteroidal anti-inflammatory drugs

Nonsteroidal anti-inflammatory drugs (NSAIDs) are a series of substances used to treat pain, fever, or inflammation. They inhibit the function of cyclooxygenases (COXs) which are strong mediators in the conversion of arachidonic acid (AA) into thromboxanes and prostaglandins (PGs). This inhibition leads to the metabolism of AA toward the 5-lipoxygenase pathway and results in an increase of cysteinyl leukotrienes release.

There are two subtypes of COXs: COX-1 and COX-2. COX-1 is a constitutive enzyme present in all cells and is significant in mucosa protection and physiological homeostasis (*86,87*). COX-2 is an inducible enzyme and is expressed only in a limited range of cell types after stimulation by inflammatory signals (*88*). NSAIDs vary in their mechanisms by inhibiting different isoforms of COXs. It has been shown that therapeutic effects of NSAIDs are primarily associated with their abilities to inhibit COX-2, while some of their frequent adverse effects are induced by COX-1 inhibition (*89*).

NSAIDs are reported to induce pseudo-allergic reactions, which are commonly described as intolerant in the medical literature (*90*). Pseudo-allergic reactions to NSAIDs account for 21% to 25% of all adverse drug reactions (*91*). Taking aspirin as an example, intolerance reactions are typically developed with the symptoms of rhinorrhea and conjunctival irritation within one hour after aspirin administration with acute asthma attacks (*92*). Szczeklik published results indicating that aspirin intolerance may be related to inhibition of COX-1, resulting in increased production of leukotrienes and decreased synthesis of PGE2, which is responsible for the symptoms of pseudo-allergic reactions observed in patients (*93*). This theory is also supported by multiple observations, including increased expression of the enzyme LTC_4 synthase (LTC4S) and LT receptors, and increased urinary leukotriene E_4 (LTE_4) levels in this patient population (*94-96*).

5. Nonclinical detection methods

Several animal models have been established to detect pseudo-allergic reactions, including pig, dog, and rat models. Szebeni *et al*. has compared the sensitivity of these models in complement-mediated hypersensitivity reactions to liposomes and other lipid-based nanoparticles, and concluded that pig and dog models were more applicable than rat models in predicting pseudo-allergic reactions of particulate "nanodrugs". Moreover, dogs can also be a model used for micellar lipids (such as CrEL), while pigs cannot (*97*). It has also been indicated that pseudo-allergic shock could be induced in porcine models by intravenous injection of calcium ionophore A23187 (*98*). If symptoms of anaphylaxis are observed in animal studies (as shown in Table 1), the following studies should be considered. Various methods should be studied to distinguish pseudo-allergic reactions from true IgE mediated type I allergy. For example, the mast cell line, as an *in vitro* model, is extensively used to detect the release of histamine induced by drugs (*99*). Among which, rat peritoneal mast cells have been the most popular model for many years (*100*). Besides, biochemical markers of pseudo-allergic reactions should be observed in nonclinical toxicology studies, including the detection of serum anaphylactic complement products in animals which show signs of anaphylaxis (*56*). Careful evaluation of the above reactions may supply valuable information on biochemical markers for clinical trials.

6. Conclusions

Pseudo-allergic reactions, which are mediated in an IgE-independent mechanism, have drawn more and more people's attention recently. Three possible mechanisms involved have been introduced, with the important drugs and agents which have been studied, in considerable detail. However, due to little understanding in this area, there is no rapid *in vivo* or *in vitro* diagnosis test in the clinic. The skin test is used for the diagnosis of type I allergy, but not for the pseudo-allergic reactions. In view of the characteristics of pseudo-allergic reactions, the provocation test may be the only way to come to a diagnosis. With the further study of the mechanism of these reactions, effective diagnosis methods in the clinic will be found.

Acknowledgments

The authors acknowledge Zhao-Hua Liu, Hui-Di Qin for the helpful comments on the manuscript. This work was supported by a Grant from the "Eleventh Five-year Plan" of Key Projects in the National Science & Technology Pillar Program (No. 2009ZX09502-001) and National Natural Science Foundation of China (No. 30973934).

References

1. Coombs R, Gell P, Laehman P. The classification of allergic reactions underlying disease. In: Clinical Aspects of Immunology (Gell PGH, Coombs RRA, eds.). F.A. Davis Company, Philadelphia, PA, USA, 1963; pp. 317-337.
2. Descotes J, Choquet-Kastylevsky G. Gell and Coombs's classification: Is it still valid? Toxicology. 2001;

158:43-49.
3. Johansson SG, Hourihane JO, Bousquet J, Bruijnzeel-Koomen C, Dreborg S, Haahtela T, Kowalski ML, Mygind N, Ring J, van Cauwenberge P, van Hage-Hamsten M, Wüthrich B; EAACI (the European Academy of Allergology and Cinical Immunology) nomenclature task force. A revised nomenclature for allergy: An EAACI position statement from the EAACI nomenclature task force. Allergy. 2001; 9:813-824.
4. Johansson S, Bieber T, Dahl R, Friedmann PS, Lanier BQ, Lockey RF, Motala C, Ortega Martell JA. Revised nomenclature for allergy for global use: Report of the Nomenclature Review Committee of the World Allergy Organization, October 2003. J Allergy Clin Immunol. 2004; 113:832-836.
5. FDA Guidance for Industry-Immunotoxicology Evaluation of Investigational New Drugs. *http://www.fda.gov/downloads/Drugs/GuidanceComplianceRegulatoryInformation/Guidances/ucm079239.pdf.*
6. Demoly P, Bousquet J. Epidemiology of drug allergy. Curr Opin Allergy Clin Immunol. 2001; 4:305-310.
7. Demoly P, Lebel B, Messaad D, Sahla H, Rongier M, Daures J, Godard P, Bousquet J. Predictive capacity of histamine release for the diagnosis of drug allergy. Allergy. 1999; 54:500-506.
8. Szebeni J. Complement activation-related pseudoallergy caused by liposomes, micellar carriers of intravenous drugs, and radiocontrast agents. Crit Rev Ther Drug Carrier Syst. 2001; 18:567-606.
9. Bohlke K, Davis RL, DeStefano F, Marcy SM, Braun MM, Thompson RS. Epidemiology of anaphylaxis among children and adolescents enrolled in a health maintenance organization. J Allergy Clin Immunol. 2004; 113:536-542.
10. Metzger H. The receptor with high affinity for IgE. Immunol Rev. 1992; 1:37-48.
11. Di Capite J, Parekh AB. CRAC channels and Ca^{2+} signaling in mast cells. Immunol Rev. 2009; 231:45-58.
12. Venkatesh P, Mukherjee PK, Kumar SN, Nema NK, Bandyopadhyay A, Fukui H, Mizuguchi H. Mast cell stabilization and antihistaminic potentials of *Curculigo orchioides* rhizomes. J Ethnopharmacol. 2009; 126:434-436.
13. Yeung CK, Law JK, Sam SW, Ingebrandt S, Lau HY, Rudd JA, Chan M. Modulatory action of potassium channel openers on field potential and histamine release from rat peritoneal mast cells. Can J Physiol Pharmacol. 2009; 87:624-632.
14. Shin K, Nigrovic PA, Crish J, Boilard E, McNeil HP, Larabee KS, Adachi R, Gurish MF, Gobezie R, Stevens RL. Mast cells contribute to autoimmune inflammatory arthritis *via* their tryptase/heparin complexes. J Immunol. 2009; 182:647-656.
15. Ono E, Taniguchi M, Mita H, Fukutomi Y, Higashi N, Miyazaki E, Kumamoto T, Akiyama K. Increased production of cysteinyl leukotrienes and prostaglandin D2 during human anaphylaxis. Clin Exp Allergy. 2009; 39:72-80.
16. Misso NL, Aggarwal S, Thompson PJ, Vally H. Increases in urinary 9alpha,11beta-prostaglandin f2 indicates mast cell activation in wine-induced asthma. Int Arch Allergy Immunol. 2009; 149:127-132.
17. Jiang Y, Borrelli L, Bacskai BJ, Kanaoka Y, Boyce JA. P2Y6 receptors require an intact cysteinyl leukotriene synthetic and signaling system to induce survival and activation of mast cells. J Immunol. 2009; 182:1129-1137.
18. Galli SJ, Nakae S, Tsai M. Mast cells in the development of adaptive immune responses. Nat Immunol. 2005; 6:135-142.
19. Guedes A, Papich M, Rude E, Rider M. Comparison of plasma histamine levels after intravenous administration of hydromorphone and morphine in dogs. J Vet Pharmacol Ther. 2007; 30:516-522.
20. Woodall HE, Chiu A, Weissman DE. Opioid allergic reactions # 175. J Palliat Med. 2008; 11:776-777.
21. Casale TB, Bowman S, Kaliner M. Induction of human cutaneous mast cell degranulation by opiates and endogenous opioid peptides: Evidence for opiate and nonopiate receptor participation. J Allergy Clin Immunol. 1984; 73:775-781.
22. Trescot A, Datta S, Lee M, Hansen H. Opioid pharmacology. Pain Physician. 2008; 11 (Suppl 2): S133-S135.
23. Liu NJ, vongizycki H, Gintzler AR. Phospholipase Cbeta1 modulates pain sensitivity, opioid antinociception and opioid tolerance formation. Brain Res. 2006; 1069:47-53.
24. Gilfillan AM, Tkaczyk C. Integrated signalling pathways for mast-cell activation. Nat Rev Immunol. 2006; 6:218-230.
25. Ferry X, Brehin S, Kamel R, Landry Y. G protein-dependent activation of mast cell by peptides and basic secretagogues. Peptides. 2002; 23:1507-1515.
26. Mukai H, Kikuchi M, Suzuki Y, Munekata E. A mastoparan analog without lytic effects and its stimulatory mechanisms in mast cells. Biochem Biophys Res Commun. 2007; 362:51-55.
27. Higashijima T, Burnier J, Ross EM. Regulation of Gi and Go by mastoparan, related amphiphilic peptides, and hydrophobic amines. Mechanism and structural determinants of activity. J Biol Chem. 1990; 265:14176-14178.
28. Song DL, Chang GD, Ho CL, Chang CH. Structural requirements of mastoparan for activation of membrane-bound guanylate cyclase. Eur J Pharmacol. 1993; 15:283-288.
29. Jones S, Howl J. Biological applications of the receptor mimetic peptide mastoparan. Curr Protein Pept Sci. 2006; 7:501-508.
30. Rocha T, Leonardo MB, De Souza BM, Palma MS, Da Cruz-Höfling MA. Mastoparan effects in skeletal muscle damage: An ultrastructural view until now concealed. Microsc Res Tech. 2008; 71:220-229.
31. de Souza BM, da Silva AV, Resende VM, Arcuri HA, Dos Santos Cabrera MP, Ruggiero Neto J, Palma MS. Characterization of two novel polyfunctional mastoparan peptides from the venom of the social wasp *Polybia paulista*. Peptides. 2009; 30:1387-1395.
32. Kim SH, Lee S, Kim IK, Kwon TK, Moon JY, Park WH, Shin TY. Suppression of mast cell-mediated allergic reaction by *Amomum xanthiodes*. Food Chem Toxicol. 2007; 45:2138-2144.
33. Chahdi A, Fraundorfer PF, Beaven MA. Compound 48/80 activates mast cell phospholipase D *via* heterotrimeric GTP-binding proteins. J Pharmacol Exp Ther. 2000; 292:122-130.
34. Mousli M, Bueb JL, Bronner C, Rouot B, Landry Y. G protein activation: A receptor-independent mode of action for cationic amphiphilic neuropeptides and venom

peptides. Trends Pharmacol Sci. 1990; 11:358-362.
35. Chahdi A, Daeffler L, Gies J, Landry Y. Drugs interacting with G protein α subunits: Selectivity and perspectives. Fundam Clin Pharmacol. 1998; 12:121-132.
36. Shelley W, Juhlin L. *In vitro* effect of licithinase A on the cytology of the human basophil. J Lab Clin Med. 1962; 60:589-597.
37. Haye KR, Schneider R. The difference in behaviour of basophil leucocytes and mast cells towards compound 48/80. Br J Pharmacol Chemother. 1966; 28:282-288.
38. Marks B, Sorgen R, Ginsburg H. Histamine-liberator and basophilic leukocytes. Biochem Pharmacol. 1959; 3:200-202.
39. Cabriales S, Bresnahan J, Testa D, Espina BM, Scadden DT, Ross M, Gill PS. Extravasation of liposomal daunorubicin in patients with AIDS-associated Kaposi's sarcoma: A report of four cases. Oncol Nurs Forum. 1998; 25:67-70.
40. Dianzani C, Pierangeli A, Chiricozzi A, Avola A, Degener AM. Cutaneous human papillomaviruses as recurrence factor in actinic keratoses. Int J Immunopathol Pharmacol. 2008; 21:145-152.
41. Ferry X, Eichwald V, Daeffler L, Landry Y. Activation of betagamma subunits of G(i2) and G(i3) proteins by basic secretagogues induces exocytosis through phospholipase Cbeta and arachidonate release through phospholipase Cgamma in mast cells. J Immunol. 2001; 167:4805-4813.
42. Bot I, de Jager SC, Bot M, van Heiningen SH, de Groot P, Veldhuizen RW, van Berkel TJ, von der Thüsen JH, Biessen EA. The neuropeptide substance P mediates adventitial mast cell activation and induces intraplaque hemorrhage in advanced atherosclerosis. Circ Res. 2010; 106:89-92.
43. Tatemoto K, Nozaki Y, Tsuda R, Konno S, Tomura K, Furuno M, Ogasawara H, Edamura K, Takagi H, Iwamura H. Immunoglobulin E-independent activation of mast cell is mediated by Mrg receptors. Biochem Biophys Res Commun. 2006; 349:1322-1328.
44. Lembo PM, Grazzini E, Groblewski T, *et al*. Proenkephalin A gene products activate a new family of sensory neuron-specific GPCRs. Nat Neurosci. 2002; 5:201-209.
45. Blank U, Cyprien B, Martin-Verdeaux S, Paumet F, Pombo I, Rivera J, Roa M, Varin-Blank N. SNAREs and associated regulators in the control of exocytosis in the RBL-2H3 mast cell line. Mol Immunol. 2002; 38:1341-1345.
46. Qin HD, Shi YQ, Liu Z, Li ZG, Wang H, Liu ZP. Effect of chlorogenic acid on mast cell-dependent anaphylactic reaction. Int Immunopharmacol. 2010; 10:1135-1141.
47. Reed PW, Lardy HA. A23187: A divalent cation ionophore. J Biol Chem. 1972; 247:6970-6977.
48. Pfeiffer D, Lardy HA. Ionophore A23187: The effect of H^+ concentration on complex formation with divalent and monovalent cations and the demonstration of K^+ transport in mitochondria mediated by A23187. Biochemistry. 1976; 15:935-943.
49. Yecies LD, Wedner HJ, Johnson SM, Jakschik BA, Parker CW. Slow reacting substance (SRS) from ionophore A23187-stimulated peritoneal mast cells of the normal rat. I. conditions of generation and initial characterization. J Immunol. 1979; 122:2083-2089.
50. Paterson NA, Wasserman SI, Said JW, Austen KF. Release of chemical mediators from partially purified human lung mast cells. J Immunol. 1976; 117:1356-1362.
51. Itoh T, Ohguchi K, Iinuma M, Nozawa Y, Akao Y. Inhibitory effect of xanthones isolated from the pericarp of *Garcinia mangostana* L. on rat basophilic leukemia RBL-2H3 cell degranulation. Bioorg Med Chem. 2008; 16:4500-4508.
52. Melendez AJ, Khaw AK. Dichotomy of Ca^{2+} signals triggered by different phospholipid pathways in antigen stimulation of human mast cells. J Biol Chem. 2002; 19:17255-17262.
53. Kabu K, Yamasaki S, Kamimura D, Ito Y, Hasegawa A, Sato E, Kitamura H, Nishida K, Hirano T. Zinc is required for Fcepsilon RI-mediated mast cell activation. J Immunol. 2006; 2177:1296-1305.
54. Walport MJ. Complement. First of Two Parts. N Engl J Med. 2001; 344:1058-1066.
55. Walport MJ. Complement. Second of two parts. N Engl J Med. 2001; 344:1140-1144.
56. Szebeni J. Complement activation-related pseudoallergy: A new class of drug-induced acute immune toxicity. Toxicology. 2005; 216:106-121.
57. Mousli M, Hugli TE, Landry Y, Bronner C. Peptidergic pathway in human skin and rat peritoneal mast cell activation. Immunopharmacology. 1994; 27:1-11.
58. Kostner KM. Activation of the complement system: A crucial link between inflammation and atherosclerosis? Eur J Clin Invest. 2004; 34:800-802.
59. Xu Y, Narayana SV, Volanakis JE. Structural biology of the alternative pathway convertase. Immunol Rev. 2001; 180:123-135.
60. Szebeni J, Baranyi L, Savay S, Milosevits J, Bodo M, Bunger R, Alving CR. The interaction of liposomes with the complement system: *In vitro* and *in vivo* assays. Methods Enzymol. 2003; 373:136-154.
61. Szebeni J. Hypersensitivity reactions to radiocontrast media: The role of complement activation. Curr Allergy Asthma Rep. 2004; 4:25-30.
62. Cochran ST. Anaphylactoid reactions to radiocontrast media. Curr Allergy Asthma Rep. 2005; 5:28-31.
63. Szebeni J, Muggia FM, Alving CR. Complement activation by Cremophor EL as a possible contributor to hypersensitivity to paclitaxel: An *in vitro* study. J Natl Cancer Inst. 1998; 90:300-306.
64. Uziely B, Jeffers S, Isacson R, Kutsch K, Wei-Tsao D, Yehoshua Z, Libson E, Muggia FM, Gabizon A. Liposomal doxorubicin: Antitumor activity and unique toxicities during two complementary phase I studies. J Clin Oncol. 1995; 13:1777-1785.
65. Chanan-Khan A, Szebeni J, Savay S, Liebes L, Rafique NM, Alving CR, Muggia FM. Complement activation following first exposure to pegylated liposomal doxorubicin (Doxil): Possible role in hypersensitivity reactions. Ann Oncol. 2003; 14:1430-1437.
66. Schneider K, Dietze S, Leschke H. Anaphylactic reaction to liposomal amphotericin (AmBisome). Br J Haematol. 1998; 4:1108-1109.
67. de Marie S. Liposomal and lipid-based formulations of amphotericin B. Leukemia. 1996; 10 (Suppl 2):S93-S96.
68. Richardson DS, Kelsey SM, Johnson SA, Tighe M, Cavenagh JD, Newland AC. Early evaluation of liposomal daunorubicin (DaunoXome, Nexstar) in the treatment of relapsed and refractory lymphoma. Invest New Drugs. 1997; 15:247-253.
69. Skubitz KM, Skubitz AP. Mechanism of transient dyspnea induced by pegylated-liposomal doxorubicin (Doxil). Anticancer Drugs. 1998; 9:45-50.

70. Szebeni J. The interaction of liposomes with the complement system. Crit Rev Ther Drug Carrier Syst. 1998; 15:57-88.
71. Corallini F, Bossi F, Gonelli A, Tripodo C, Castellino G, Mollnes TE, Tedesco F, Rizzi L, Trotta F, Zauli G. The soluble terminal complement complex (SC5b-9) up-regulates osteoprotegerin expression and release by endothelial cells: Implications in rheumatoid arthritis. Rheumatology (Oxford). 2009; 48:293-298.
72. Hong SJ, Wong JT, Bloch KJ. Reactions to radiocontrast media. Allergy Ashma Proc. 2002; 23:347-351.
73. Cashman J, McCredie J, Henry D. Intravenous contrast media: Use and associated mortality. Med J Austral. 1991; 155:618-623.
74. Lasser EC, Sovak M, Lang JH. Development of contrast media idiosyncrasy in the dog. Radiology. 1976; 119:91-95.
75. Small P, Satin R, Palayew M, Hyams B. Prophylactic antihistamines in the management of radiographic contrast reactions. Clin Allergy. 1982; 12:289-294.
76. Barrett BJ, Parfrey PS, Vavasour HM, O'Dea F, Kent G, Stone E. A comparison of nonionic, low-osmolality radiocontrast agents with ionic, high-osmolality agents during cardiac catheterization. N Engl J Med. 1992; 326:431-436.
77. Hirshfeld JW Jr, Kussmaul WG, DiBattiste PM. Safety of cardiac angiography with conventional ionic contrast agents. Am J Cardiol. 1990; 66:355-361.
78. Katayama H, Yamaguchi K, Kozuka T, Takashima T, Seez P, Matsuura K. Adverse reactions to ionic and nonionic contrast media. A report from the Japanese Committee on the Safety of Contrast Media. Radiology. 1990; 175:621-628.
79. Bhat KN, Arroyave CM, Crown R. Reaction to radiographic contrast agents: New developments in etiology. Ann Allergy. 1976; 37:169-173.
80. Siegle RL, Lieberman P. Measurement of histamine, complement components and immune complexes during patient reactions to iodinated contrast material. Invest Radiol. 1976; 11:98-101.
81. Ring J, Arroyave CM, Frizler MJ, Tan EM. *In vitro* histamine and serotonin release by radiographic contrast media (RCM). Complement-dependent and-independent release reaction and changes in ultrastructure of human blood cells. Clin Exp Immunol. 1978; 32:105-118.
82. Noguchi T, Kamiyama N, Kashiwayanagi M. Modulation of voltage-gated ion channels on SH-SY5Y neuroblastoma by non-ionic surfactant, Cremophor EL. Biol Pharm Bull. 2010; 33:2013-2017.
83. Weiss RB, Donehower RC, Wiernik PH, Ohnuma T, Gralla RJ, Trump DL, Baker JR Jr, Van Echo DA, Von Hoff DD, Leyland-Jones B. Hypersensitivity reactions from taxol. J Clin Oncol. 1990; 8:1263-1268.
84. Szebeni J, Alving CR, Savay S, Barenholz Y, Priev A, Danino D, Talmon Y. Formation of complement-activating particles in aqueous solutions of Taxol: Possible role in hypersensitivity reactions. Int Immunopharmacol. 2001; 1:721-735.
85. Kessel D, Woodburn K, Decker D, Sykes E. Fractionation of Cremophor EL delineates components responsible for plasma lipoprotein alterations and multidrug resistance reversal. Oncol Res. 1995; 7:207-212.
86. Cha YI, Solnica-Krezel L, DuBois RN. Fishing for prostanoids: Deciphering the developmental functions of cyclooxygenase-derived prostaglandins. Dev Biol. 2006; 289:263-272.
87. Fortier M, Krishnaswamy K, Danyod G, Boucher-Kovalik S, Chapdelaine J. A postgenomic integratred view of prostaglandins in reproduction: Implications for other body systems. J Physiol Pharmacol. 2008; 59 (Suppl 1):65-89.
88. Murphey LJ, Williams MK, Sanchez SC, Byrne LM, Csiki I, Oates JA, Johnson DH, Morrow JD. Quantification of the major urinary metabolite of PGE2 by a liquid chromatographic/mass spectrometric assay: Determination of cyclooxygenase-specific PGE2 synthesis in healthy humans and those with lung cancer. Anal Biochem. 2004; 334:266-275.
89. Dannhardt G, Kiefer W. Cyclooxygenase inhibitors-current status and future prospects. Eur J Med Chem. 2001; 36:109-126.
90. Berges-Gimeno MP, Martín-Lázaro J. Allergic reactions to nonsteroidal anti-inflammatory drugs: Is newer better? Curr Allergy Asthma Rep. 2007; 7:35-40.
91. Weberschock TB, Müller SM, Boehncke S, Boehncke WH. Tolerance to coxibs in patients with intolerance to non-steroidal anti-inflammatory drugs (NSAIDs): A systematic structured review of the literature. Arch Dermatol Res. 2007; 299:169-175.
92. Stevenson DD. Aspirin and NSAID sensitivity. Immunol Allergy Clin North Am. 2004; 24:491-505.
93. Szczeklik A. The cyclooxygenase theory of aspirin-induced asthma. Eur Respir J. 1990; 3:588-593.
94. Picado C. The role of cyclooxygenase in acetylsalicylic acid sensitivity. Allergy Clin Immunol Int. 2006; 18:154-157.
95. Kowalski ML, Makowska JS. Aspirin-exacerbated respiratory disease. An update of diagnose and managment. Allergy Clin Immunol Int. 2006; 4:140-149.
96. Szczeklik A, Sanak M, Nizankowska-Mogilnicka E, Kielbasa B. Aspirin intolerance and the cyclooxygenase-leukotriene pathways. Curr Opin Pulm Med. 2004; 10:51-56.
97. Szebeni J, Alving CR, Rosivall L, Bünger R, Baranyi L, Bedöcs P, Tóth M, Barenholz Y. Animal models of complement-mediated hypersensitivity reactions to liposomes and other lipid-based nanoparticles. J Liposome Res. 2007; 17:107-117.
98. Heflin CR, Brewer KL, Hack JB, Meggs WJ. Heparin reverses anaphylactoid shock in a porcine model. Ann Emerg Med. 2006; 48:190-193.
99. Ennis M, Nehring E, Schneider C. Adverse reactions to drugs: *In vitro* studies with isolated cells. Inflamm Res. 2004; 53 (Suppl 2):S105-S108.
100. Sugimoto Y, Iba Y, Utsugi K, Kamei C. Influences of everninomicin, vancomycin and teicoplanin on chemical mediator release from rat peritoneal mast cells. Jpn J Pharmacol. 2000; 83:300-305.

(Received March 08, 2011; Revised August 15, 2011; Accepted August 26, 2011)

Original Article

DOI: 10.5582/ddt.2011.v5.5.220

A sensitive near-infrared fluorescent probe for caspase-mediated apoptosis: Synthesis and application in cell imaging

Yepeng Luan[1,2], Qiuhong Yang[2], Yumei Xie[2], Shaofeng Duan[2], Shuang Cai[2], M.L Forrest[2,*]

[1] *Department of Medicinal Chemistry, College of Pharmacy, Shandong University, Ji'nan, Shandong, China;*
[2] *Department of Pharmaceutical Chemistry, University of Kansas, Lawrence, KS, USA.*

ABSTRACT: Near-infrared (NIR) absorbing dyes represent an intriguing avenue for extracting biological information from living subjects since they can be monitored with noninvasive optical imaging techniques. We designed and synthesized an imaging agent which contains a NIR fluorochrome (IR780) and peptidyl fluoromethyl ketone (FMK) for caspase-9 imaging of cells undergoing apoptosis. The IR780-FMK fluorescent probe had a Strokes shift of 79 nm and quantum yield 0.75. Prostate cancer DU145 cells undergoing apoptosis were successfully imaged using as little as 0.1 μM of IR780-FMK.

Keywords: Cell death, cancer, screening, apoptosis, fluoromethyl ketone

1. Introduction

Apoptosis is the process of programmed cell death by which multicellular organisms regulate cell number and maintain homeostasis. Within the series of biochemical events involved in apoptosis, the activation of caspases is recognized a critical marker. Apoptosis can be triggered by extrinsic or intrinsic signals such as physiological activators (TNF family, neurotransmitters, calcium, glucocorticoids), damage-related inducers (heat shock, viral infection, tumor suppressors p53, oxidants, free radicals), therapy-associated agents (chemotherapeutic agents, gamma radiation and UV radiation) and toxins (ethanol, β-amyloid peptide) (*1-5*). Defective apoptosis processes can lead to severe pathological disorders, for example, downregulated apoptosis is involved in autoimmune diseases, cancer and viral infections (*6,7*); abnormal upregulation of apoptosis is associated with AIDS, neurodegenerative disorders and ischemic injury (*7,8*). Therefore, the development of caspase inhibitors could be novel treatments for a variety apoptosis associated diseases.

A number of peptidyl caspase inhibitors have been developed including peptidyl chloromethyl ketones, peptidyl fluoromethyl ketones and peptidyl aldehydes. The chloromethyl ketones have strong electrophilicity and are not stable to high concentrations of thiol which limits their use *in vivo* (*9*). The aldehyde based inhibitors are poorly cell permeable and are not effective caspase inhibitors under concentrations of 1 μM (*10*). The fluoromethyl ketone (FMK) inhibitors, which are more stable *in vivo* and cell permeable (*10,11*), act as broad-spectrum, irreversible caspase inhibitors (*12*) with no added cytotoxic effects. Inhibitors synthesized with a benzyloxycarbonyl group (such as Boc- or Z-) at the N-terminus and *O*-methyl side chains such as Z-Val-Ala-Asp(OMe)-FMK display improved cellular permeability facilitating their use in both *in vitro* cell culture and *in vivo* animal studies (*13,14*).

In this work, we synthesized an imaging agent containing a NIR fluorochrome IR780 with high quantum yield and the cell permeable fluoromethyl ketone Z-Val-Ala-Glu(OMe). The structure of it is shown in Figure 1. The agent irreversibly binds caspase-9 in cells undergoing apoptosis and can be used to monitor live cells undergoing apoptosis. Fluorochromes with absorption and emission maxima between 650 and 900 nm are within the NIR range and are ideally suited for imaging in tissue due to the minimal optical absorption from hemoglobin, water,

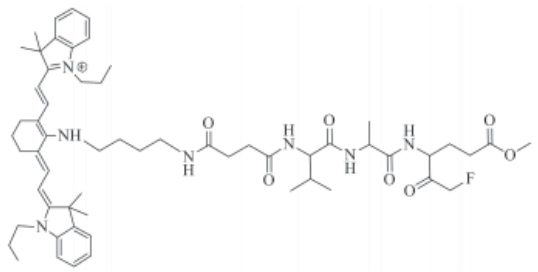

Figure 1. Structure of cell permeable fluoromethyl ketone Z-Val-Ala-Glu (OMe) (IR780-linker-Val-Ala-Glu(OMe)-FMK).

**Address correspondence to:*
Dr. M.L Forrest, Department of Pharmaceutical Chemistry, University of Kansas, 2095 Constant Ave., Lawrence, KS, 66047 USA.
e-mail: mforrest@ku.edu

and lipids over this range (*15-17*). This is a significant benefit over current commerical cell caspase imaging agents, such as FLIVO™, which use fluorophores wavelengths less than 600 nm, *e.g.* fluorescein and rhodamine, where there is significantly more tissue autofluorescence and optical attenuation.

2. Materials and Methods

2.1. *Chemicals*

All chemicals were obtained from Sigma-Aldrich (St. Louis, MO, USA) and used as received unless stated otherwise. Solvents were distilled under argon immediately before use. NMR spectra were taken on a 400-MHz Bruker with the TMS peak as internal reference. Mass spectra were run in the electrospray ionization mass spectrometry (ESI-MS) mode or atmospheric pressure chemical ionization (APCI-MS) mode. Reactions were carried out under dry argon with flame-dried glassware. Dichloromethane (DCM), *N*,*N*-dimethylformamide (DMF) and triethylamine (TEA) were freshly distilled from CaH_2, and tetrahydrafuran (THF) was freshly distilled from sodium benzophenone. The NIR fluorescent imaging agent 4' C-[4-[2-(fluoromethylketone-Ala-Val-NH)carbonyl]ethyl]carbonyl]amino]butyl]amino-IR780 [IR780-linker-Val-Ala-Glu(OMe)-FMK] (compound 10) was synthesized in 11 steps (Figure 2; Appendix).

2.2. *Spectral properties of IR780-linker-Val-Ala-Glu(OMe)-FMK*

The fluorescent spectrum of a 1-μM solution of IR780-linker-Val-Ala-Glu(OMe)-FMK in DMSO was recorded using a Shimadzu RF-5301 PC spectrofluorophotometer. The Stokes shift was determined by the difference in wavelength between excitation and emission maxima. The quantum yield was measured according to a reported protocol (*18,19*) using cresyl violet as a reference.

2.3. *Cell imaging for apoptosis*

The DU145 cell line was cultured in Eagle's Minimum Essential Medium (MEM) supplemented with 10% fetal bovine serum and 1% L-glutamine. Cells were seeded into an 8-chamber culture slide at a density of 40,000 per well,

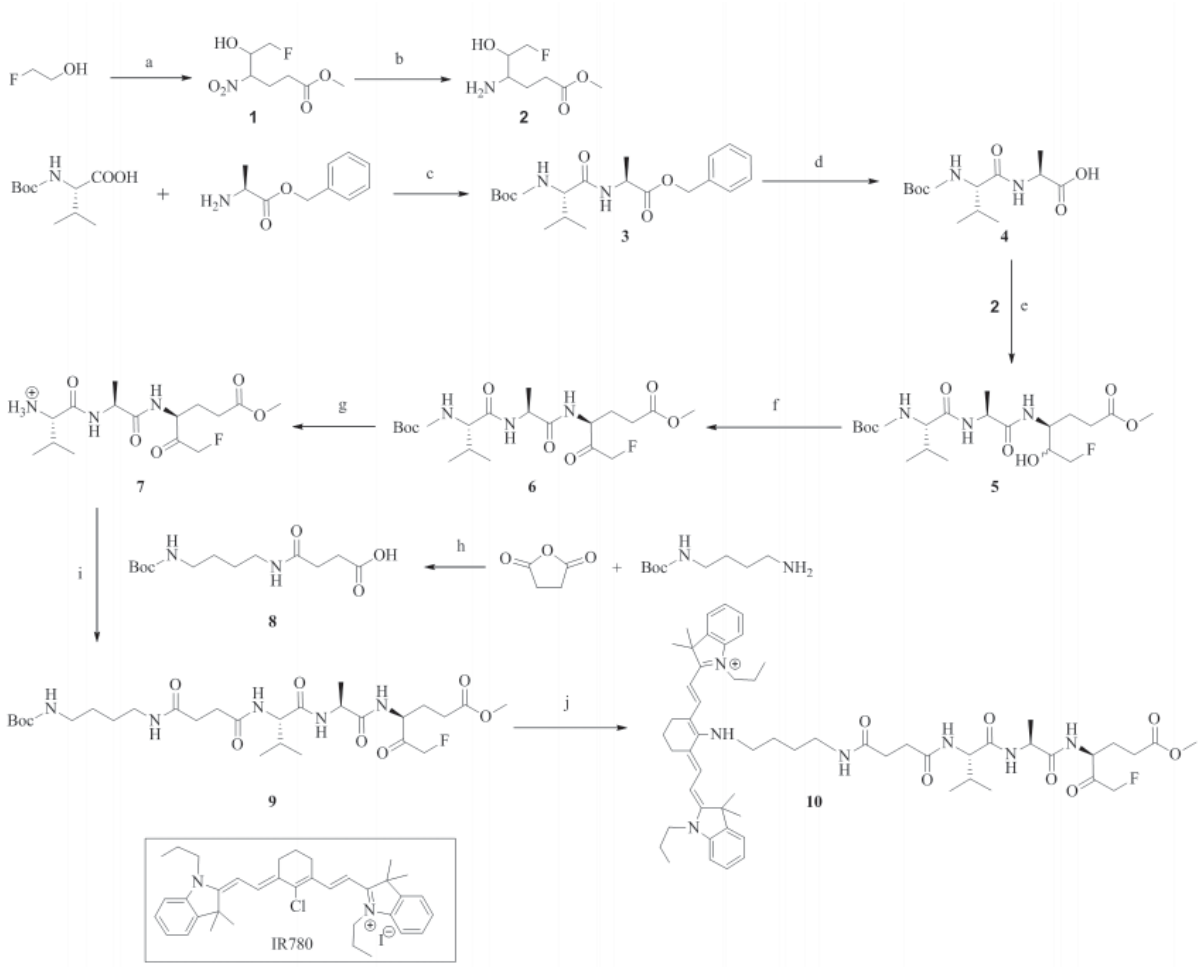

Figure 2. Synthetic scheme of IR780-linker-Val-Ala-Glu(OMe)-FMK imaging agent. Reagents: **a)** *i*, Swern oxidation; *ii*, methyl 4-nitrobutyrate, TEA; **b)** 10% Pd/C, H_2, in MeOH; **c)** TEA, HBTU, DMF; **d)** 10% Pd/C, H_2, in THF; **e)** EDCI, DMAP, THF; **f)** Dess-Martin periodinane, in DCM; **g)** 4M HCl/EtOAc; **h)** 1,4-dioxan, DMAP, reflux; **i)** EDCI, HOBt, DMAP, THF; **j)** *i*, 4M HCl/EtOAc; *ii*, IR 780, TEA, DMF.

and after overnight incubation, they were treated with or without 1 μM of camptothecin. After 24 h, IR780-linker-Val-Ala-Glu(OMe)-FMK (compound 10) or IR780 iodide at different concentrations (0.1, 0.2, 0.5 and 1.0 μM) was applied, and the cells were incubated at 37°C for 30 min. Fresh MEM medium was exchanged once every hour for 3 h. The cells were washed once with sterile phosphate buffered saline (PBS) for fluorescent imaging using a Nikon Eclipse 80i microscope coupled with a Hamamatsu ORCA-ER digital camera. The fluorescent images were analyzed using the MetaMorph software.

For the nuclear counterstain, DU145 cells were seeded onto a 12-mm coverslip in 6-well plate at a density of 1.5 × 10^5 cells per well for overnight. After cells were treated with or without 1 μM of camptothecin for 24 h, IR780-linker-Val-Ala-Glu(OMe)-FMK at concentrations of 0.1 or 0.5 μM was incubated with cells for 30 min at 37°C. Then the cells were washed twice with sterile PBS and subsequently incubated with 5-μg/mL DAPI in MEM for at 37°C for 5 min. Finally, the cells were washed with sterile PBS twice and imaged using the system described above.

The acute toxicity of the IR780-linker-Val-Ala-Glu(OMe)-FMK in cell culture was determined by incubating the cells with the imaging agent for 30 min and then measuring the ratio of dead to live (attached cells). DU145 cells had been seeded at 1.5 × 10^5 cells/well in a 6-well plate and allowed to attach overnight before addition of the imaging agent.

2.4. *Western blotting*

DU145 cells were treated with 1 μM of camptothecin as described in the previous section, and cell lysates were prepared with a solution of 1% Nonidet P-40, 50-mM Tris, 150-mM NaCl, APL protease inhibitors, and PMSF adjusted to pH 7.4. After treatment, floating cells were collected by aspiration, and attached cells were collected by trypsinization followed by centrifugation at 350 × g for 5 min. Cell pellets were incubated with lysis buffer on ice for 20 min and then centrifuged at 3,000 × g for 20 min at 4°C. The protein concentration was determined by BCA assay. Samples (40 μg of protein/sample) were separated by 10% polyacrylaminde gel and then transferred onto 0.45-μm nitrocellulose membrane, which was then blocked with 5% (w/v) non-fat milk in TBS and 0.1% Tween 20 (TBS/T). After washing with TBS/T, the nitrocellulose membrane was incubated with the anti-caspase-9 polyclonal antibody (diluted 1:1,000, Cell Signaling Technology #9502, Danvers, MA, USA) overnight at 4°C, followed by horseradish peroxidase-conjugated secondary antibody (diluted 1:2,000, Santa Cruz Biotechnology #sc-2004, Santa Cruz, CA, USA) for 1 h at ambient temperature. Proteins were visualized with the Western Lightening® ECL detection system from Perkin Elmer.

2.5. *TUNEL assay*

DU145 cells were treated with 1 μM of camptothecin as described in section 2.3 for 24 h and then were fixed in freshly prepared 4% paraformaldehyde in PBS, pH 7.4, for 1 h at ambient temperature. After washing with PBS, cells were permeabilized with 0.1% Triton X-100 in 0.1% sodium citrate for 2 min on ice. Cells were incubated with TUNEL reaction mixture (Roche Diagnostics, Indianapolis, IN, USA) at 37°C in a humidified atmosphere for 1 h. Samples were directly imaged under a Nikon Eclipse 80i microscope coupled with a Hamamatsu ORCA-ER digital camera at 465-495 nm excitation and 515-555 nm emission.

3. Results and Discussion

3.1. *Synthesis of the NIR fluorescent imaging agent [IR780-linker-Val-Ala-Glu(OMe)-FMK]*

We successfully synthesized the NIR fluorescent imaging agent [IR780-linker-Val-Ala-Glu(OMe)-FMK] in 11 steps with an overall yield 0.75%. The structure of each compound was determined by ^{1}H-NMR or together with APCI-MS (ESI-MS). Optically pure starting materials were used in the synthesis; however, isomers may have been introduced during the synthesis at the three chiral centers. During the purification of compound 5, only the major compound was collected, a pair of enantiomers, which resulted in the low yield of 32%. The enantiomers were not separated further before proceeding.

3.2. *Absorption and emission spectrum of IR780-linker-Val-Ala-Glu(OMe)-FMK*

The structure of IR780-linker-Val-Ala-Glu(OMe)-FMK consists of three parts: the IR780 fluorophore, the linker, and the fluoromethyl ketone of the tripeptides valine, alanine, and *O*-methyle-glutamic acid [Val-Ala-Glu(OMe)-FMK] as the reactive part to the caspase-9. IR780-linker-Val-Ala-Glu(OMe)-FMK had a maximum excitation at 650 nm (Figure 3) and emission at 729 nm respectively. By contrast, the λ_{max} of unconjugated IR780 dye was at 685 and 760 nm for excitation and emission,

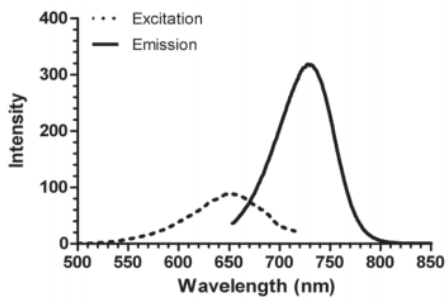

Figure 3. Excitation (dashed) and emission (solid) spectrum of IR780-linker-Val-Ala-Glu(OMe)-FMK.

respectively. The fluorescence quantum yield (Φ) was calculated as 0.75, which was determined in methanol with reference compound cresyl violet (Φ = 0.54 in methanol, (*20*)). The quantum yield is high enough to be employed as a fluorescent label in cell imaging studies.

3.3. *Camptothecin induces apoptosis via activation of caspases-9*

The caspase proteases can be activate either though the death signal-induced or stress-induced pathways. Caspase-9 is an activator of apoptosis in the mitochondrion-mediated or stress-induced pathway, wherein it subsequently activates caspases-3/6/7. Caspase-9 can be bypassed in the death signal-induced pathway when death receptors (*e.g.* TNF receptor) activate caspases-3/6/7 directly *via* caspase-10 (*21*). Camptothecin inhibits DNA synthesis and was expected to induce apoptosis *via* the caspase-9 pathway. After treatment with camptothecin, TUNEL assay indicated DNA fragmentation characteristic of apoptosis (Figure 4) and immunoblotting found cleaved caspase-9 fragments (Figure 5), which are the target of the IR780-linker-Val-Ala-Glu(OMe)-FMK imaging agent.

The normal DU145 cells had no uptake of IR780 dye in the tested concentration range (0.1-1 μM). The unconjugated IR780 dye is highly polar and cell membrane impregnable, and we did not observe nonspecific uptake of the unconjugated IR780 dye in normal or apoptotic DU145 cells (images not shown). DU145 cells undergoing apoptosis showed fluorescent signals, because IR780-linker-Val-Ala-Glu(OMe)-FMK bound to the cleaved caspase-9 induced by camptothecin, which caused it to be retained within the cells (Figures 6D, 6E, and 6F). Furthermore, counter-staining of the cells with DAPI confirmed that the IR780-linker-Val-Ala-Glu(OMe)-FMK was confined to the cytoplasm (Figure 7). The inhibition and binding of IR780-linker-Val-Ala-Glu(OMe)-FMK to cleaved caspase-9 is a result

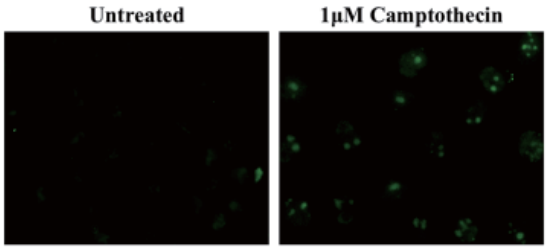

Figure 4. TUNEL assay. Apoptotic DU145 cells that have been treated with 1 μM camptothecin for 24 h were labeled by TUNEL staining of the DNA fragments. In comparison, untreated cells did not undergo apoptosis.

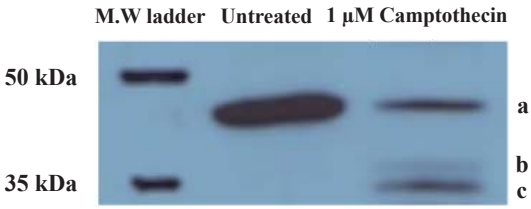

Figure 5. Western blot analysis of caspase-9 cleavage in untreated DU145 cells, or cells treated with 1-μM camptothecin for 24 h. a, full length; b, cleaved caspase-9 (37 kDa); c, cleaved caspase-9 (35 kDa).

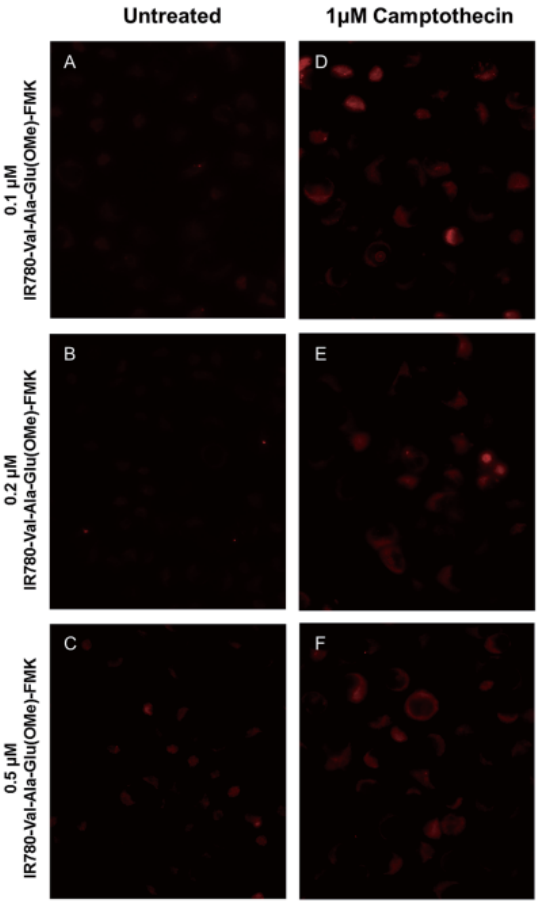

Figure 6. DU145 cell imaging after treatment with IR780-linker-Val-Ala-Glu(OMe)-FMK at concentrations of: A) 0.1 μM; B) 0.2 μM; C) 0.5 μM; IR780-linker-Val-Ala-Glu(OMe)-FMK with 1 μM of camptothecin at concentrations of: D) 0.1 μM; E) 0.2 μM; F) 0.5 μM.

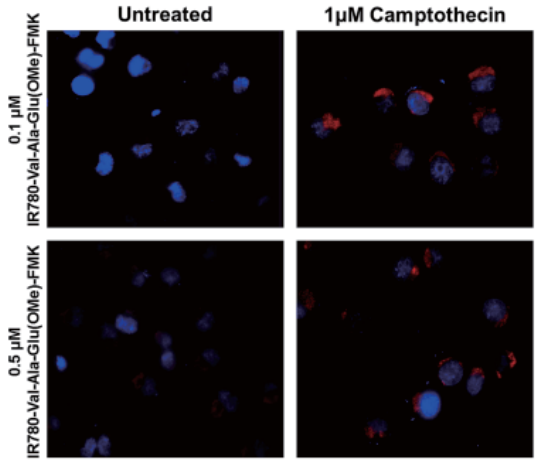

Figure 7. Fluorescent microscopic images of IR780-linker-Val-Ala-Glu(OMe)-FMK-stained DU145 cells; DAPI counter stain. The IR780-linker-Val-Ala-Glu(OMe)-FMK fluorescent label (red) is distributed within the cytoplasm of the cells.

of the peptide sequence recognition and the nucleophilic substitution of the fluoro- by a sulfhydryl group of the cysteine protease (*22*). By contrast, after untreated DU145 cells (~ 90% cell confluence) were incubated with IR780-linker-Val-Ala-Glu(OMe)-FMK, there was no accumulation of fluorescence either on the cell membrane or inside the cells at 0.1- or 0.2-μM IR780-Val-Ala-Glu(OMe)-FMK concentrations (Figures 6A and 6B). However, there was a small amount of fluorescence detected when the cells were incubated with 0.5-μM IR780-linker-Val-Ala-Glu(OMe)-FMK (Figure 6C). This was probably due to the high cell confluence (~ 90%) used for the imaging, as this non-specific binding was not observed in the cells at 60% confluency used for the DAPI counterstaining (Figure 7), and the imaging agent alone was not toxic. When the cells were incubated with the imaging agent for 30 min, there were no statistically significant differences in cell death between 0, 0.1 and 0.5 μM of agent, which resulted in 3.17 ± 0.85, 3.01 ± 1.17, and 3.34 ± 1.01% dead cells, respectively.

4. Conclusion

The synthesis of a new NIR fluorescent imaging agent [IR780-Val-Ala-Glu(OMe)-FMK] for caspase-9 was successfully accomplished in 11 steps (0.75% overall yield), which has a maxima excitation at 650 nm and emission at 729 nm. The *in vitro* cell imaging demonstrated the sensitivity of this imaging agent for caspase-9-mediated cell apoptosis. At high confluences and dye concentrations, the dye uptake lost specificity. The NIR fluorescent probe could be ideally suited for *in vivo* imaging to monitor tumor cell progress and cell apoptosis induced by chemotherapeutics.

Acknowledgements

This work was supported by awards from the National Institutes of Health (R21 CA132033) and the American Cancer Society (RSG-08-133-01-CDD). In addition, YL was partially supported by a generous exchange fellowship from the government of the People's Republic of China. QY and SD contributed equally to this work.

References

1. Bosman FT, Visser BC, van Oeveren J. Apoptosis: Pathophysiology of programmed cell death. Pathol Res Pract. 1996; 192:676-683.
2. Buttke TM, Sandstrom PA. Oxidative stress as a mediator of apoptosis. Immunol Today. 1994; 15:7-10.
3. Reed JC. Bcl-2 and the regulation of programmed cell-death. J Cell Biol. 1994; 124:1-6.
4. Sachs L, Lotem J. Control of programmed cell-death in normal and leukemic-cells: New implications for therapy. Blood. 1993; 82:15-21.
5. Vaux DL, Weissman IL, Kim SK. Prevention of programmed cell-death in caenorhabditis-elegans by human bcl-2. Science. 1992; 258:1955-1957.
6. Hanahan D, Weinberg RA. The hallmarks of cancer. Cell. 2000; 100:57-70.
7. Thompson CB. Apoptosis in the pathogenesis and treatment of disease. Science. 1995; 267:1456-1462.
8. Yuan J, Yankner BA. Apoptosis in the nervous system. Nature. 2000; 407:802-809.
9. Smith RE, Rasnick D, Burdick CO, Cho K, Rose JC, Vahratian A. Visualization of time-dependent inactivation of human-tumor cathepsin-b isozymes by a peptidyl fluoromethyl ketone using a fluorescent print technique. Anticancer Res. 1988; 8:525-529.
10. Ekert PG, Silke J, Vaux DL. Caspase inhibitors. Cell Death Differ. 1999; 6:1081-1086.
11. Yang W, Guastella J, Huang JC, Wang Y, Zhang L, Xue D, Tran M, Woodward R, Kasibhatla S, Tseng B, Drewe J, Cai SX. MX1013, a dipeptide caspase inhibitor with potent *in vivo* antiapoptotic activity. Br J Pharmacol. 2003; 140:402-412.
12. Sadhukhan R, Leone JW, Lull J, Wang Z, Kletzien RF, Heinrikson RL, Tomasselli AG. An efficient method to express and refold a truncated human procaspase-9: A caspase with activity toward Glu-X bonds. Protein Expr Purif. 2006; 46:299-308.
13. Guo YP, Kyprianou N. Restoration of transforming growth factor beta signaling pathway in human prostate cancer cells suppresses tumorigenicity *via* induction of caspase-1-mediated apoptosis. Cancer Research. 1999; 59:1366-1371.
14. Schlegel J, Peters I, Orrenius S, Miller DK, Thornberry NA, Yamin TT, Nicholson DW. CPP32/apopain is a key interleukin 1 beta converting enzyme-like protease involved in Fas-mediated apoptosis. J Biol Chem. 1996; 271:1841-1844.
15. Wang W, Ke S, Kwon S, Yallampalli S, Cameron AG, Adams KE, Mawad ME, Sevick-Muraca EM. A new optical and nuclear dual-labeled imaging agent targeting interleukin 11 receptor alpha-chain. Bioconjug Chem. 2007; 18:397-402.
16. Hilderbrand SA, Kelly KA, Weissleder R, Tung CH. Monofunctional near-infrared fluorochromes for imaging applications. Bioconjug Chem. 2005; 16:1275-1281.
17. Bouteiller C, Clavé G, Bernardin A, Chipon B, Massonneau M, Renard PY, Romieu A. Novel water-soluble near-infrared cyanine dyes: Synthesis, spectral properties, and use in the preparation of internally quenched fluorescent probes. Bioconjug Chem. 2007; 18:1303-1317.
18. Williams ATR, Winfield SA, Miller JN. Relative fluorescence quantum yields using a computer-controlled luminescence spectrometer. Analyst. 1983; 108:1067-1071.
19. Dhami S, De Mello AJ, Rumbles G, Bishop SM, Phillips D, Beeby A. Phthalocyanine fluorescence at high-concentration - dimers or reabsorption effect? Photochem Photobiol. 1995; 61:341-346.
20. Magde D, Brannon JH, Cremers TL, Olmsted J. Absolute luminescence yield of cresyl violet. A standard for the red. J Phys Chem. 1979; 83:696-699.
21. Fan TJ, Han LH, Cong RS, Liang J. Caspase family proteases and apoptosis. Acta Biochim Biophys Sin (Shanghai). 2005; 37:719-727.
22. Haberkorn U, Kinscherf R, Krammer PH, Mier W, Eisenhut M. Investigation of a potential scintigraphic marker of apoptosis: radioiodinated Z-Val-Ala-DL-Asp(*O*-methyl)-fluoromethyl ketone. Nucl Med Biol.

2001; 28:793-798.
23. Zhang HZ, Zhang H, Kemnitzer W, Tseng B, Cinatl J, Michaelis M, Doerr HW, Cai SX. Design and synthesis of dipeptidyl glutaminyl fluoromethyl ketones as potent severe acute respiratory syndrome coronovirus (SARS-CoV) inhibitors. J Med Chem. 2006; 49:1198-1201.
24. Montero A, Goya P, Jagerovic N, Callado LF, Meana JJ, Girón R, Goicoechea C, Martín MI. Guanidinium and aminoimidazolinium derivatives of *N*-(4-piperidyl)propanamides as potential ligands for mu opioid and I2-imidazoline receptors: Synthesis and pharmacological screening. Bioorg Med Chem. 2002; 10:1009-1018.
25. Unciti-Broceta A, Diezmann F, Ou-Yang CY, Fara MA, Bradley M. Synthesis, penetrability and intracellular targeting of fluorescein-tagged peptoids and peptide-peptoid hybrids. Bioorg Med Chem. 2009; 17:959-966.
26. Strekowski L, Lipowska M, Patonay G. Substitution-reactions of a nucleofugal group in heptamethine cyanine dyes. Synthesis of an isothiocyanato derivative for labeling of proteins with a near-infrared chromophore. J Org Chem. 1992; 57:4578-4580.
27. Masotti A, Vicennati P, Boschi F, Calderan L, Sbarbati A, Ortaggi G. A novel near-infrared indocyanine dye-polyethylenimine conjugate allows DNA delivery imaging *in vivo*. Bioconjug Chem. 2008; 19:983-987.

(Received June 23, 2011; Revised October 05, 2011; Accepted October 08, 2011)

Appendix

Steps of synthesis of IR780-linker-Val-Ala-Glu(OMe)-FMK.

6-Fluoro-5-hydroxy-4-nitrohexanoic acid methyl ester (compound 1). Anhydrous DMSO (1.4 mL, 19 mmol) was added dropwise to the solution of oxalyl chloride (0.9 mL, 9.6 mmol) in DCM (5 mL) at −78°C. To this solution was added 2-fluoroethanol (0.44 mL, 7.5 mmol) in DCM (2 mL). Fifteen minutes later, the reaction mixture was diluted with DCM (60 mL), followed by addition of TEA (4.4 mL, 31 mmol). The mixture was allowed to warm up to 0°C and stirred for 2 h followed by the addition of methyl 4-nitrobutyrate (0.93 g, 6.3 mmol) in DCM (5 mL). The mixture was stirred at 0°C for 3 h and then ambient temperature (ca. 20°C) overnight (*23*). The solution was concentrated and washed with ethyl acetate (EtOAc). Removal of the solvent followed by purification by silica gel column (hexanes:EtOAc = 5:1) gave the desired compound (1.0 g, 76%) as a yellow viscous oil. ^{1}H-NMR (400 MHz, $CDCl_3$): 2.40-2.45 (m, 4H), 3.69 (s, 3H), 4.20 (brs) and 4.25 (brs, 1H), 4.40-4.80 (m, 3H), 5.02 (brs) and 5.19 (brs, 1H).

4-Amino-6-fluoro-5-hydroxyhexanoic acid methyl ester (compound 2). A solution of 6-fluoro-5-hydroxy-4-nitrohexanoic acid methyl ester (compound 1, 1.15 g, 5.5 mmol) in methanol (20 mL) and acetic acid (0.5 mL) was hydrogenated with H_2 (40-45 psi) at ambient temperature for 5 h using 10% Pd/C (0.5 g) catalyst. The Pd/C was filtered off and the solvent was evaporated under reduced pressure. The desired compound was obtained as colorless viscous oil (0.92 g, yield 87%), which was used for the next step without further purification. ^{1}H-NMR (400 MHz, MeOD): 1.65-2.00 (m, 2H), 2.90-3.42 (m, 2H), 3.65 (s, 3H), 3.66-3.3.95 (m, 2H), 4.41-4.55 (m, 2H).

Boc-Val-Ala-OBn (compound 3). Boc-Val (3.0 g, 13.8 mmol), alanine benzyl ester hydrochloride salt (3.3 g, 15.3 mmol) and *O*-benzotriazole-*N*,*N*,*N'*,*N'*-tetramethyl-uronium-hexafluoro-phosphate (HBTU, 5.76 g, 15.3 mmol) were dissolved in DMF (100 mL) followed by addition of TEA (4.3 mL). The reaction was stirred at ambient temperature for 24 h and then diluted with saturated citric acid (100 mL). Then the mixture was washed with EtOAc (100 mL × 2), and the combined organic layers were washed with brine, saturated $NaHCO_3$ and brine, respectively, and then dried over Na_2SO_4. Removal of the solvent under reduced pressure followed by purification on silica gel (EtOAc:hexanes = 1:3) gave the desired compound (4.48 g, 86%) as a white solid. ^{1}H-NMR (400 MHz, $CDCl_3$): 0.93 (d, J = 7.0 Hz, 3H), 0.97 (d, J = 6.8 Hz, 3H), 1.44 (d, J = 7.2 Hz, 3H), 1.46 (s, 9H), 2.08-2.20 (m, 1H), 3.94 (t, J = 7.6 Hz, 1H), 4.62-4.69 (m, 1H), 5.08 (d, J = 8.8, 1H), 5.19 (dd, J = 12.3, 8.2 Hz, 2H), 6.44 (d, J = 5.8 Hz, 1H) , 7.32-7.44 (m, 5H).

Boc-Val-Ala-COOH (compound 4). Boc-Val-Ala-OBn (Compound 3, 5.0 g, 12.7 mmol) was dissolved in THF (100 mL), and the solution was hydrogenated with H_2 (1 atm) using 10% Pd/C catalyst (0.50 g) for 24 h. The solid Pd/C was removed by filtration, and the solvent was evaporated under reduced pressure. The desired compound was obtained as a white solid (3.4 g, 82%). ^{1}H-NMR (400 MHz, $CDCl_3$): 0.92 (d, J = 6.7 Hz, 3H), 0.96 (d, J = 6.7 Hz, 3H), 1.42-1.47 (m, 12H, overlap), 2.00-2.11 (m, 1H), 4.01 (t, J = 8.0 Hz, 1H), 4.57 (t, J = 7.0 Hz, 1H), 5.51 (brs, 1H), 7.04 (brs, 1H), 9.66 (brs, 1H).

4-(Boc-Val-Ala-amido)-6-fluoro-5-hydroxylhexanoic acid methyl ester (compound 5). Boc-Val-Ala-COOH (compound 4, 1.0 g, 3.5 mmol), 4-dimethylaminopyridine (DMAP, 0.25 g, 1.9 mmol), and *N*-(3-dimethylaminopropyl)-*N*-ethylcarbodiimide hydrochloride (EDAC, 0.74 g, 3.9 mmol) were dissolved in anhydrous THF (10 mL) at ambient temperature. After 10 min a solution of 4-amino-6-fluoro-5-hydroxyhexanoic acid methyl ester (compound 2, 0.69 g, 3.9 mmol) in anhydrous THF (10 mL) was added directly to the above solution, and the reaction was stirred at ambient temperature overnight. The solvent was removed under reduced pressure, and the residue was dissolved in EtOAc, washed with saturated $NaHCO_3$, brine, and citric

acid, respectively. The organic layer was dried with Na_2SO_4, and the product was purified over silica gel (EtOAc:hexanes = 3:1) to give the desired compound as a white solid (0.5 g, 32%). APCI -MS: [M + 1] = 450.3, [M + 1-C_4H_8] = 394.2, [M-Boc] = 350.2. ^{1}H-NMR (400 MHz, $CDCl_3$): 0.95 (d, *J* = 7.0 Hz, 3H), 0.98 (d, *J* = 6.6 Hz, 3H), 1.40 (d, *J* = 7.6 Hz, 3H), 1.45 (s, 9H), 1.85-1.97 (m, 2H), 2.08-2.18 (m, 1H), 2.41 (t, *J* = 7.2 Hz, 2H), 3.69 (s, 3H), 3.83-3.95 (m, 1H), 3.96-4.10 (m, 1H), 4.29-4.55 (m, 3H), 6.54 (brs, 1H), 6.58 (brs, 1H).

4-(Boc-Val-Ala-amido)-6-fluoro-5-oxohexanoic acid methyl ester (compound 6). A solution of compound 5 (0.898 g, 2.0 mmol) in DCM (20 mL) was treated with Dess-Martin periodinane solution (20 mL, 0.3 M in DCM). The reaction mixture was stirred at ambient temperature for 12 h. The solvent was removed under reduced pressure, and the crude product was purified by silica gel chromatography (EtOAc:hexanes = 1:1) to give the desired compound as a white solid (0.749 g, 81%). APCI-MS: [M + 1] = 448.3, [M + 1-C_4H_8] = 392.2, [M-Boc] = 348.2. ^{1}H-NMR (400 MHz, $CDCl_3$): 0.95 (d, *J* = 7.0 Hz, 3H), 0.99 (d, *J* = 6.6 Hz, 3H), 1.40 (d, *J* = 7.6 Hz, 3H), 1.45 (s, 9H), 1.88-1.96 (m, 2H), 2.12-2.22 (m, 1H), 2.43 (t, *J* = 7.2 Hz, 2H), 3.68 (s, 3H), 3.87-3.99 (m, 1H), 4.46-4.59 (m, 1H), 5.09-5.21 (m, 2H), 6.76 (brs, 1H), 7.37 (brs, 1H).

4-(Val-Ala-amido)-6-fluoro-5-oxohexanoic acid methyl ester [Val-Ala-Glu(OMe), compound 7]. A solution of 4-M HCl in anhydrous EtOAc (20 mL) was cooled to 0°C, 4-(Boc-Val-Ala-amido)-6-fluoro-5-oxohexanoic acid methyl ester (compound 6, 0.749 g, 1.62 mmol) was added, and the mixture was stirred at ambient temperature overnight. Collection of the precipitated solid followed by washing with EtOAc (50 mL) gave a pale yellow solid (0.564 g, quantitative yield), which was used for the next step without further purification.

4-(4-(Tert-butoxycarbonyl)ethylamino)-4-oxobutanoic acid (Boc-linker, compound 8). Mono-Boc-protected butane-1,4-diamine (2.82 g, 15 mmol; prepared according to previous reports (*24,25*)) in 10 mL of dioxane was added slowly to a solution of succinic anhydride (1.5 g, 15 mmol) in 10 mL of dioxane and then stirred at 80°C for 3 h. Removal of the solvent followed by purification of the residue through silica gel chromatography (EtOAc:hexanes:acetic acid = 50:5:1) gave the desired compound as a white solid (2.64 g, 63%). ^{1}H-NMR (400 MHz, MeOD): 1.46 (s, 9H), 1.46-1.57 (m, 4H), 2.39-2.50 (m, 2H), 2.55-2.67 (m, 2H), 3.06 (t, *J* = 4.6 Hz, 2H), 3.19 (t, *J* = 6.5 Hz, 2H), 6.53 (brs, 1H), 7.90 (brs, 1H), 12.10 (brs, 1H).

Boc-linker-Val-Ala-Glu(OMe)-FMK (compound 9). To a solution of compound 8 (1.44 g, 5.0 mmol) in THF (30 mL) was added *N*-(3-dimethylaminopropyl)-*N*-ethylcarbodiimide hydrochloride (EDCI, 0.96 g, 5.0 mmol), 1-hydroxybenzotriazole (HOBt; 0.68 g, 5.0 mmol), and 4-dimethylaminopyridine (DMAP) (0.31 g, 2.5 mmol). The mixture was stirred for 10 min at ambient temperature followed by the addition of compound 7 (2.24 g, 5.0 mmol) in THF (15 mL). The mixture was stirred at ambient temperature overnight. After removing the solvent under reduced pressure, the residue was diluted with EtOAc (100 mL) and washed with brine (50 mL). The organic layer was dried over sodium sulfate the solvent was removed under reduced pressure. Purification of the residue by silica gel chromatography (EtOAc:MeOH = 20:1) gave the desired compound as a yellow solid (1.17 g, 38%). APCI-MS: [M + 1] = 618.7, [M-Boc] = 518.5. ^{1}H-NMR (400 MHz, $CDCl_3$): 0.95 (d, *J* = 7.0 Hz, 3H), 0.99 (d, *J* = 6.6 Hz, 3H), 1.40 (d, *J* = 7.6 Hz, 3H), 1.46 (s, 9H), 1.47-1.55 (m, 4H), 1.67-1.78 (m, 2H), 2.14-2.26 (m, 1H), 2.39-2.50 (m, 4H), 2.55-2.68 (m, 2H), 3.07 (t, *J* = 4.7 Hz, 2H), 3.20 (t, *J* = 6.4, 2H), 3.68 (s, 3H), 4.08-4.20 (m, 1H), 4.45-4.58 (m, 1H), 4.48-4.59 (m, 1H), 4.99-5.30 (m, 2H), 6.19 (brs, 1H), 6.50 (brs, 1H), 7.45 (brs, 1H), 7.53 (brs, 1H), 7.56 (brs, 1H).

IR780-linker-Val-Ala-Glu(OMe)-FMK (compound 10). To a solution of Boc-linker-Val-Ala-Glu(OMe)-FMK (compound 9, 0.46 g, 0.75 mmol) in dry DMF (5 mL) was added a solution of 4-M HCl/EtOAc (10 mL) at 0°C. The mixture was stirred for 12 h at ambient temperature, followed by the addition of TEA (55 µL, 0.75 mmol) and IR780 iodide (0.1 g, 0.15 mmol) in dry DMF (5 mL) (*26,27*). The mixture was then heated to 85°C and stirred continuously for 24 h in the dark. Removal of the solvent followed by purification of the obtained residue through silica gel chromatography ($CHCl_3$:MeOH = 50:1) gave the desired compound as a blue solid (0.038 g, 25%). ESI-MS: [M^+ + 1] = 1022.3. ^{1}H-NMR (400 MHz, DMSO-d_6): 0.95 (d, *J* = 7.0 Hz, 3H), 0.98 (d, *J* = 6.6 Hz, 3H), 1.03-1.07 (m, 6H), 1.32-1.41 (m, 2H), 1.42-1.51 (m, 5H), 1.52-1.57 (m, 4H), 1.59-1.70 (m, 15H), 1.71-1.76 (m, 4H), 2.07-2.15 (m, 2H), 2.18-2.27 (m, 1H), 2.34 (t, *J* = 7.2 Hz, 2H), 2.49 (t, *J* = 6.8 Hz, 2H), 2.57 (t, *J* = 6.8 Hz, 2H), 2.83 (t, *J* = 7.5 Hz, 4H), 2.89 (t, *J* = 6.8 Hz, 2H), 3.05 (t, *J* = 6.8 Hz, 2H), 3.64 (s, 3H), 3.79 (t, *J* = 6.8, 2H), 3.94 (t, *J* = 7.2 Hz, 2H), 4.10-4.20 (m, 1H), 4.26-4.37(m, 1H), 4.48-4.56 (m, 1H), 5.13-5.25 (m, 2H), 5.86 (d, *J* = 13.0 Hz, 2H), 7.06-7.15 (m, 4H), 7.29-7.36 (m, 1H), 7.62-7.71 (m, 1H), 7.77 (d, *J* = 13.0 Hz, 2H), 8.13-8.25 (m, 2H).

Original Article

DOI: 10.5582/ddt.2011.v5.5.227

Design, synthesis, anticonvulsant screening and $5HT_{1A/2A}$ receptor affinity of *N*(3)-substituted 2,4-imidazolidinediones and oxazolidinediones

Meenakshi Dhanawat, Nirupam Das, Sushant Kumar Shrivastava*

Department of Pharmaceutics, Institute of Technology, Banaras Hindu University, Varanasi, India.

ABSTRACT: In the present study, a series of *N*(3)-substituted 2,4-imidazolidinediones and oxazolidinediones derivatives (1-16) were synthesized and tested for anticonvulsant activity using the maximal electroshock seizure test. Affinity towards receptor (5-$HT_{1A/2A}$) was also studied. Their neurotoxicity was determined using the rotarod test. Structures of compounds were confirmed by spectroscopic methods. Compounds 1, 2, 5, 7, 9, and 10 exhibited significant anticonvulsant activity as compared to the standard drug phenytoin. Affinity toward receptor (5-$HT_{1A/2A}$) was studied *in vivo* for compounds 1, 2, 5, 7, 9, and 10. Rectal body temperature, lower lip retractions and head twitch responses in Wistar rats/albino mice were determined for this purpose. The tested compounds showed affinity for 5-HT_{1A} and 5-HT_{2A} receptors (agonists/antagonists and presynaptic/postsynaptic). Replacement of piperazine by aniline derivatives provides good outcomes in terms of affinity for 5-$HT_{1A/2A}$.

Keywords: Epilepsy, anticonvulsant, acetamide, phenytoin, oxazolidine-2,4-dione, aniline, piperazine

1. Introduction

Serotonin (5-HT) plays an important role in many physiological and pathophysiological processes in the brain (*1*). The link between 5-HT and the inhibition of epilepsy was suggested by Bonnycastle (*2*). They demonstrated that a series of anticonvulsants raise the brain 5-HT level. Serotonergic neurotransmission modulates a wide variety of experimentally induced seizures and is involved in the enhanced seizure susceptibility observed in rodents genetically prone to epilepsy (*3*). Welsh *et al*. observed in their study that the rat model of myoclonic epilepsy is associated with a profound loss of 5-HT throughout the brain (*4*). Drugs *viz*. valproic acid, lamotrigine, carbamazepine, phenytoin, and zonisamide are found to stimulate basal 5-HT levels, as part of their anticonvulsant action. Generally, agents that elevate the extracellular 5-HT levels, such as 5-hydroxytryptophan and serotonin reuptake blockers, inhibit both focal and generalized seizures (*5*).

The 5-HT_{1A} receptors are to date one of the best characterized subtypes and it is generally accepted that they are involved in psychiatric disorders such as depression and anxiety. Several compounds from different chemical classes possess high affinity for 5-$HT_{1A/2A}$ receptors. Among them, 5-HT_{1A} receptor partial agonists and 5-HT_{2A} receptor antagonists are of particular interest, since clinical studies indicate that these drugs are effective in treating mood disorders. Consequently, it has been suggested that compounds which interact simultaneously with 5-HT_{1A} and 5-HT_{2A} receptors may have a more advantageous therapeutic profile.

Autoradiographic analysis of 5-HT receptors in fully kindled rat brain showed a selective increase in 5-HT_{1A} binding in the dentate gyrus. These findings suggest that 5-HT_{1A} receptors may have an inhibitory role in the generation of hippocampal seizures. According to the studies by Gariboldi *et al.*, intrahippocampal or systemic administration of 8-hydroxy-*N,N*-dipropyl-2-aminotetralin (8-OH-DPAT), a specific 5-HT_{1A} receptor agonist, to rats resulted in protective effects against seizure activity induced in the hippocampus by kainic acid (*6*). Several classes of compounds are known to bind to 5-HT_{1A} receptor sites. Among them, 4-arylpiperazines that are linked to a terminal cyclic amide *via* a long chain are effective as antianxiety and antidepressant drugs (*7*). It has also been found that stimulation of 5-HT_2 receptors is linked to the anticonvulsant action of some methylphenylpiperazine derivatives (5-HT_{2A}/5-HT_{2C}) in an animal maximal electroshock seizure (MES) test (*8,9*). Presently the effectiveness of antiepileptic drugs (AEDs) in reducing the severity and number of seizures is less than 70%. Moreover the treatment is coupled with adverse side effects ranging from cosmetic (gingival hyperplasia) to life threatening

**Address correspondence to:*
Dr. S. K. Shrivastava, Department of Pharmaceutics, Institute of Technology, Banaras Hindu University, Varanasi-221005, India.
e-mail: skshrivastava.phe@itbhu.ac.in; mdanawat.rs.phe@itbhu.ac.in

(hepatotoxicity, megaloblastic anemia) (*10-12*).

One of the structures among the compounds studied for anticonvulsant activity is the acetamide and propionamide nucleus. Ameltolide (*13*), ralitoline (*14*), and some phthalimide derivatives (*15*) are the best examples with potent anticonvulsant activity in the MES test (Figure 1). Ameltolide was developed by Eli Lilly (Indianapolis, IN, USA), which originated from the approach of Clark *et al*. This research group isolated the 4-aminobenzamide pharmacophore, which subsequently led to the design of a number of new and potent anticonvulsant agents (*16-20*). Apart from the acetamide and propionamide nucleus, hydantoin and oxazolidine-2,4-dione are also one of the most commonly used antiepileptic pharmacophores. Many heterocyclic compounds attached to piperazine *via* an alkyl linkage have already been proved as potent anticonvulsants by many scientists (*21-23*). The molecules contain 5- or 6-member heterocyclic rings, one or two carbonyl groups as well as a required aromatic system which was confirmed by the structure-activity relationship studies of clinically available AEDs and other anticonvulsant active compounds. Many studies on the structure-affinity relationship of the 1-arylpiperazineclass of 5-HT_{1A} receptor ligands have been reported (*24,25*). Misztal *et al*. (*26*) assumed that the terminal amide fragment in buspirone-like ligands stabilized the 5-HT_{1A} receptor-ligand complex by either *p*-electron or local dipole-dipole interaction.

Based on the above findings, in the present study our interest was focused to target the 5-$HT_{1A/2A}$ receptor. Herein derivatives of 5-phenyloxazolidine-2,4-dione and 5,5-diphenyl hydantoin (these moieties are already well established prototypes for antiepileptic drugs) attached to piperazine and aniline derivatives *via* an acetamide linkage (*18,20*) have been synthesized. Various electron donating and electron-attracting groups in the *para* position of aniline and piperazine were synthesized. Compound **4** (*p*-tolyl-acetamide derivative of 2,4-imidazolidinedione) reported earlier for anticonvulsant activity (*27*) has been included in the present study for the purpose of comparison with other synthesized compounds. Based on potency-structure relationships, we designed analogues related to ameltolide and hydantoin/oxazolidinedione. The synthesized compounds were evaluated for anticonvulsant, neurotoxicity and $5HT_{1A/2A}$ *in vivo* receptor affinity.

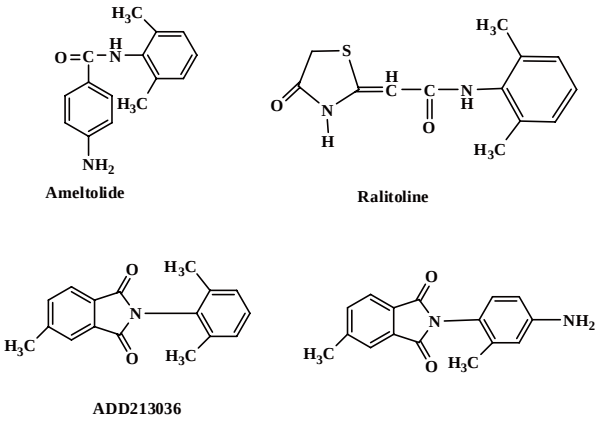

Figure 1. Potent anticonvulsant compounds bearing anilide (acetamide linkage) function.

2. Materials and Methods

All the substituted aniline and piperazine derivatives, 8-OH-DPAT, WAY 100653 (*N*-[2-[4-(2-methoxyphenyl)piperazin-1-yl]ethyl]-*N*-pyridin-2-yl-cyclohexanecarboxamide trihydrochloride), (±)-DOI ((±)-1-(2,5-dimethoxy-4-iodophenyl)-2-aminopropane), ketanserine were purchased from Sigma-Aldrich Chemicals Pvt. Ltd. (St. Louis, MO, USA) and solvents were purchased from Merck (Darmstadt, Germany) and were used without further purification. The purity of the compounds was confirmed by thin-layer chromatography (TLC) performed on Merck silica gel 60 F254 aluminium sheets (Merck), using various developing systems. Spots were detected by their absorption under UV light (λ = 254 nm) and by visualization with I_2. The ^1H and ^{13}C NMR spectra were recorded on a Bruker Avance DPX (300 MHz) spectrometer. Chemical shifts are reported in parts per million units relative to Tetramethylsilane (TMS) used as an internal standard. Coupling constants (*J*) are reported in Hertz (Hz). The infrared spectras were generated using a Shimadzu 8300 FTIR Spectrophotometer using KBr pellets and the nujol mull method. Spectral outputs were recorded either in absorbance or in transmittance mode as a function of wave number. The spectrum was collected from 4,000 to 400 cm^{-1}. Mass spectra were analyzed on a Finnigan MAT LCQ (APCI). Elemental analysis was carried out on EXTER analytical inc. CE-440 Elemental analysis, autosampler. Melting points (M.P.) were determined in open capillaries on a STUART SMP10, UK and are uncorrected. Signal multiplicities are represented by the following abbreviations: s (singlet), b (broad singlet), d (doublet), dd (doublet of doublets), t (triplet), q (quartet), m (multiplet).

2.1. *Chemistry*

In the present investigation a new series of *N*(3)-substituted 2,4-imidazolidinediones and oxazolidinediones derivatives (Scheme 1, Figure 2) were synthesized using procedures explained in the literature (*28-30*). All the compounds were synthesized by classic two-step methods as illustrated in Scheme 1 (Table 1). In the first step, reacting 2-chloroacetylchloride with appropriately substituted anilines and piperazine yielded acetamide derivatives (**1a-8a**). In the second step, those intermediates were condensed with 5,5-diphenyl hydantoin and 5-phenyl oxazolidine-2,4-dione to furnish the title compounds **1-6**, **7**, **8** and **9-14**, **15**,

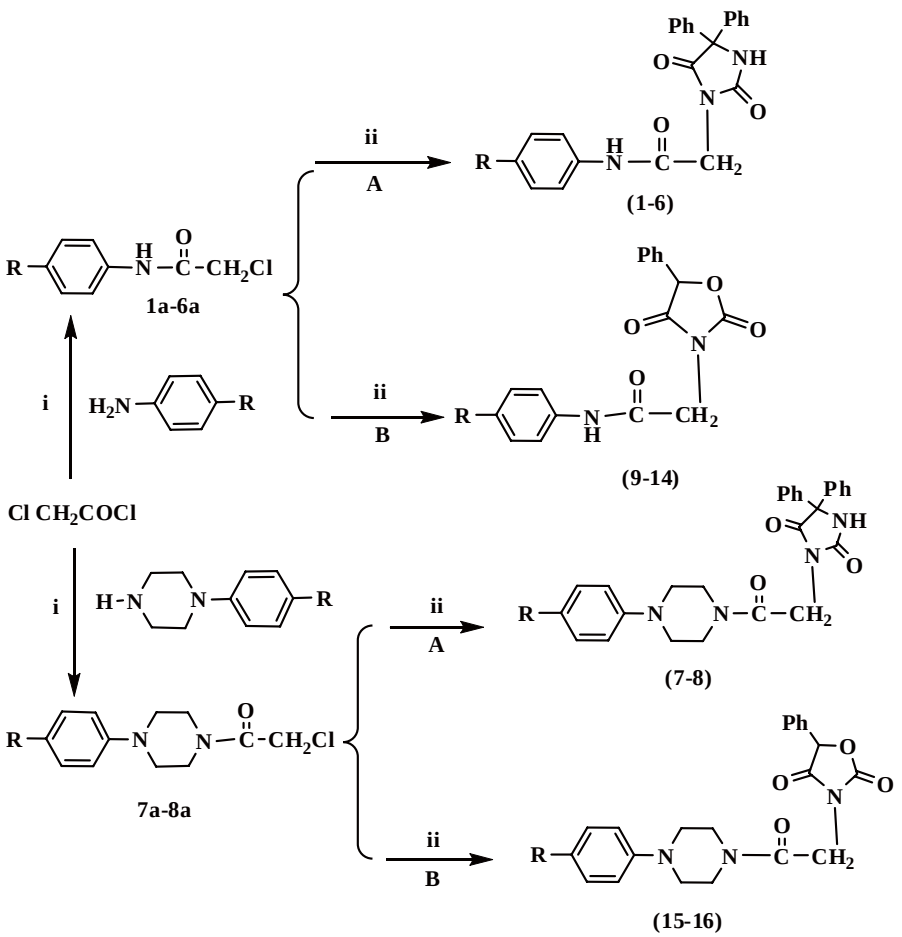

A= 5, 5-diphenyl hydantoin; B=5-phenyl oxazolidine-2,4 dione

Scheme 1. Synthesis of the compounds: (*i*) Glacial acetic acid, ice bath (30 min)-RT (1 h); (*ii*) DMF; reflux.

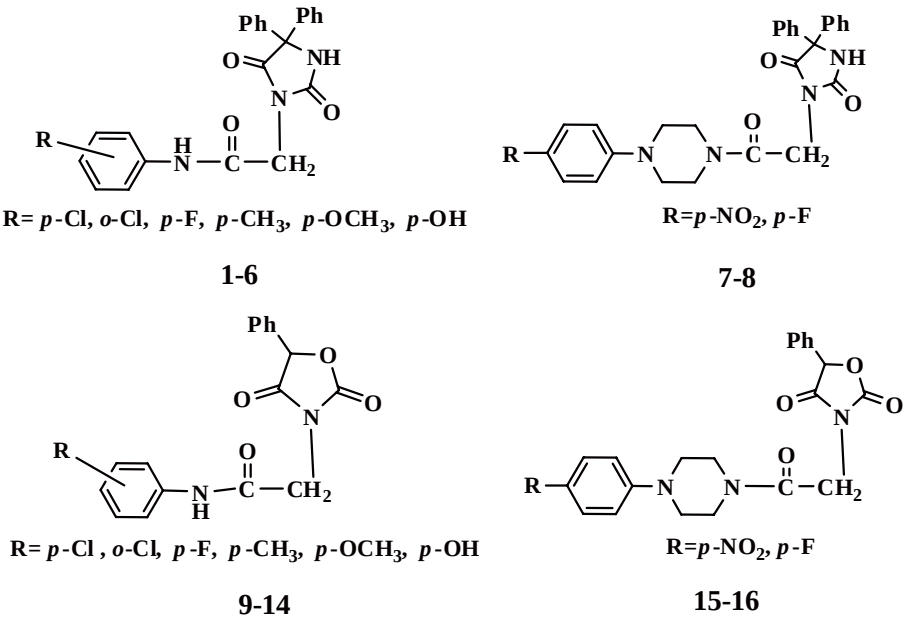

Figure 2. Chemical structures of the synthesized compounds.

Table 1. Structures and physicochemical data of compounds

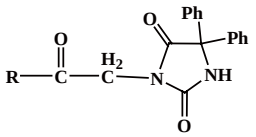

1-8

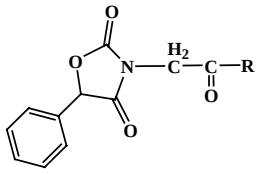

9-16

No.	R	Formula	Yield in %	Mol wt (calc)
1	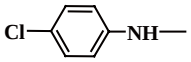	$C_{23}H_{18}ClN_3O_3$	55	419.86
2	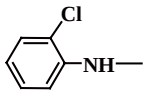	$C_{23}H_{18}ClN_3O_3$	57	419.86
3	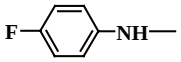	$C_{23}H_{18}FN_3O_3$	60	403.41
4	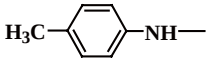	$C_{24}H_{21}N_3O_3$	45	399.44
5	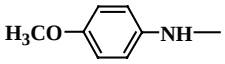	$C_{24}H_{21}N_3O_4$	54	415.44
6	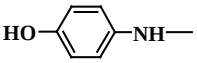	$C_{23}H_{19}N_3O_4$	60	401.41
7	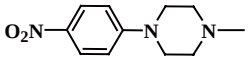	$C_{27}H_{25}N_5O_5$	58	499.52
8	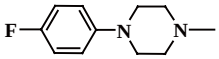	$C_{27}H_{25}FN_4O_3$	62	472.51
9	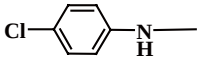	$C_{17}H_{13}ClN_2O_4$	55	344.75
10	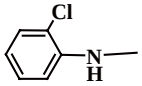	$C_{17}H_{13}ClN_2O_4$	56	344.75
11	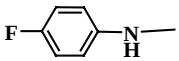	$C_{17}H_{13}FN_2O_4$	45	328.29
12	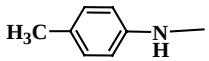	$C_{18}H_{16}N_2O_4$	45	324.33
13	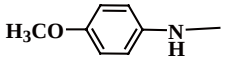	$C_{18}H_{16}N_2O_5$	45	340.33
14	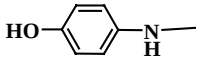	$C_{17}H_{14}N_2O_5$	40	326.30
15	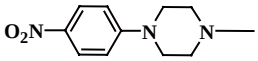	$C_{21}H_{20}N_4O_6$	50	424.14
16	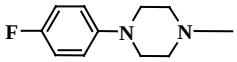	$C_{21}H_{20}FN_3O_4$	53	397.40

16, respectively. 5-Phenyl oxazolidine-2,4-dione and 5,5-diphenyl hydantoin were synthesized in the lab using reported procedures (*31-34*). The title compounds were evaluated for anti-MES activity, neurotoxicity and *in vivo* receptor affinity for 5-$HT_{1A/2A}$.

2.1.1. *Synthesis of acetamide derivatives (**1a-8a**)*

Intermediates were prepared according to methods reported in the literature (*28-30*). For this purpose, appropriately substituted aniline/piperazine (0.066 mol)

was dissolved in 25 mL glacial acetic acid. 2-Chloroacetyl chloride (0.074 mol) was added dropwise to this solution while cooling in an ice-bath. The reaction mixture was stirred in an ice-bath for 0.5 h followed by 1 h at room temperature. The mixtures were poured into saturated sodium acetate solution. Obtained precipitates were filtered off and washed with cold water and purified by recrystallization from ethanol/water.

2.1.2. *General procedure for the synthesis of compounds* ***(1-16)***

Acetamide derivatives (0.002 mol) (**1a-8a**) and 5,5-diphenyl hydantoin (A)/5-phenyl oxazolidine-2,4-dione (B) (0.01 mol) in 20 mL *N,N*-dimethylformamide (DMF) were refluxed. The reaction was terminated, using monitoring of products with TLC. The reaction mixture was poured into cold water. The precipitates were filtered off and washed with water. After drying, the precipitate was purified by crystallization from ethanol. The physicochemical data of compounds are reported in Table 1.

2.2. *Pharmacology*

2.2.1. *MES*

Banaras Hindu University, Institute of Medical Sciences, Institutional Animal Ethical Committee (IAEC), approved all experiments for animal testing. MES is recognized as the 'gold standard' in the early stages of testing (*35*). Male albino mice (25-35 g) and Wistar rats (200-250 g) of either sex were used. Laboratory temperature was maintained at 20 ± 1°C under conditions of a 12 h light and dark schedule. Before experimentation, animals were allowed 1 week of adaptation. Food was withdrawn 12-15 h before commencing the experiment, while water was withdrawn immediately before the experiment. Each group consisted of 6 animals per dose. Each animal was used once.

The compounds were administered orally (suspension in a 1% Tween 80/water mixture) and intraperitoneally (suspension in 0.5% methylcellulose). The rotarod test was carried out to determine minimal neurotoxicity before the experiments.

The anticonvulsive activity of the compounds was evaluated by defining the abolition of the hind-leg tonic maximal extension component of the seizure (*36*). Maximal seizure is induced by application of an electrical current across the brain through corneal electrodes. The stimulus parameters are 50 mA, AC in a pulse of 60 Hz for 200 Ms (0.2 sec). After applying shock, mice/rats were observed for the type of convulsion produced and the hind limb extensor response was taken as the end point. Animals were tested at 0.5 and 4 h after administration of compounds. The animals that showed a positive hind limb extensor response were used for testing drug substances.

2.2.2. *Neurotoxicity test*

A neurological toxicity test (TOX) induced by a compound was detected in mice using the standardized rotarod test. Untreated control mice, when placed on a 6 rpm rotation rod, can maintain their equilibrium for a prolonged period of time. Neurological impairment is demonstrated by the inability of mice to maintain equilibrium for 1 min in each of three successive trials.

2.2.3. *In vivo receptor binding studies*

All drug solutions were prepared in a 1% aqueous solution of Tween 80 and were freshly prepared before use [Investigated compounds: 8-OH-DPAT, WAY 100653, (±)-DOI, and ketanserine]. 8-OH-DPAT and WAY 100653 were injected subcutaneously (*s.c.*), and (±)-DOI was given intraperitoneally (*i.p.*). The data obtained were analyzed by one-way analysis of variance followed by Dunnet's test. All scoring were carried out by an observer who was unaware of the specific drug treatment. Male albino mice (25-35 g) and Wistar rats (200-250 g) of either sex, were used. Groups consisted of 6-8 animals per dose.

2.2.3.1. *Lower lip retraction (LLR)*

The LLR was assessed according to the method described by Berendsen *et al.* (*38*). The rats were individually placed in cages and were scored three times (at 15, 30, and 45 min) after the administration of the tested compounds or 8-OH-DPAT (0 = lower incisors not visible, 0.5 = partly visible, 1 = clearly visible). The total maximum score amounted to 3/rat. In a separate experiment, the effect of the investigated compounds or WAY 100635 on LLR induced by 8-OH-DPAT (1 mg/kg) was tested. The investigated compounds or WAY 100635 were administered 45 and 15 min, respectively, prior to 8-OH-DPAT, and the animals were scored 15, 30, and 45 min after 8-OH-DPAT administration.

2.2.3.2. *Rectal body temperature of rats*

8-OH-DPAT (5 mg/kg) decreases rectal body temperature in rats. Effects of tested compounds given alone on rectal body temperature of rats (measured with an Ellab thermometer) were recorded 30, 60, 90, and 120 min after administration and compared with the effect of WAY 100635 (0.1 mg/kg). Results were expressed as change in body temperature (Δt) compared to basal body temperature, as measured at the beginning of the experiment. Compounds were administered 45 min prior to 8-OH-DPAT.

2.2.3.3. *Head twitch method*

In order to habituate the rats to the experimental

environment, each animal was randomly transferred to a cage, 30 min before injection of the compound (±)-DOI or vehicle. Head twitches were induced in mice by (±)-DOI (2.5 mg/kg). Immediately after treatment, head twitches (rapid right and left movements of the head with little or no involvement of the trunk) were counted for 20 min (*37*). The investigated compounds were administered 60 min before (±)-DOI. Their 5-HT_{2A} antagonistic activity was compared to ketanserin (ID_{50} = 0.14 mg/kg), a well-known 5-HT_{2A} receptor antagonist.

3. Results and Discussion

3.1. *Chemistry*

In this study, sixteen new *N*(3)-substituted 2,4-imidazolidinediones and oxazolidinediones derivatives were synthesized to evaluate anticonvulsant activity using the MES test. Chemical structures of title compounds were confirmed by elemental analysis, ^{1}H, ^{13}C NMR, IR and mass spectra data. Intermediates (compounds **1a-16a**) were verified by FT-IR spectra (spectra not shown).

IR spectra of compounds shows N-H and C=O stretching bands in the region of 3,486-3,112 cm^{-1} and 1,620-1,680 cm^{-1} respectively, indicating the presence of an -CONH-. Nitro groups show two intense peaks, one is in the range of 1,300-1,400 cm^{-1} for the symmetric stretching mode while the other one is 1,500-1,600 cm^{-1} for the asymmetric stretching mode. The -OH group has a distinct peak at 3,550-3,600 cm^{-1}. The strong bands in the 3,000-2,850 cm^{-1} regions are due to C-H stretch. In the acetamide series, ^{1}H NMR spectra confirmed the presence of expected proton signals with relevant splitting patterns and integrations. The chemical shifts and splitting patterns of protons in each compound differed depending on the nature of the substituent and substitution patterns. The compounds were further verified by mass spectral analyses where the molecular ion peaks were in complete agreement with the calculated molecular weight for individual compounds. The compounds having chloro substituent (compounds **1**, **2**, **9**, **10**) have relatively small molecular ions whereas the $[M\text{-}Cl]^{+}$ ions derived by loss of chlorine were more intense. C, H, N and O determinations were found to be within range.

3.2. *Anticonvulsant activity*

3.2.1. *MES & Rota- Rod test*

The anticonvulsant activity for all synthesized compounds was established by the MES tests after intraperitoneal injection (*i.p.*) to mice at doses of 30, 100, and 300 mg/kg. The neurotoxicity (NT) was determined by the minimal motor impairment-rotarod screening. Preliminary screening results indicated that some of the title compounds have diversified anti-MES activity.

Compound **1**, **2**, **5**, **7**, **9**, and **10** showed protection against MES and in addition they were devoid of neurotoxicity. While compounds **3**, **4**, **11**, **12**, **13**, and **16** are active but also impart neurotoxicity and compounds **6**, **8**, **14**, and **15** were inactive. All results are presented in Table 2.

On the basis of obtained data in *i.p.* MES screening in mice and according to the anticonvulsant screening project (ASP) procedure selected, compounds (**1**, **2**, **5**, **7**, **9**, and **10**) were evaluated orally in rats at doses of 30 mg/kg for two different time intervals (0.5 and 4 h) for both anticonvulsant and neurotoxic properties (Table 3) (*39*).

Compounds **1** and **9** were found to be the most active among all synthesized ones with dose levels of 30 and 100 mg/kg for 4 h, while others (**2**, **5**, **7**, and **10**) were active at high dose levels (100/300 mg/kg). Compound **3**, **4**, **11**, **12**, **13**, and **16** are also active but suffer from neurotoxicity and therefore these compounds will not be considered for further study. Compounds **6**, **8**, **14**,

Table 2. Evaluation of all synthesized compounds in MES tests after intraperitonial injection (30, 100, 300 mg/kg) to mice (Phase 1)

No.	MES (h)[a]		NT (h)[b]	
	0.5	4	0.5	4
1	30	100	-	-
2	-	100	-	-
3	100	300	100	-
4	100	-	100	-
5	100	300	-	-
6	-	-	-	-
7	100	300	-	-
8	-	-	-	-
9	30	100	-	-
10	100	300	-	-
11	100	300	-	100
12	30	100	-	100
13	100	300	100	-
14	-	-	-	-
15	-	-	-	-
16	-	300	100	300
Phenytoin	30	30	100	100

[a] Maximal electroshock seizure test (h, hours); [b] Neurotoxicity (Determined by rotarod).

Table 3. Evaluation of compounds 1, 2, 5, 7, 9, 10 in MES tests after oral administration (30 mg/kg) to rats (Phase 6a)

No.	MES (h)[a]		NT (h)[b]	
	0.5	4	0.5	4
1	1/6	4/6	0/6	0/6
2	0/6	3/6	0/6	0/6
5	2/6	4/6	0/6	0/6
7	3/6	4/6	0/6	0/6
9	2/6	4/6	0/6	0/6
10	2/6	3/6	0/6	0/6
Phenytoin	6/6	5/6	-	-

[a] MES test (number of animals protected/number of animals tested); [b] Neurotoxicity (number of animals exhibiting toxicity/number of animals tested).

and **15** were found to be inactive in this test and were also excluded from further consideration. Some of the compounds (**3**, **4**, **11**, **12**, **13**, and **16**) were found to be neurotoxic according to the rotarod test. Preliminary screening results are presented in Tables 2 and 3.

3.2.2. *In vivo receptor binding studies*

Compounds, which are active in MES and devoid of neurotoxicity were further considered for *in vivo* receptor binding studies (Tables 4-7). Various animal models were used for estimation of receptor affinity for 5-HT_{1A} (*i*) rectal body temperature (measured with an Ellab thermometer), (*ii*) lower lip retraction in rats were recorded, while (*iii*) head twitches were recorded in mice for the determination of probable affinity towards 5-HT_{2A} receptors (*37,40*). The standards used in the study are 8-OH-DPAT (5-HT_{1A} agonist), WAY 100653 (5-HT_{1A} antagonist), (±)-DOI (5-HT_{2A} agonist), and ketanserine (5-HT_{2A} antagonist).

In the presynaptic model, compounds which produced hypothermia like 8-OH-DPAT (5-HT_{1A} agonist) were considered as presynaptic agonists and *vice versa*. Among the tested one, **2**, **7**, and **9** produced hypothermia while **1**, **5**, and **10** were not active in the test. In another experiment induction of lower lip retraction was studied using 8-OH-DPAT compared to WAY 100635 (5-HT_{1A} antogonist). Compounds **1**, **2**, and **9** served as post synaptic agonist while **5**, **7**, and **10** were found to be antagonist. To estimate affinity toward 5-HT_{2A} receptors the head twitch method was used. Like ketanserin, a reference 5-HT_{2A} receptor antagonist

Table 4. The effect of the investigated compounds and WAY 100635 on the body temperature in rats

Treatment	Dose (mg/kg)	Δt SEM			
		30 min	60 min	90 min	120 min
Vehicle	-	-0.1 ± 0.1	0.0 ± 0.1	-0.2 ± 0.1	0.0 ± 0.1
1	10	-0.7 ± 0.2	-0.7 ± 0.1	-0.8 ± 0.2	-0.7 ± 0.2
	20	-1.8 ± 0.3	-1.8 ± 0.3	-1.6 ± 0.2	-1.7 ± 0.2
2	10	-0.6 ± 0.1	-0.8 ± 0.1	-0.9 ± 0.3	-1.9 ± 0.2
	20	-2.0 ± 0.1	-2.5 ± 0.2	-2.9 ± 0.1	-1.5 ± 0.1
5	10	-0.5 ± 0.1	-0.6 ± 0.2	-0.6 ± 0.1	-0.6 ± 0.1
	20	-1.2 ± 0.3	-1.1 ± 0.2	-1.2 ± 0.2	-1.1 ± 0.1
7	10	-0.4 ± 0.2	-0.8 ± 0.1	-0.9 ± 0.2	-0.6 ± 0.3
	20	-1.5 ± 0.3	-1.7 ± 0.1	-1.9 ± 0.1	-1.5 ± 0.1
9	10	-0.4 ± 0.1	-0.6 ± 0.2	-0.7 ± 0.1	-0.5 ± 0.1
	20	-1.0 ± 0.1	-1.1 ± 0.1	-1.4 ± 0.1	-1.1 ± 0.1
10	10	-0.2 ± 0.1	-0.2 ± 0.1	-0.3 ± 0.2	-0.2 ± 0.1
	20	-1.2 ± 0.2	-1.3 ± 0.3	-1.2 ± 0.1	-1.2 ± 0.1
WAY100635	0.1	0.2 ± 0.1	0.2 ± 0.1	0.1 ± 0.1	0.2 ± 0.1

The investigated compounds (*i.p.*) and WAY 100635 (*s.c.*) were administered 30 min before the test. The absolute mean initial body temperatures were within a range of 36.3 ± 0.5°C. $p < 0.001$ *vs.* vehicle.

Table 5. Induction of lower lip retraction (LLR) by the investigated compounds and WAY 100635 (A) and their effect on 8-OH-DPAT (B)

Treatment	Dose (mg/kg)	Mean SEM LLR score	
		A	B
Vehicle	-	0.1 ± 0.1	2.8 ± 0.2
1	10	1.0 ± 0.1	2.3 ± 0.2
	20	1.8 ± 0.3	2.4 ± 0.2
2	10	1.5 ± 0.2	2.8 ± 0.2
	20	2.2 ± 0.1	NT
5	10	0.1 ± 0.2	0.4 ± 0.1
	20	0.9 ± 0.1	0.8 ± 0.1
7	10	0.1 ± 0.1	0.4 ± 0.1
	20	0.5 ± 0.3	0.6 ± 0.2
9	10	1.4 ± 0.1	2.2 ± 0.1
	20	2.5 ± 0.2	NT
10	10	0.1 ± 0.1	0.4 ± 0.2
	20	0.3 ± 0.2	0.6 ± 0.3
WAY 100635	0.1	0.1 ± 0.1	0.3 ± 0.2

The investigated compounds (*i.p.*) and WAY 100635 (*s.c.*) were administrated 15 min before the test **(A)**, or 45 min before 8-OH-DPAT (1 mg/kg, *s.c.*) **(B)**. $p < 0.01$ *vs.* vehicle **(A)** or *vs.* vehicle + 8-OH-DPAT (**B**). NT: not tested.

Table 6. The effect of compounds 5, 7, 10 and ketanserin on the (±)-DOI-induced head twitch response in mice

Treatment	ID_{50} (mg/kg, *i.p.*)[a]
5	7 (5.4-9.2)
7	10 (6.2-15.3)
10	8 (5.9-11.7)
Ketanserine	0.12 (0.07-0.20)

[a] ID_{50}, the dose inhibiting head twitches in mice by 50%; confidence limit (90%) given in parenthesis. Investigated compounds were administrated *i.p.* 60 min before (±)-DOI (2.5 mg/kg, *i.p.*).

Table 7. Functional *in vivo* 5-$HT_{1A/2A}$ receptor activity of the investigated compounds

Compound	5HT_{1A} activity		5HT_{2A} activity
	Presynaptic	Postsynaptic	
1	Non active	Agonist	NA
2	Agonist	Agonist	NA
5	Non active	Antagonist	Antagonist
7	Agonist	Antagonist	Antagonist
9	Agonist	Agonist	NA
10	Non active	Antagonist	Antagonist

compounds **5**, **7**, and **10** (which exhibited the highest 5-HT_{2A} receptor affinity) inhibited head twitches induced by (±)-DOI, a 5-HT_{2A} receptor agonist, in mice. Hence, compound **5**, **7**, and **10** may be classified as 5-HT_{2A} receptor antagonist.

It has already been reported that alone 5-HT_{2A} is not responsible for inhibition of the head twitch response evoked by (±)-DOI. Selective antagonists of dopamine D1 and D2 receptors or α1-adrenoreceptors can also be responsible for the same response (*41*,*42*). Thus, it cannot be excluded that mechanisms other than 5-HT_{2A} receptor blockade are involved in reduction of (±)-DOI-induced head twitches by these compounds.

4. Conclusion

In this investigation *N*(3)-substituted 2,4-imidazolidinediones and oxazolidinediones derivatives were obtained by utilizing various *para*-substituted aniline and piperazine derivatives. The results showed that selected compounds (**1**, **2**, **5**, **7**, **9**, and **10**) can be assumed to be potential ligands for 5-$HT_{1A/2A}$ and the piperazine ring can be replaced by the aniline nucleus. This not only decreases the bulkiness but also increases the activity of the entity. Considering the functional profile of the investigated compounds few of them can act as potential anticonvulsant compounds.

Synthesized compounds in phase 1 (anticonvulsant screening) show that electronegative substitution was more active than electropositive substitution, whereas in the subsequent phase 6a trial, compounds with *para* substitution are more active than *ortho* substitution among the electronegative substituents.

In the functional receptor activity for 5-HT_{1A} the chloro derivatives **1**, **2**, and **9** act as agonist whereas compound **7**, which is a piperazine derivative, acts as a presynaptic agonist and post synaptic antagonist. For 5-HT_{2A} compounds **5**, **7**, and **10** act as antagonist.

Acknowledgements

The authors are grateful to The Head, Department of Chemistry, Faculty of Science, Banaras Hindu University (BHU), Varanasi, India for ^{1}H NMR, ^{13}C NMR and IR spectroscopy. We gratefully acknowledge the financial assistance given by University Grants Commission (UGC), New Delhi for the grant of senior research fellowship to Ms. Meenakshi Dhanawat.

References

1. Peroutka SJ, Sleight AJ, McCarthy BG, Pierce PA, Schmidt AW, Hekmatpanah CR. The clinical utility of pharmacological agents that act at serotonin receptors. J Neuropsychiatry Clin Neurosci. 1989; 1:253-262.
2. Bonnycastle DD, Giarman NJ, Paasonen MK. Anticonvulsant compounds and 5-hydroxytryptamine in rat brain. Br J Pharmacol Chemother. 1957; 12:228-231.
3. Filakovszky J, Gerber K, Bagdy G. A serotonin-1A receptor agonist and an *N*-methyl-D-aspartate receptor antagonist oppose each others effects in a genetic rat epilepsy model. Neurosci Lett. 1999; 261:89-92.
4. Welsh JP, Placantonakis DG, Warsetsky SI, Marquez RG, Bernstein L, Aicher SA. The serotonin hypothesis of myoclonus from the perspective of neuronal rhythmicity. Adv Neurol. 2002; 89:307-329.
5. Ahmad S, Fowler LJ, Whitton PS. Lamotrigine, carbamazepine and phenytoin differentially alter extracellular levels of 5-hydroxytryptamine, dopamine and amino acids. Epilepsy Res. 2005; 63:141-149.
6. Gariboldi M, Tutka P, Samanin R, Vezzani A. Stimulation of 5-HT_{1A} receptors in the dorsal hippocampus and inhibition of limbic seizures induced by kainic acid in rats. Br J Pharmacol. 1996; 119:813-818.
7. Blier P, de Montigny C. Current advances and trends in the treatment of depression. Trends Pharmacol Sci. 1994; 15:220-226.
8. Przegaliński E, Baran L, Siwanowicz J. Role of 5-hydroxytryptamine receptor subtypes in the 1-[3-(trifluoromethyl)phenyl] piperazine-induced increase in threshold for maximal electroconvulsions in mice. Epilepsia. 1994; 35:889-894.
9. Upton N, Stean T, Middlemiss D, Blackburn T, Kennett G. Studies on the role of 5-HT_{2C} and 5-HT_{2B} receptors in regulating generalised seizure threshold in rodents. Eur J Pharmacol. 1988; 359:33-40.
10. Löscher W, Schmidt D. New horizons in the development of antiepileptic drugs. Epilepsy Res. 2002; 50:3-16.
11. Greenwood RS. Adverse effects of antiepileptic drugs. Epilepsia. 2000; 41:S42-52.
12. Chkhenkeli SA, Sramka M, Lortkipanidze GS, Rakviashvili TN, Bregvadze ESh, Magalashvili GE, Gagoshidze TSh, Chkhenkeli IS. Electrophysiological effects and clinical results of direct brain stimulation for intractable epilepsy. Clin Neurol Neurosurg. 2004; 106:318-329.
13. Clark CR. Comparative anticonvulsant activity and neurotoxicity of 4-amino-*N*-(2,6-dimethylphenyl)benzamide and prototype antiepileptic drugs in mice and rats. Epilepsia. 1998; 29:198-203.
14. Leppik IE. Antiepileptic drugs in development: Prospects for the near future. Epilepsia. 1994; 35:S29-40.
15. Bailleux V, Vallée L, Nuyts JP, Hamoir G, Poupaert JH, Stables JP, Vamecq J. Comparative anticonvulsant activity and neurotoxicity of 4-amino-*N*-(2,6-dimethylphenyl)phthalimide and prototype antiepileptic drugs in mice and rats. Epilepsia. 1995; 36:559-565.
16. Clark CR, Lin CM, Sansom RT. Anticonvulsant activity of 2- and 3-aminobenzanilides. J Med Chem. 1986; 29:1534-1537.
17. Clark CR, Davenport TW. Synthesis and anticonvulsant activity of analogues of 4-amino-*N*-(1-phenylethyl)benzamide. J Med Chem. 1997; 30:1214-1218.
18. Clark CR, Sansom RT, Lin CM, Norris GN. Anticonvulsant activity of some 4-aminobenzanilides. J Med Chem. 1985; 28:1259-1262.
19. Clark CR, Wells MJ, Sansom RT, Norris GN, Dockens RC, Ravis WR. Anticonvulsant activity of some 4-aminobenzamides. J Med Chem. 1984; 27:779-782.
20. Leander JD, Robertson DW, Clark CR, Lawson RR, Rathbun RC. Pharmacological effects of enantiomers of 4-amino-*N*-(alpha-methylbenzyl)benzamide, a

chemically novel anticonvulsant. Epilepsia. 1988; 29:83-90.
21. Zajdel P, Subra G, Bojarski AJ, Duszynska B, Pawłowski M, Martinez J. A new class of arylpiperazine derivatives: The library synthesis on SynPhase lanterns and biological evaluation on serotonin 5-HT(1A) and 5-HT(2A) receptors. J Comb Chem. 2004; 6:761-767.
22. Obniska J, Kolaczkowski M, Bojarski AJ, Duszyńska B. Synthesis, anticonvulsant activity and 5-HT_{1A}, 5-HT_{2A} receptor affinity of new *N*-[(4-arylpiperazin-1-yl)-alkyl] derivatives of 2-azaspiro[4.4]nonane and [4.5]decane-1,3-dione. Eur J Med Chem. 2006; 41:874-881.
23. Obniska J, Kaminski K, Skrzynska D, Pichor J. Synthesis and anticonvulsant activity of new *N*-[(4-arylpiperazin-1-yl)-alkyl] derivatives of 3-phenyl-pyrrolidine-2,5-dione. Eur J Med Chem. 2009; 44:2224-2233.
24. van Steen BJ, van Wijngaarden I, Tulp MT, Soudijn W. Structure-affinity relationship studies on 5-HT_{1A} receptor ligands. 1. Heterobicyclic phenylpiperazines with *N*4-alkyl substituents. J Med Chem. 1993; 36:2751-2760.
25. Perrone R, Berardi F, Leopoldo M, Tortorella V, Fornaretto MG, Caccia C, McArthur RA. 1-aryl-4-[(1-tetralinyl)alkyl]piperazines: Alkylamido and alkylamino derivatives. Synthesis, 5-HT_{1A} receptor affinity, and selectivity. 3. J Med Chem. 1996; 39:3195-3202.
26. Misztal S, Bojarski A, Mackowiak M, Boska J, Bielecka Z, Mokrosz JL. Structure-activity relationship studies of CNS agents. 6. Effect of terminal amide fragment on 5-HT_{1A} and 5-HT_2 receptor affinity for *N*-[3-(4-aryl-1-piperazinyl)propyl] derivatives of 3,4-dihydroquinolin-2-(1H)-one and its isomeric isoquinolinones. Med Chem Res. 1992; 2:82-87.
27. Winstead MB, Hamel CK. Substitution in the hydantoin ring. II. *N*-3-Acetic acid derivatives. J Med Chem. 1965; 8:120-122.
28. Vamecq J, Lambert D, Poupaert JH, Masereel B, Stables JP. Anticonvulsant activity and interactions with neuronal voltage-dependent sodium channel of analogues of ameltolide. J Med Chem. 1998; 41:3307-3313.
29. Soyer Z, Kiliç FS, Erol K, Pabuçcuoğlu V. Synthesis and anticonvulsant activity of some omega-(1H-imidazol-1-yl)-*N*-phenylacetamide and propionamide derivatives. Farmaco. 2003; 59:595-600.
30. Soyer Z, Kilic FS, Erol K, Pabuccuoglu V. The synthesis and anticonvulsant activity of some omega-phthalimido-*N*-phenylacetamide and propionamide derivatives. Arch Pharm (Weinheim). 2004; 337:105-111.
31. Ernest LE, Fisk MT, Prosser T. α-Chlorophenylacetic acid. Org Synth. 1956; 36:3-6.
32. Shapiro SL, Rose IM, Freedman L. Aminoalkylamides and oxazolidinediones. J Am Chem Soc. 1959; 81:3083-3088.
33. Muccioli GG, Poupaert JH, Wouters J, Norberg B, Poppitz W, Scriba GKE, Lambert DMA. A rapid and efficient microwave-assisted synthesis of hydantoins and thiohydantoins. Tetrahedron. 2003; 59:1301-1307.
34. Hayward RC. Synthesis of the anticonvulsant drug 5,5-diphenylhydantoin: An under-graduate organic chemistry experiment. J Chem Educ. 1983; 60:512-515.
35. Rogawski MA. Molecular targets versus models for new antiepileptic drug discovery. Epilepsy Res. 2006; 68:22-28.
36. Ucar H, Van derpoorten K, Cacciaguerra S, Spampinato S, Stables JP, Depovere P, Isa M, Masereel B, Delarge J, Poupaert JH. Synthesis and anticonvulsant activity of 2(3H)-benzoxazolone and 2(3H)-benzothiazolone derivatives. J Med Chem. 1998; 41:1138-1145.
37. Berendsen HH, Jenck F, Broekkamp CL. Selective activation of 5HT_{1A} receptors induces lower lip retraction in the rat. Pharmacol Biochem Behav. 1989; 33:821-827.
38. Krall RL, Penry JK, White BG, Kupferberg HJ, Swinyar EA. Antiepileptic drug development: II. Anticonvulsant drug screening. Epilepsia. 1978; 19:409-428.
39. Stables JP, Kupferberg HJ. The NIH anticonvulsant drug development (ADD) program: Preclinical anticonvulsant screening project. In: Molecular and cellular targets for antiepileptic drugs (Avanzini G, Tanganelli P, Avoli M, eds.). John Libbey & Company Ltd., London, England, 1997; pp. 4-17.
40. Jurczyk S, Kołaczkowski M, Maryniak E, Zajdel P, Pawłowski M, Tatarczyńska E, Kłodzińska A, Chojnacka-Wójcik E, Bojarski AJ, Charakchieva-Minol S, Duszyńska B, Nowak G, Maci D. New arylpiperazine 5-HT(1A) receptor ligands containing the pyrimido[2,1-f]purine fragment: Synthesis, *in vitro*, and *in vivo* pharmacological evaluation. J Med Chem. 2004; 47:2659-2666.
41. Dursun SM, Handley SL. Similarities in the pharmacology of spontaneous and DOI-induced head-shakes suggest 5HT_{2A} receptors are active under physiological conditions. Psychopharmacology. 1996; 128:198-205.
42. Schreiber R, Brocco M, Audinot V, Gobert A, Veiga S, Millan MJ. (1-(2,5-dimethoxy-4 iodophenyl)-2-aminopropane)-induced head-twitches in the rat are mediated by 5-hydroxytryptamine 5-HT_{2A} receptors: Modulation by novel 5-$HT_{2A/2C}$ antagonists, D1 antagonists and 5-HT_{1A} agonists. J Pharmacol Exp Ther. 1995; 273:101-112.

(Received April 30, 2011; Revised August 01, 2011; Accepted September 11, 2011)

Appendix

Characterization data of compounds synthesized in the current study.

***N*-(4-chlorophenyl)-2-(2,5-dioxo-4,4-diphenyl-imidazolidin-1-yl)-acetamide (1)**: Melting point: 294-296°C; Yield: 55%; IR (KBr, ν_{max} cm^{-1}): 3,254 (NH Str), 2,945 (C-H), 1,721 (C=O), 1,672 (NH Bend), 790 (C-Cl Str); Mass: 420 (M + 1), 421 (M + 2); ^1H NMR ($CDCl_3$, 300 MHz): δ 8.062 (s, NH, sec amide), 7.685-7.371 (m, 4H, 1Ph), 7.249-7.019 (m, 10H, 2Ph), 6.146 (s, 1H, N-H, phenytoin), 3.960 (s, 2H, -CH_2-); ^{13}C NMR ($CDCl_3$): 169.2, 168.2, 161.2, 143, 138.9, 129.4, 128, 126, 121, 72.6, 47.1; Elemental analysis: calcd for $C_{23}H_{18}ClN_3O_3$: C, 65.79; H, 4.32; Cl, 8.44; N, 10.01; O, 11.43%. Found: C, 65.72; H, 4.28; Cl, 8.39; N, 9.97; O, 11.39%.

***N*-(2-chlorophenyl)-2-(2,5-dioxo-4,4-diphenyl-**

imidazolidin-1-yl)-acetamide (2): Melting point: 298-300°C; Yield: 57%; IR (KBr, v_{max} cm^{-1}): 3,265 (NH Str), 2,980 (C-H), 1,726 (C=O), 1,622 (NH Bend), 810 (C-Cl Str); Mass: 420 (M + 1), 421 (M + 2); ^1H NMR ($CDCl_3$, 300 MHz): δ 8.192 (s, NH, sec amide), 7.198-7.009 (m, 10H, 2Ph), 7.149-6.94 (m, 4H, 1Ph), 6.210 (s, 1H, N-H, phenytoin), 4.095 (s, 2H, -CH_2-); ^{13}C NMR ($CDCl_3$): 169.2, 168.2, 161.2, 143, 141.2, 138.9, 129, 129.1, 128.4, 126.8, 126, 125.7, 125.5, 72.6, 47.1; Elemental analysis: calcd for $C_{23}H_{18}ClN_3O_3$: C, 65.79; H, 4.32; Cl, 8.44; N, 10.01; O, 11.43%. Found: C, 65.73; H, 4.29; Cl, 8.38; N, 9.99; O, 11.41%.

2-(2,5-Dioxo-4,4-diphenyl-imidazolidin-1-yl)-*N*-(4-fluoro-phenyl)-acetamide (3): Melting point: 272-173°C; Yield: 60%; IR (KBr, v_{max} cm^{-1}): 3,305 (NH), 2,900 (CH), 1,722 (C=O), 1,656 (NH Bend), 1,120 (C-F Str); Mass: 404 (M + 1), 405 (M + 2); ^1H NMR ($CDCl_3$, 300 MHz): δ 8.090 (s, NH, sec amide), 7.585-7.271 (m, 4H, 1Ph), 7.149-7.019 (m, 10H, 2Ph), 6.208 (s, 1H, N-H, phenytoin), 3.890 (s, 2H, -CH_2-); ^{13}C NMR ($CDCl_3$): 169.2, 168.2, 161.2, 157.7, 143.0, 136.4, 129, 128.4, 126, 122.0, 115.7, 72.6, 47.1; Elemental analysis: calcd for $C_{23}H_{18}FN_3O_3$: C, 68.48; H, 4.50; F, 4.71; N, 10.42; O, 11.90%. Found: C, 68.41; H, 4.48; F, 4.69; N, 10.38; O, 11.87%.

2-(2,5-Dioxo-4,4-diphenyl-imidazolidin-1-yl)-*N*-*p*-tolyl-acetamide (4): Melting point: 292-294°C; Yield: 45%; IR (KBr, v_{max} cm^{-1}): 3,323 (NH), 2,900 (-CH_3 Str), 1,722 (C=O), 1,656 (NH Bend), 1,380 (C-H Bend); Mass: 400 (M + 1), 401 (M + 2); ^1H NMR ($CDCl_3$, 300 MHz): δ 8.174 (s, NH, sec amide), 7.549-7.319 (m, 10H, 2Ph), 7.295-7.156 (m, 4H, 1Ph), 6.001 (s, 1H, N-H, phenytoin), 4.160 (s, 2H, -CH_2-), 2.355 (s, 3H, -CH_3); ^{13}C NMR ($CDCl_3$): 169.2, 168.2, 161.2, 143.0, 137.8, 133.3, 129.4, 129.0, 128.4, 126, 120.3, 72.6, 47.1, 20.9; Elemental analysis: calcd for $C_{24}H_{21}N_3O_3$: C, 72.16; H, 5.30; N, 10.52; O, 12.02%. Found: C, 72.14; H, 5.29; N, 10.49; O, 12.00%.

2-(2,5-Dioxo-4,4-diphenyl-imidazolidin-1-yl)-*N*-(4-methoxy-phenyl)-acetamide (5): Melting point: 294-296°C; IR (KBr, v_{max} cm^{-1}): 3,355 (NH), 2,967 (-CH_3 Str), 1,730 (C=O), 1,612 (NH Bend), 1,012 (C-H Bend); Mass: 416 (M + 1), 417 (M + 2); ^1H NMR ($CDCl_3$, 300 MHz): δ 8.098 (s, NH, sec amide), 7.440-7.309 (m, 10H, 2Ph), 7.295-6.750 (m, 4H, 1Ph), 6.098 (s, 1H, N-H, phenytoin), 4.160 (s, 2H, -CH_2-), 3.734 (s, 3H, -OCH_3); ^{13}C NMR ($CDCl_3$): 169.2, 168.2, 161.2, 157.6, 143.0, 133.3, 129.0, 128.4, 126, 121.4, 114.3, 72.6, 56.0, 47.1; Elemental analysis: calcd for $C_{24}H_{21}N_3O_4$: C, 69.39; H, 5.10; N, 10.11; O, 15.40 %. Found: C, 69.35; H, 5.13; N, 10.12; O, 15.39%.

2-(2,5-Dioxo-4,4-diphenyl-imidazolidin-1-yl)-*N*-(4-hydroxy-phenyl)-acetamide (6): Melting point: 296-298°C; Yield: 60%; IR (KBr, v_{max} cm^{-1}): 3,590 (OH Str), 3,335 (NH), 2,912 (-CH_3 Str), 1,711 (C=O), 1,638 (N-H Bend); Mass: 402 (M + 1), 403 (M + 2); ^1H NMR ($CDCl_3$, 300 MHz): δ 8.190 (s, NH, sec amide), 7.340-7.209 (m, 10H, 2Ph), 7.195-6.750 (m, 4H, 1Ph), 6.098 (s, 1H, N-H, phenytoin), 5.172 (brs, 1H, -OH), 4.060 (s, 2H, -CH_2-); ^{13}C NMR ($CDCl_3$): 168.2, 161.2, 152.9, 143.0, 133.3, 129.0, 128.4, 126, 121.8, 115.9, 72.6, 47.1; Elemental analysis: calcd for $C_{23}H_{19}N_3O_4$: C, 68.82; H, 4.77; N, 10.47; O, 15.94%. Found: C, 68.83; H, 4.72; N, 10.42; O, 15.90%.

3-{2-[4-(4-Nitrophenyl)-piperazin-1-yl]-2-oxo-ethyl}-5,5-diphenyl-imidazolidine-2,4-dione (7): Melting point: 280-282°C; Yield: 58%; IR (KBr, v_{max} cm^{-1}): 3,335 (NH), 2,912 (-CH_3 Str), 1,711(C=O), 1,635 (N-H Bend), 1,545 (-NO_2), 1,350 (-NO_2), 1,290 (CN Str), 1,180; Mass: 500 (M + 1), 501 (M + 2); ^1H NMR ($CDCl_3$, 300 MHz): δ 7.370-7.116 (m, 10H, 2Ph), 6.990-6.873 (m, 4H, Ar-H), 5.906 (s, 1H, N-H, phenytoin), 4.060 (s, 2H, -CH_2-), 3.616-3.436 (m, 8H, Piperazine); ^{13}C NMR ($CDCl_3$): 169.1, 161.2, 150.6, 143.0, 137.9, 128.4, 124.5, 114.0, 72.6, 57.4, 48.7, 45.3; Elemental analysis: calcd for $C_{27}H_{25}N_5O_5$: C, 64.92; H, 5.04; N, 14.02; O, 16.01%. Found: C, 64.93; H, 5.05; N, 14.00; O, 16.02%.

3-{2-[4-(4-Fluorophenyl)-piperazin-1-yl]-2-oxo-ethyl}-5,5-diphenyl-imidazolidine-2,4-dione (8): Melting point: 281-283°C; Yield: 62%; IR (KBr, v_{max} cm^{-1}): 3,335 (NH), 2,912 (-CH_3 Str), 1,711 (C=O), 1,638 (N-H Bend), 1,350 (CN Str), 1,120 (C-F Str); Mass: 473 (M + 1), 474 (M + 2); ^1H NMR ($CDCl_3$, 300 MHz): δ 7.870-7.116 (m, 10H, 2Ph), 6.790-6.573 (m, 4H, Ar-H), 5.986 (s, 1H, N-H, phenytoin), 4.380 (s, 2H, -CH_2-), 3.516-3.336 (m, 8H, Piperazine); ^{13}C NMR ($CDCl_3$): 169.1, 161.2, 151.6, 140.1, 129.0, 128.4, 116.4, 114.0, 72.6, 57.4, 48.7, 45.3; Elemental analysis: calcd for $C_{27}H_{25}FN_4O_3$: C, 68.63; H, 5.33; F, 4.02; N, 11.86; O, 10.16%. Found: C, 68.64; H, 5.31; F, 4.03; N, 11.84; O, 10.12%.

***N*-(4-chlorophenyl)-2-(2,4-dioxo-5-phenyl-oxazolidin-3-yl)-acetamide (9)**: Melting point: 117-119°C; Yield: 55%; IR (KBr, v_{max} cm^{-1}): 3,254 (NH), 2,932 (-CH_3 Str), 1,719 (C=O), 1,656 (N-H Bend), 790 (C-Cl Str); Mass: 345 (M + 1), 346 (M + 2); ^1H NMR ($CDCl_3$, 300 MHz): δ 8.190 (s, 1H, NH, sec amide), 7.587-7.260 (m, 4H, Ar-H), 7.235-6.116 (m, 5H, 1Ph), 6.201 (1H, methine) 4.460 (s, 2H, -CH_2-); ^{13}C NMR ($CDCl_3$): 169.1, 168.2, 155.8, 138.9, 135.9, 129.8, 129.4, 129.1, 121.8, 89.5, 46.2; Elemental analysis: calcd for $C_{17}H_{13}ClN_2O_4$: C, 59.23; H, 3.80; Cl, 10.28; N, 8.13; O, 18.56%. Found: C, 59.20; H, 3.81; Cl, 10.25; N, 8.15; O, 18.54%.

***N*-(2-chlorophenyl)-2-(2,4-dioxo-5-phenyl-oxazolidin-3-yl)-acetamide (10)**: Melting point:

114-116°C; Yield: 56%; IR (KBr, v_{max} cm^{-1}): 3,245 (NH), 2,911(-CH_3 Str), 1,767 (C=O), 1,621 (N-H Bend), 778 (C-Cl Str); Mass: 345 (M + 1), 346 (M + 2); ^{1}H NMR: ($CDCl_3$, 300 MHz): δ 8.090 (s, 1H, NH, sec amide), 7.480 (s, 1H, O-H, Ar), 7.250-7.120 (s, 1H, m-H, Ar), 7.197-7.019 (m, 5H, 1Ph), 6.945 (dd, 1H, p-H, Ar), 6.105 (1H, methine), 4.460 (s, 2H, -CH_2-); ^{13}C NMR ($CDCl_3$): 169.1, 168.2, 155.8, 141.2, 135.9, 129.8, 129.1, 127.4, 126.8, 125.7, 125.5, 121.8, 89.5, 46.2; Elemental analysis: calcd for $C_{17}H_{13}ClN_2O_4$: C, 59.23; H, 3.80; Cl, 10.28; N, 8.13; O, 18.56%. Found: C, 59.25; H, 3.80; Cl, 10.29; N, 8.16; O, 18.52%.

2-(2,4-Dioxo-5-phenyl-oxazolidin-3-yl)-*N*-(4-fluoro-phenyl)-acetamide (11): Melting point: 150-152°C; Yield: 45%; IR (KBr, v_{max} cm^{-1}): 3,314 (NH), 2,935 (-CH_3 Str), 1,726 (C=O), 1,645 (N-H Bend), 1,112 (C-F Str); Mass: 329 (M + 1), 330 (M + 2); ^{1}H NMR ($CDCl_3$, 300 MHz): δ 8.117 (s, 1H, NH, sec amide), 7.620-7.450 (s, 4H, Ar), 7.197-7.019 (m, 5H, 1Ph), 6.167 (1H, methine), 4.460 (s, 2H, -CH_2-); ^{13}C NMR ($CDCl_3$): 169.1, 168.2, 155.8, 136.4, 135.9, 129.8, 129.0, 122.0, 115.7, 89.5, 46.2; Elemental analysis: calcd for $C_{17}H_{13}FN_2O_4$: C, 62.19; H, 3.99; F, 5.79; N, 8.53; O, 19.49%. Found: C, 62.16; H, 3.94; F, 5.72; N, 8.54; O, 19.42%.

2-(2,4-Dioxo-5-phenyl-oxazolidin-3-yl)-*N*-*p*-tolyl-acetamide (12): Melting point: 150-152°C; Yield; 45%; IR (KBr, v_{max} cm^{-1}): 3,343 (NH), 2,934 (-CH_3 Str), 1,723 (C=O), 1,645 (N-H Bend), 1,368 (C-H Bend); Mass: 325 (M + 1), 326 (M + 2); ^{1}H NMR ($CDCl_3$, 300 MHz): δ 8.117 (s, 1H, NH, sec amide), 7.570-7.390 (m, 4H, Ar), 7.197-7.019 (m, 5H, 1Ph), 6.134 (1H, methine), 4.298 (s, 2H, -CH_2-), 2.307 (s, 2H, -CH_3); ^{13}C NMR ($CDCl_3$): 169.2, 168.2, 155.8, 137.8, 135.9, 133.3, 129.8, 129.4, 129.0, 127.4, 120.3, 89.5, 46.2, 20.9; Elemental analysis: calcd for $C_{18}H_{16}N_2O_4$: C, 66.66; H, 4.97; N, 8.64; O, 19.73%. Found: C, 66.60; H, 4.95; N, 8.61; O, 19.72%.

2-(2,4-Dioxo-5-phenyl-oxazolidin-3-yl)-*N*-(4-methoxy-phenyl)-acetamide (13): Melting point: 152-154°C; Yield: 45%; IR (KBr, v_{max} cm^{-1}): 3,323 (NH), 2,956 (-CH_3 Str), 1,722 (C=O), 1,609 (N-H Bend), 1,016 (C-H Bend); Mass: 341 (M + 1), 342 (M + 2); ^{1}H NMR ($CDCl_3$, 300 MHz): δ 8.117 (s, 1H, NH, sec amide), 7.620-7.420 (m, 4H, Ar), 7.197-7.019 (m, 5H, 1Ph), 6.156 (1H, methine), 4.298 (s, 2H, -CH_2-), 3.607 (s, 3H, -OCH_3); ^{13}C NMR ($CDCl_3$): 169.2, 168.2, 157.6, 155.8, 135.9, 133.3, 129.0, 129.8, 127.4, 121.4, 114.3, 89.5, 56.0, 46.2; Elemental analysis: calcd for $C_{18}H_{16}N_2O_5$: C, 63.52; H, 4.74; N, 8.23; O, 23.51%. Found: C, 63.50; H, 4.71; N, 8.24; O, 23.50%.

2-(2,4-Dioxo-5-phenyl-oxazolidin-3-yl)-*N*-(4-hydroxy-phenyl)-acetamide (14): Melting point: 152-154°C; Yield: 40%; IR (KBr, v_{max} cm^{-1}): 3,578 (OH), 3,323 (NH), 2,922 (-CH_3 Str), 1,709 (C=O), 1,628 (N-H Bend); Mass: 327 (M + 1), 328 (M + 2); ^{1}H NMR ($CDCl_3$, 300 MHz): δ 8.117 (s, 1H, NH, sec amide), 7.620-7.460 (m, 4H, Ar), 7.197-7.019 (m, 5H, 1Ph), 6.189 (1H, methine), 5.048 (brs, 1H, OH), 4.298 (s, 2H, -CH_2-); ^{13}C NMR ($CDCl_3$): 169.2, 168.2, 155.8, 152.9, 135.9, 133.3, 129.8, 129, 127.4, 121.8, 115.9, 89.5, 46.2; Elemental analysis: calcd for $C_{17}H_{14}N_2O_5$: C, 62.57; H, 4.32; N, 8.59; O, 24.52%. Found: C, 62.56; H, 4.33; N, 8.55; O, 24.51%.

3-{2-[4-(4-Nitrophenyl)-piperazin-1-yl]-2-oxo-ethyl}-5-phenyl-oxazolidine-2,4-dione (15): Melting point: 98-100°C; Yield: 50%; IR (KBr, v_{max} cm^{-1}): 3,354 (NH), 2,909 (-CH_3 Str), 1,723 (C=O), 1,644 (N-H Bend), 1,534 (-NO_2), 1,352 (-NO_2), 1,278 (CN Str), 1,178; Mass: 425 (M + 1), 426 (M + 2); ^{1}H NMR ($CDCl_3$, 300 MHz): δ 7.2970-7.016 (m, 5H, 1Ph), 6.890-6.773 (m, 4H, Ar), 6.209 (1H, methine), 4.102 (s, 2H, -CH_2-), 3.706-3.536 (m, 8H, Piperazine); ^{13}C NMR ($CDCl_3$):169.1, 155.8, 150.6, 137.9, 135.9, 129.8, 129.0, 127.4, 124.5, 114.0, 89.5, 57.4, 48.7, 44.4; Elemental analysis: calcd for $C_{21}H_{20}N_4O_6$: C, 59.43; H, 4.75; N, 13.20; O, 22.62%. Found: C, 59.40; H, 4.72; N, 13.21; O, 22.60%.

3-{2-[4-(4-Fluorophenyl)-piperazin-1-yl]-2-oxo-ethyl}-5-phenyl-oxazolidine-2,4-dione (16): Melting point: 97-99°C; Yield: 53%; IR (KBr, v_{max} cm^{-1}): 3,334 (NH), 2,923 (-CH_3 Str), 1,721 (C=O), 1,622 (N-H Bend), 1,333 (CN Str), 1,130 (C-F Str); Mass: 398 (M + 1), 399 (M + 2); ^{1}H NMR ($CDCl_3$, 300 MHz): δ 7.2970-7.016 (m, 5H, 1Ph), 6.790-6.573 (m, 4H, Ar), 6.145 (1H, methine), 4.022 (s, 2H, -CH_2-), 3.706-3.536 (m, 8H, Piperazine); ^{13}C NMR ($CDCl_3$): 169.1, 155.8, 140.1, 135.9, 129.8, 129.0, 114.7, 89.5, 57.4, 48.7, 44.4; Elemental analysis: calcd for $C_{21}H_{20}FN_3O_4$: C, 63.47; H, 5.07; F, 4.78; N, 10.57; O, 16.10%. Found: C, 63.45; H, 5.01; F, 4.72; N, 10.54; O, 16.11%.

Original Article

DOI: 10.5582/ddt.2011.v5.5.238

Anti-*Candida* and radical scavenging activities of essential oils and oleoresins of *Zingiber officinale* Roscoe and essential oils of other plants belonging to the family Zingiberaceae

Miki Takahashi*, Shigeharu Inouye, Shigeru Abe

Teikyo University Institute of Medical Mycology, Tokyo, Japan.

ABSTRACT: Essential oils of young and mature rhizomes, air-dried and steamed rhizomes, and seed rhizomes of *Zingiber officinale* Roscoe (ginger) were prepared, and their inhibition of filamentation by *Candida albicans* was examined. Ginger essential oils, and particularly those from seed and air-dried rhizomes, had potent inhibitory activity compared to ginger oleoresins obtained by ethanol and hypercritical carbon dioxide extraction and essential oils of 5 other plants in the family Zingiberaceae. Of the constituents, [6]-shogaol was most active against filament formation and growth of *C. albicans*, followed by citral and [6]-gingerol. Ginger oleoresin, and especially that obtained by ethanol extraction, with a high [6]-gingerol content exhibited potent scavenging activity against 1,1-diphenyl-2-picrylhydrazyl radicals in comparison to essential oils of ginger and other Zingiberaceae plants.

Keywords: Essential oil, oleoresin, *Z. officinale*, [6]-gingerol, [6]-shogaol, citral, *Candida albicans*, radical scavenging activity

1. Introduction

Oral candidiasis is common in patients with AIDS, hypo-salvation, and diabetes mellitus and in individuals with poor oral hygiene. Chemotherapy is usually effective at treating oral candidiasis but causes new problems clinically, such as frequent recurrence of the disease and the emergence of drug-resistant *Candida* strains. Therefore, new therapies such as oral administration of edible materials that have anti-*Candida* activity should be developed.

Essential oil from rhizomes of *Zingiber officinale* Roscoe (abbreviated as ginger below) has been the subject of numerous studies worldwide. The oil has been reported to have stimulating action (*1*), anti-spasmodic action (*2*), immunomodulation (*3,4*), anti-inflammatory action (*5*), and other types of activity. However, there are relatively few reports on the oil's antimicrobial action, which is probably because of the weakness of that action (*6*). Most recently, essential oil of *Alpinia galanga*, a plant of the Zingiberaceae family, has been reported to have strong anti-microbial activity (*7*).

The current study focused on the anti-*Candida* activity of ginger essential oil. Ginger oils were prepared using young and mature rhizomes and air-dried and steamed rhizomes, and their inhibition of filamentation and growth of *C. albicans* was determined. The anti-*Candida* activity of ginger oils was compared to that of 2 ginger oleoresins obtained by ethanol and hypercritical carbon dioxide (CO_2) extraction and 5 other oils belonging to the family Zingiberaceae. These oils were plai (rhizomes of *Z. cassumunar* Roxb.), ginger lily (flower and leaves of *Hedychium coronarium* Koenig), kapurkachri (rhizomes of *H. spicatum*), gettou (leaves of *Alpinia zerumbet* B.L. Burtt et R.M. Sm.), and myoga (flower buds of *Z. mioga*). Plai is native to Indonesia, Thailand, and India and is used in folk medicine. Ginger lily is an erect shrub grown in the tropical and semi-tropical portions of India. It is cultivated for ornamental use and also for Chinese medicine. Kapurkachri is grown in mountainous areas of India and southern China and is used in Chinese medicine. Gettou is grown in tropical and subtropical regions and is known as wild ginger or bitter ginger. It is cultivated in Okinawa and the Ogasawara Islands of Japan for decoration. Myoga is a traditional Japanese vegetable with edible flower buds produced in the summer/autumn. Young ginger rhizomes are called "hashouga" in Japanese and are eaten raw in Japan.

The current study sought to evaluate the anti-*Candida* activity of ginger essential oil, and particularly its inhibition of filament formation by *C. albicans*, and to evaluate its scavenging activity against 1,1-diphenyl-2-picrylhydrazyl (DPPH) radicals by comparing ginger essential oil to ginger oleoresins and other related essential oils.

**Address correspondence to:*
Dr. Miki Takahashi, Teikyo University Institute of Medical Mycology, 359 Otsuka, Hachioji, Tokyo 192-0395, Japan.
e-mail: miki-391@main.teikyo-u.ac.jp

2. Materials and Methods

2.1. *Essential oils, oleoresins, and chemicals*

Young and mature ginger oils were obtained by steam distillation of fresh rhizomes collected from a farm in the Town of Shimanto, Kochi Prefecture, Japan in August and November 2010, along with the seed rhizome (propagation rhizome) connected to the fresh rhizome underground. Air-dried ginger oil was prepared from mature rhizomes dried for a week in the shade, and steamed oil was obtained from mature rhizomes after steam-heating for 2 h followed by drying. Myoga oil was prepared from fresh flower buds of myoga cultivated in the City of Suzaki, Kochi Prefecture, Japan in August 2009. Details of steam distillation were described in a separate paper (Inouye *et al*., submitted for publication).

Ethanol oleoresin was prepared by two cycles of extraction of fresh mature rhizomes (231 g) with ethanol (300 mL). The first ethanol extract contained much of the rhizome's water content, and most constituents were extracted with the second extraction. Both extracts were combined and evaporated under reduced pressure to dryness to yield 290 mg of resinous oleoresin.

Plai oil prepared in Indonesia and ginger lily, kapurkachri oils, and CO_2 oleoresin of ginger rhizomes prepared in India were supplied by Phyto-aroma Laboratories, Yokohama, Japan. Gettou oil prepared in Okinawa was supplied by Yumejin Limited, Okinawa, Japan. [6]-Gingerol, [6]-shogaol, citral, β-bisabolene and dextrose were purchased from Wako Pure Chemical Co., Ltd., Osaka, Japan. RPMI-1640 medium containing phenol red was obtained from Sigma Chemical, Ltd. (St. Louis, MO, USA). Calf serum was obtained from Thermo Trace, Ltd. (Melbourne, Australia). Bacto™ Yeast Extract and Bacto™ Peptone were purchased from Becton-Dickinson & Company (MD, USA). Alamar Blue was obtained from Trek Diagnostic Systems, Inc. (Cleveland, OH, USA).

2.2. *Compositional analysis*

GC/MS analysis of essential oils and oleoresins was performed using a Shimadzu QP-2010 instrument (Shimadzu, Kyoto, Japan) with a TC-5 column. Quantitative analysis was carried out using a Model 353B GC instrument equipped with a TC-5 column and a hydrogen flame detector. GC conditions were as previously described (*8*).

HPLC analysis was carried out using a Waters Alliance instrument (Tokyo, Japan) coupled to a Waters ZQ MS ESI instrument with a mobile phase of 50 mM ammonium acetate (A), acetonitrile (B), and water (C) at a ratio of A:B:C = 10:10:80 (0-10 min, linear gradient flow) and 10:10:0 (10-20 min, fixed flow). The flow rate was 0.4 mL/min at 30°C, and peaks were detected using UV absorption at 280 nm.

[6]-Gingerol content was determined by HPLC using an authentic sample as an external standard and absorbance at 280 nm or MS intensity at m/z 293. The correlation coefficient was 0.9999 for 280 nm and 0.9983 for m/z 293.

2.3. *Assay of the inhibition of filament formation and growth of Candida albicans*

C. albicans TIMM1678, a stock culture of Teikyo University Institute of Medical Institute, was used in an inhibition assay. An assay of filamentation inhibition was carried out according to the method used by Abe *et al*. (*9*) and is briefly described below.

An essential oil or oleoresin was dissolved in DMSO in a series of two-fold dilutions. Each DMSO solution was diluted with RPMI-1640 medium so as to obtain a 0.25% DMSO concentration for the final assay medium. A sample (100 μL) and a fungal solution (500 cells/mL, 100 μL) suspended in RPMI-1640 containing 2.0% calf serum were mixed in a 96-well flat microplate. The mixture was cultured at 37°C for 16 h. After the yeast form was washed out with distilled water, the filamentous form was stained with 0.02% crystal violet (10 μL) for 15 min. The dye adsorbed on the filamentous cells was eluted with isopropanol (150 μL) containing 0.25% dodecyl sulfate and 0.04 N hydrochloric acid, and the extract's absorbance at 620 nm was recorded. The rate of inhibition of filamentous formation was expressed as follows:

Rate of inhibition (%) = $(1 - OD_{sample}/OD_{control}) \times 100$, where OD_{sample} is the optical density of a sample solution, and $OD_{control}$ is the optical density of a control solution.

The assay of growth inhibition was carried out using the same RPMI-1640 medium used for the assay of filamentation inhibition, and YPD medium (yeast 1%, peptone 2% and dextrose 5%) as previously reported (*10*). A sample solution in a series of two-fold dilutions containing less than 0.5% DMSO (100 μL) and a fungal suspension (2×10^3 cells/mL) in medium (100 μL) were mixed in the wells of a microplate. Alamar Blue (10 μL) was added when RPMI-1640 was used. The microplate was incubated at 30°C, and growth was stopped when a control well turned red in the event RPMI-1640 was used or absorbance at 620 nm exceeded 0.2 in of the event YPD was used. The minimum concentration needed for the well to remain blue was defined as the MIC. *C. albicans* TIMM1678 grows in both filamentous and yeast forms in RPMI-1640 medium, and turbidimetry was difficult. However, *C. albicans* TIMM1678 grows in the yeast form in YPD medium, and turbidimetry was used when that medium was used. When absorbance at 620 nm was 50% of the control, the IC_{50} value (minimum concentration to reduce the growth 50%) was obtained. At the same time,

inhibition percentage at 4,000 μg/mL was recorded since the IC_{50} value could not be obtained for many oils because of their weak activity.

2.4. *DPPH radical scavenging assay*

The detailed procedures for an assay of DPPH radical scavenging have previously been reported (*11*) and briefly described here. An essential oil or a pure compound was dissolved in ethanol in a series of two-fold dilutions, starting at 4,000 μg/mL to 3.9 μg/mL. Eugenol and α-tochopherol were used as positive controls. Each ethanol solution (75 μL) was added to 150 μL of 100 mM (0.012%) tri-(hydroxymethyl)-aminomethane hydrochloride buffer (pH 6.5) in 50% ethanol in wells of a microplate (Multi Well Plate, Sumitomo Bakelite Co., Ltd., Tokyo, Japan). A DPPH solution (0.2 mg/mL) in ethanol (75 μL) was added to the mixture, and the microplate was covered with a plastic film (Sumitomo Bakelite Co., Ltd.), shaken vigorously with an agitator, and allowed to stand at room temperature in a dark room. The absorbance at 540 nm was measured after 6 h using a multiscan photometer (Multiskan FC (Skanlt 3.1), Thermo Fisher Scientific Ltd., Yokohama, Japan). Relative scavenging activity (RSA) was calculated using the following equation:

RSA (%) = (1 – As/Ac) × 100, where Ac is the absorbance of a control sample, and As is the absorbance of a test sample. The EC_{50} value (effective concentration to decrease the initial DPPH concentration by 50%) was calculated.

3. Results

Table 1 shows the composition of essential oils, oleoresins, and ethyl acetate extracts from various forms of ginger rhizomes. The major constituent of essential oils was citral, which increased in the oils obtained from air-dried rhizomes and seed rhizomes. A particularly high percentage (70%) was noted in air-dried specimens. In contrast, young rhizomes had the lowest content of citral and highest content of geranyl

Table 1. Composition of essential oils, oleoresins, and solvent extracts of ginger as determined by GC

Table 1A. Compositions of essential oils

Constituent[a]	Ginger oil (fresh rhizomes)			Ginger oil (dry rhizomes)	
	Young (%)	Mature (%)	Seed (%)	Air-dried (%)	Steamed (%)
Zingiberene	6.3	17.1	14.2	3.8	10.3
Ar-curcumene	1.3	2.8	5.2	1.9	18.1
β-Bisabolene	4.2	6.8	7.2	1.8	18.7
Farnesene	0.3	0.5	0.7	0.2	7.0
β-Sesquiphellandrene	2.8	5.9	6.4	2.1	14.1
Citral[b]	12.6	24.9	46.0	70.5	7.0
Geraniol	8.6	4.7	2.4	1.7	1.9
Geranyl acetate	45.0	6.7	0.2	0.1	7.6
1,8-Cineole	1.6	6.1	1.7	0.8	-
Camphene	0.1	3.1	0.6	-	0.8
Sabinene	0.7	6.3	1.7	0.5	-
[6]-Gingerol	-	-	-	-	-
[6]-Shogaol	-	-	-	-	-

Table 1B. Composition of oleoresins and solvent extracts

Constituent[a]	Oleoresin		Ethyl acetate extract		
	EtOH[c] (%)	CO_2[d] (%)	Young (%)	Mature (%)	Steamed (%)
Zingiberene	11.8	27.1	28.8	26.2	30.4
Ar-curcumene	4.2	15.1	3.4	6.0	9.7
Bisabolene	7.1	11.8	11.7	10.8	20.2
Farnesene	0.4	3.1	0.3	1.3	3.3
β-Sesquiphellandrene	8.0	14.0	10.8	10.3	14.8
Citral[b]	-	-	0.6	5.1	-
Geraniol	-	-	2.8	-	-
Geranyl acetate	-	-	8.9	0.2	1.5
1,8-Cineole	-	1.8	2.3	3.1	0.2
Camphene	-	2.1	0.2	5.3	1.1
Sabinene	-	2.3	0.6	4.8	1.1
[6]-Gingerol	19.4	1.6	3.6	2.9	1.0
[6]-Shogaol	14.0	0.6	-	-	6.5

[a] Listed are constituents at levels of more than 3.0% in at least one oil, oleoresin, or extract; [b] Combined content from geranial and neral; [c] Oleoresin obtained by ethanol extraction; [d] Oleoresin obtained by supercritical carbon dioxide extraction.

acetate. The lowest citral content was found in steam-heated rhizomes.

The next major constituents were sesquiterpenes consisting of zingiberene, β-sesquiphellandrene, β-bisabolene, and ar-curcumene while the sesquiterpene farnesene was a minor constituent. The steam-heated sample had a higher content of ar-curcumene. 1,8-Cineole, camphene, and sabinene were present as minor constituents.

A similar composition was noted for oleoresins and ethyl acetate extracts of ginger, with had five sesquiterpenes as major constituents. 1,8-Cineole, camphene, and sabinene were found to be minor constituents except in ethanol oleoresin, in which no monoterpene hydrocarbon was detected. However, oleoresins and ethyl acetate extracts had quite a low citral, geraniol, and geranyl acetate content; the extract of young rhizomes, however, had a relatively high geranyl acetate content.

Gingerol and shogaol, two major pungent principals of ginger rhizomes, were not present in the essential oils but were present in the oleoresins and solvent extracts according to GC analysis. [6]-Gingerol was found to be a major constituent of ethanol oleoresin while [6]-shogaol was a minor constituent. Although ethanol oleoresin had a high percentage of [6]-gingerol, it contained many other compounds with a high molecular weight, such as stigmasta-4,22-dien-3-ol (C_{29}), clionasterol (C_{29}), and other unidentified compounds. These less volatile constituents were detected by the QP-2010 GC/MS instrument but not by the 353B GC instrument. These high molecular compounds were not present in CO_2 oleoresin.

Since some gingerol was converted to shogaol due to thermal decomposition during GC, HPLC analysis was performed to determine the [6]-gingerol content and relative ratio of gingerol and shogaol. As shown in Table 2, [6]-gingerol was found to be a major constituent of ethanol oleoresin while [8]- and [10]-gingerols were minor constituents. [6]-Shogaol content was 1/3 of the [6]-gingerol content in ethanol oleoresin. CO_2 oleoresin prepared in India had a composition of gingerol and shogaol similar to that of ethanol oleoresin, although the concentration of [6]-gingerol was lower. Ethyl acetate extract of young and mature rhizomes contained only gingerols and no shogaol, but the [6]-shogaol content increased markedly in steam-heated rhizomes.

Table 3 shows the composition of the reference oils. Plai essential oil mainly consisted of sabinene (40.1%), terpinen-4-ol (24.8%), β-terpinene, *p*-cymene, γ-terpinene, and β-sesquiphellandrene. 1,4-Bis-methoxy-triquinacene was detected only by the QP-2010 GC/MS instrument.

The flower essential oil of ginger lily consisted mainly of sesquiterpenes such as 6-ethenyl-3-

Table 2. Composition of gingerol and shogaol in ginger oleoresins and ethyl acetate extracts as determined by HPLC

Source	Relative percentage (concentration, μg/mg)[a]			
	[6]-Gingerol	[6]-Shogaol	[8]-Gingerol	[10]-Gingerol
Ethanol oleoresin	46.9% (256.8)	15.1%	7.7%	12.2%
CO_2 oleoresin	3.2% (115.5)	12.9%	4.5%	7.3%
Young rhizome extract[b]	77.9%	-	22.1%	-
Fresh rhizome extract[c]	65.2%	-	6.4%	10.9%
Steamed rhizome extract[d]	46.1%	25.6%	7.1%	8.6%

[a] Absorbance at 280 nm. [6]-gingerol content determined using m/z 293 was 284.2 μg/mg in ethanol oleoresin and 156.6 μg/mg in CO_2 oleoresin; [b] Ethyl acetate-ethanol extract from fresh young rhizomes; [c] Ethyl acetate extract from fresh mature rhizomes; [d] Ethyl acetate extract from steam-heated and dried mature rhizomes.

Table 3. Composition of essential oils from plants belonging to the family Zingiberaceae except for ginger

Essential oil	Constituent[a]
Plai (rhizomes)	Sabinene (40.1%), terpinen-4-ol (24.8%), β-terpinene (7.9%), *p*-cymene (4.5%), γ-terpinene (4.1%), β-sesquiphellanderene (3.0%), 1,4-bismethoxy-triquinacene[b]
Ginger lily (flowers, leaves)	Methoxy-sesquiterpene[c] (32.4%), camphor (13.7%), germacra-trien-6-one (8.4%), 1,8-cineole (6.0%), furanosesquiterpene[d] (6.1%), β-elemene (5.4%), camphene (3.9%), borneol (3.5%)
Kapukachri (rhizomes)	1,8-Cineole (25.4%), agarospirol (10.6%), β-eudesmol (9.9%), cadina-1(10),4-diene (7.5%), β-elemol (5.8%), α-eudesmol (5.2%), cadina-1(11),4-diene (4.3%), α-cadinol (4.3%), cubenol (4.1%)
Gettou (leaves)	β-Phellandrene (25.5%), 1,8-cineole (17.3%), γ-terpinene (10.7%), *p*-cymene (10.1%), terpinen-4-ol (7.5%), β-pinene (7.2%), α-thujene (4.9%)
Myoga (flower buds)	Eudesma-4 (14%), 11-diene (28.8%), β-elemene (26.5%), germacrene B (9.8%), β-eudesmol (4.0%), cycloundecatriene (4.0%), sabinene (3.5%)
Spearmint (leaves)	Carvone (80.0%)
Tea tree (leaves)	Terpinen-4-ol (39%)

[a] Constituents at levels of more than 3.0% are listed; [b] This constituent was detected only by GC/MS; [c] 6-Ethenyl-3-isopropyl-2-methoxy-6-methyl-5-isopropyl-cyclohex-3-ene; [d] 6-Ethenyl-3,6-dimethyl-5-iopropenyl-tetrahydrobenzofuran.

isopropyl-5-isopropenyl-6-methyl-2-methoxy-cyclohexane (a positional isomer of methyl-elemol), germacra-trien-6-one, furanosesquiterpene, and β-elemene, along with monoterpenes such as 1,8-cineole, camphene, and borneol. Kapurkachri oil mainly consisted of 1,8-cineole, β-eudesmol, elemol, and α-cadinol.

Gettou oil obtained in Okinawa contained mainly monoterpenes such as β-phellandrene, 1,8-cineole, γ-terpinene, *p*-cymene, and terpinen-4-ol. Myoga oil consisted of sesquiterpenes such as eudesma-4,11-diene, β-elemene, germacrene B, and β-eudesmol. Spearmint and tea tree oils used as reference oils contained mainly (-)-carvone and terpinen-4-ol, respectively.

Figure 1 illustrates the inhibition of filamentation by ginger oil, ethanol oleoresin, and major constituents (citral, [6]-gingerol, and [6]-shogaol) at 50 μg/mL. In contrast to the non-treated control with filamentous forms, ginger oil from fresh mature rhizomes (Figure 1A) provided almost complete inhibition of filamentation, with only the yeast form appearing. Oleoresin (Figure 1B) inhibited both filament and yeast forms at a rate of 54.6%. Citral and [6]-shogaol (Figures 1D and 1E) almost completely inhibited filamentation, and [6]-gingerol (Figure 1C) inhibited filamentation at a rate of 70.7%.

Table 4 shows the anti-*Candida* activity of five ginger oils, along with two ginger oleoresins and seven reference oils. Ginger oils had potent inhibitory activity against filamentous formation by *C. albicans*. As is apparent from the IC_{50} and IC_{90}, 5 ginger oils had 4~8 times more potent than 2 ginger oleoresins and other oils belonging to Zingiberaceae family as well as reference oils. The IC_{50} value of ethanol oleoresin was 50 μg/mL, those of CO_2 oleoresin, ginger lillylily, and kapurkachri oils was 100 μg/mL. The remaining plai, spearmint, and tea tree oils had an IC_{50} of 200 μg/mL. Gettou oil was weakest, with an IC_{50} of 400 μg/mL.

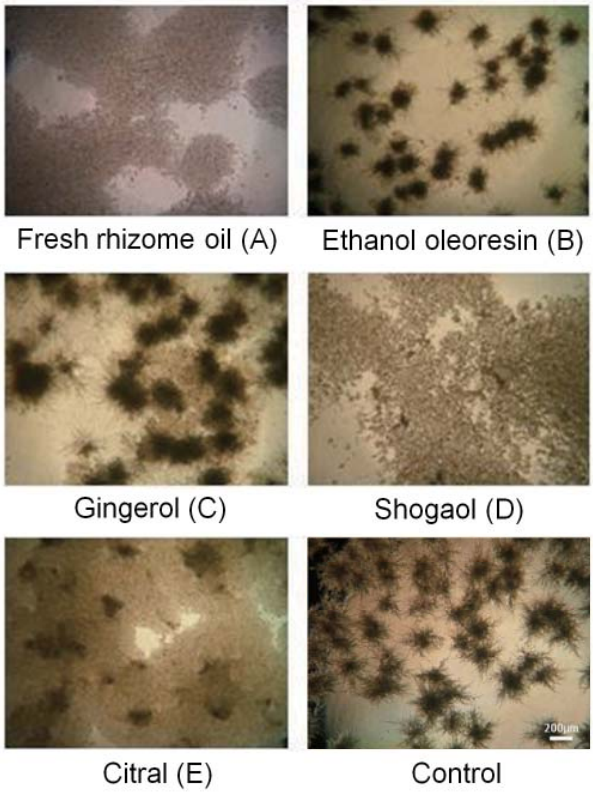

Figure 1. Inhibition of filamentation by fresh rhizome oil (A), ethanol oleoresin (B), [6]-gingerol (C), [6]-shogaol (D), and citral (E) at 50 μg/mL.

Table 4. Anti-*Candida* activity of ginger oils, oleoresins, and other essential oils belonging to the family Zingiberaceae and constituents

Agents	Inhibitory activity				
	Filament		Growth (RPMI)	Growth (YPG)	
	IC_{50} (μg/mL)	IC_{90} (μg/mL)	MIC (μg/mL)	Inhibition rate at 4,000 μg/mL (%)	IC_{50} (μg/mL)
Ginger oils					
Young	12.5	50	400	75.9%	2,000
Mature	12.5	50	400	98.0%	2,000
Seed	12.5	25	400	97.8%	1,000
Air-dried	12.5	25	200	97.5%	1,000
Steamed	12.5	50	nt	nt	nt
Ginger oleoresins					
CO_2 extract	100	200	> 800	65.9%	2,000
Ethanol extract	50	100	400	70.3%	2,000
Plai oil	200	400	1,600	56.2%	4,000
Ginger lily oil	100	200	> 3,200	39.9%	> 4,000
Kapurkachri oil	100	200	> 3,200	36.7%	> 4,000
Gettou oil	400	400	3,200	48.8%	4,000
Myoga oil	100	200	nt	nt	nt
Spearmint oil	200	400	1,600	43.9%	> 4,000
Tea tree oil	200	400	3,200	35.0%	> 4,000
[6]-Gingerol	50	100	> 100	nt	nt
[6]-Shogaol	6.25	25	100	nt	nt
β-Bisabolene	400	> 400	> 400	nt	nt
Citral	25	50	200	nt	nt

nt: not tested.

Table 5. DPPH radical scavenging activity of essential oils of Zingiberaceae plants, ginger oleoresins, [6]-gingerol, citral, and reference compounds

Oil, oleoresin, constituent	EC_{50}* (μg/mL)
Ginger oil (fresh mature rhizomes)	> 4,000
Plai oil	4,000
Ginger lily oil	4,000
Kapurkachri oil	> 4,000
Gettou oil	> 4,000
Ethanol oleoresin of ginger	62.5
CO_2 oleoresin of ginger	125
[6]-Gingerol	7.8
Citral	> 4,000
Eugenol	7.8
α-Tochopherol	62.5

* EC_{50}: effective concentration to decrease the initial DPPH concentration by 50%.

Ginger oils had more potent inhibition of *C. albicans* growth than did other oils. Ginger oils from air-dried rhizomes had an MIC of 200 μg/mL in RPMI-1640 medium. Three other ginger oils had an MIC of 400 μg/mL. Ethanol oleoresin had activity comparable to that of mature and young rhizomes, while CO_2 oleoresin and other oils were less able to inhibit growth compared to ginger oils. When the medium was changed from RPMI-1640 to YPD, the anti-*Candida* activity decreased considerably to an IC_{50} value of 1,000-2,000 μg/mL. Two oleoresins had comparable activity, but other oils, including the reference oils, had weaker activity.

Table 5 shows the DPPH radical scavenging activity of essential oils and oleoresins, expressed as EC_{50} values. Ethanol oleoresin from fresh ginger rhizomes exhibited potent activity as indicated by an EC_{50} of 62.5 μg/mL, comparable to that of α-tochopherol. CO_2 oleoresin had an EC_{50} of 125 μg/mL, but 5 essential oils including ginger, plai, ginger lily, kapurkachri, and gettou oils had very weak activity ≥ 4,000 μg/mL. [6]-Gingerol alone had an EC_{50} of 7.8 μg/mL, which was comparable to that of eugenol but more potent than that of α-tochopherol. Essentially, citral had no activity under the conditions tested.

4. Discussion

4.1. *Oil compositions*

In the growing stage, geranyl acetate is reportedly converted to geraniol and then to citral (*11*). This may be the reason for the high geranyl acetate content in young rhizomes. Terpinen-4-ol was major constituent of young hydrosol but was not detected in the young rhizome oil, suggesting that terpinen-4-ol was mostly transferred to the aqueous layer by steam distillation. Citral content increased more in seed rhizome oil than in fresh rhizomes, which agrees with the literature (*11*). The high citral content in the air-dried rhizomes may be due to the increased production of citral during the drying process. Citral content is reported to increase during storage at 15°C (*11*).

Oleoresins and ethyl acetate extracts had quite a low citral, geraniol, and geranyl acetate content. The low citral content in oleoresin in comparison to essential oil has been noted by other researchers (*12*). This suggests that citral and geraniol might be formed during steam distillation as a result of thermal decomposition. An increase in ar-curcumene to compensate for zingiberene in steam-heated rhizomes may be due to the thermal conversion of zingiberene (*13*). Lack of monoterpene hydrocarbon in ethanol oleoresin may be due, at least partly, to evaporation loss being accompanied by solvent distillation of ethanol and water.

As the current study determined, plai oil had a composition similar to that of oils found in Indonesia (*14*) and Bangladesh (*15*).

Ginger lily oil had a composition that differed vastly from that the composition reported in China, which included β-*trans*-ocimenone (28.05%) and linalool (18.5%) (*16*), suggesting a different chemo-type.

Kapurkachri oil had a composition similar to that reported by Bottini *et al*. (*17*). However, agarospirol, cadina-dienes, and cubenol were detected only in the oil studied here. Kapurkachri from southern India had a considerably different composition, according to Sabulal *et al*. (*18*).

Seasonal changes in the composition of gettou oil were studied in detail by Murakami *et al*. (*19*), and they reported that *p*-cymene, 1,8-cineole, and terpinen-4-ol were major constituents. These results agree with those of the current study. Qing *et al*. reported that oil from the flowers of myoga had a composition that included β-phellandrene, α-humulene, β-elemene, α-phellandrene, β-pinene, and β-caryophyllene (*20*). β-Elemene was found to be a common constituent, but other constituents were not found in the oil studied here.

4.2. *Anti-Candida activity*

Singh *et al*. reported that ginger oil had potent activity against *Fusarium moniliforme* but moderate or weak activity against other fungi and bacteria (*12*). They also stated that essential oil of ginger had more potent activity than did the corresponding oleoresin, which agrees with the current study.

Ginger oil is reported to have an MIC ranging from 1,600-3,200 μg/mL (average: 3,100 μg/mL) against *C. albicans* (*21*); in the current study, the oil had an MIC of 1,000-2,000 μg/mL in YPD medium but an MIC of 200-400 μg/mL in RPMI-1640 medium. The larger MIC in YPD medium was probably due to the faster rate of growth.

Citral was dominant in ginger oils except for that from steam-heated rhizomes. Since citral itself

exhibited potent activity as shown in Table 4, it may be responsible for the oils' inhibition of filamentation and growth of *C. albicans*. β-bisabolene, one of the major sesquiterpenes in ginger oil, and β-caryophyllene had weak activity. Although they were not tested, other sesquiterpenes in ginger oil such as zingiberene did not appear to have significant activity.

Two oleoresins did not contain citral, and their inhibitory activity may be due to the potent activity by [6]-gingerol itself, as shown in Table 4. Ethanol oleoresin had a higher level of activity than did CO_2 oleoresin, which may be attributed to higher [6]-gingerol content as shown in Table 2. The inhibition of *C. albicans* growth by ginger oil has previously been reported (*22*), but inhibition of filamentation by ginger oil, oleoresin, or gingerol has not been reported. The mechanisms of inhibition of growth and filamentation may differ (*23*), and the inhibition of filamentation cannot not be predicted based on inhibition of growth.

C. albicans displays dimorphism with yeast and filamentous, or hyphal, forms and its filamentous form causes candidiasis (*24,25*). Furthermore, the filamentous form contributes to biofilm formation at the infection site to disturb the action of antimicrobial agents (*26*). Since ginger oil inhibits filamentation as well as growth of the yeast form, it may have use as a mouthwash to prevent oral candidiasis.

However, ginger oil had no significant DPPH radical scavenging activity. Instead, ginger oleoresin, and especially ethanol oleoresin, exhibited scavenging activity comparable to α-tochopherol. Since [6]-gingerol is an active pungent principal of ginger and is reported to have anti-oxidative (*27*) and anti-inflammatory activities (*28*), gingerol-rich oleoresin may provide protection from skin disorders and offer antioxidant and health benefits as a food additive.

Acknowledgements

The authors wish to thank Takako Miyara, CMC Research Laboratory, Meiji Seika Kaisha Ltd., Yokohama, Japan for her help with GC/MS and HPLC analyses and Hidemoto Kojima, Phyto-aroma Laboratories for providing samples of oils and CO_2 oleoresin.

References

1. Lim WC, Seo JM, Lee CI, Pyo HB, Lee BC. Stimulative and sedative effects of essential oils upon inhalation in mice. Arch Pharm Res. 2005; 28:770-774.
2. Riyazi A, Hensel A, Bauer K, Geissler N, Schaaf S, Verspohl EJ. The effect of the volatile oil from ginger rhizomes (*Zingiber officinale*), its fractions and isolated compounds on the 5-HT3 receptor complex and the serotoninergic system of the rat ileum. Planta Med. 2007; 73:355-362.
3. Zhou HL, Deng YM, Xie QM. The modulatory effects of the volatile oil of ginger on the cellular immune response *in vitro* and *in vivo* in mice. J Ethnopharmacol. 2006; 105:301-305.
4. Carrasco FR, Schmidt G, Romero AL, Sartoretto JL, Caparroz-Assef SM, Bersani-Amado CA, Cuman RK. Immunomodulating activity of *Zingiber officinale* Roscoe, *Salvia officinalis* L. and *Syzygium aromaticum* L. essential oils: Evidence for humor- and cell-mediated responses. J Pharm Pharmacol. 2009; 61:961-967.
5. Nogueira de Melo GA, Grespan R, Fonseca JP, Farinhc TO, da Silva EL, Romero AL, Bersani-Amado CA, Cuman RK. Inhibitiory effects of ginger (*Zingiber officinale* Roscoe) volatile essential oil on leucocyte migration in migration *in vivo* and *in vitro*. J Nat Med. 2011; 65:241-246.
6. López P, Sánchez C, Batlle R, Nerín C. Solid- and vapor-phase antimicrobial activities of six essential oils: Susceptibility of selected foodborne bacteria and fungal strains. J Agric Food Chem. 2005; 53:6939-6946.
7. Waranee P, Srikanjana K, Siriporn O. Bactericidal action of *Alpinia galangal* essential oil food-borne bacteria. Drug Discov Ther. 2011; 5:84-89.
8. Inouye S, Takahashi M, Abe S. Composition, antifungal and radical scavenging activities of 15 rare essential oils. Int J Essent Oil Ther. 2010; 4:1-10.
9. Abe S, Sato Y, Inoue S, Ishibashi H, Maruyama N, Takizawa T, Oshima H, Yamaguchi H. Anti-*Candida* albicans activity of essential oils including lemongrass (*Cymbopogon citratus*) oil and its component, citral. Nihon Ishinkin Gakkai Zasshi. 2003; 44:285-291.
10. Takahashi M, Inouye S, Abe S. Composition and antifungal activity of 15 essential oils obtained from Japanese trees. Aroma Res. 2011. (In press)
11. Sakamura F. Changes in volatile constituents of *Zingiber officinale* rhizomes during storage and cultivation. Phytochemistry. 1987; 26:2207-2212.
12. Singh G, Kapoor IP, Singh P, de Heluani CS, de Lampasona MP, Catalan CA. Chemistry, antioxidant and antimicrobial investigations on essential oil and oleoresins of *Zingiber officinale*. Food Chem Toxicol. 2008; 46:3295-3302.
13. Chen CC, Ho CT. Volatile compounds in ginger oil generated by thermal treatment. In: Thermal Generation of Aromas: Vol. 409. ACS publication, Washington, DC, USA, 1989; pp. 366-375.
14. Taroeno, Brophy JJ, Zwaving JH. Analysis of the essential oil of *Zingiber cassumumar* Roxb. from Indonesia. Flavour Fragr J. 1991; 6:161-163.
15. Bhuiyan MNI, Chowdhury JU, Begum J. Volatile constituents of essential oils isolated from leaf and rhizome of *Zingiber cassumumar* Roxb. Bangladesh J Pharmacol. 2008; 3:69-73.
16. Lu Y, Zhong CX, Wang L, Lu C, Li XL, Wang PJ. Anti-inflammatory activity and chemical composition of flower essential oil from *Hedychium coronarium*. Afr J Biotechnol. 2009; 8:5373-5377.
17. Bottini AT, Garfagnoli DJ, Delgado LS, Dev V, Duong ST, Kelley CG, Keyer R, Raffel R, Joshi P, Mathela CS. Sesquiterpenes alcohol from *Hedychium spicatum* var. *acuminatum*. J Nat Prod. 1987; 50:732-734.
18. Sabulal B, George V, Dan M, Pradeep NS. Chemical composition and antimicrobial activities of the essential oils from the rhizomes of four *Hedychium* species from south India. J Essent Oil Res. 2007; 19:93-97.
19. Murakami S, Li W, Matsuura M, Satou T, Hayashi S, Koike K. Composition and seasonal variation of essential oil in *Alpinia zerumbet* from Okinawa Island. J Nat Med.

2009; 63:204-208.
20. Lv Q, Qin J, Chen T. GC-MS Analysis of chemical components in volatile oil from the flowers of *Zingiber myoga* Rosc. Physical Testing and Chemical Analysis Part B Chemical Analysis. 2004; 40:405-407.
21 Pozzatti P, Scheid LA, Spader TB, Atayde ML, Santurio JM, Alves SH. *In vitro* activity of essential oils extracted from plants used as spices against fluconazole-resistant and fluconazole-susceptible Candida spp. Can J Microbiol. 2008; 54:950-956.
22. Ficker C, Smith ML, Akpagana K, Gbeassor M, Zhang J, Durst T, Assabgui R, Arnason JT. Bioassay-guided isolation and identification of antifungal compounds from ginger. Phytother Res. 2003; 17:897-902.
23. Inouye S, Takahashi M, Abe S. Inhibitory activity of hydrosols, herbal teas and related essential oils against filament formation and the growth of *Candida albicans*. Jpn J Med Mycol. 2009; 50:243-251.
24. Villar CC, Kashleva H, Dongari-Bagtzoglou A. Role of *Candia albicans* polymorphism in interactions with oral epithelian cells. Oral Microbiol Immunol. 2004; 19:262-269.
25. Hisajima T, Ishibashi H, Yamada T, Nishiyama Y, Yamaguchi H, Funakoshi K, Abe S. Invasion process of *Candida albicans* to tongue surface in early stages of experimental murine oral candidiasis. Med Mycol. 2008; 46:697-710.
26. Katsuyama M, Ichikawa H, Ogawa S, Ikezawa Z. A novel method to control the balance of skin microflora. Part 1. Attack on biofilm of *Staphylococcus aureus* without antibiotics. J Dermatol Sci. 2005; 38:197-205.
27. Masuda Y, Kikuzaki H, Hisamoto M, Nakatani N. Antioxidant properties of gingerol related compounds from ginger. Biofactors. 2004; 21:293-296.
28. Young HY, Luo YL, Cheng HY, Hsieh WC, Liao JC, Peng WH. Analgesic and anti-inflammatory activities of [6]-gingerol. J Ethnopharmacol. 2005; 96:207-210.

(*Received September 13, 2011; Accepted September 21, 2011****)***

Original Article

DOI: 10.5582/ddt.2011.v5.5.246

Development of microemulsion of a potent anti-tyrosinase essential oil of an edible plant

Kiattisak Saeio[1], Songwut Yotsawimonwat[1], Songyot Anuchapreeda[2], Siriporn Okonogi[1,*]

[1] *Faculty of Pharmacy, Chiang Mai University, Chiang Mai, Thailand;*
[2] *Faculty of Associated Medical Sciences, Chiang Mai University, Chiang Mai, Thailand.*

ABSTRACT: The aim of this study is to develop a microemulsion product from a plant essential oil having the highest anti-tyrosinase activity. The *in vitro* anti-tyrosinase activity of six essential oils extracted from six edible plants was compared. The oil of *Cymbopogon citratus* demonstrated the highest activity which was significantly nontoxic to normal human cells. The GC-MS data indicated that geranial and neral are the major compounds in the oil. The phase diagram composed of *C. citratus* oil, water, and surfactant mixture was conducted by a titration method. Ethyl alcohol was found to be the most suitable cosurfactant for the *C. citratus* oil microemulsion. The results revealed that the amount of oil and water played an important role in microemulsion conductivity and type. The most desirable o/w type of *C. citratus* oil microemulsion was found to be composed of 20% oil, 30% water, and 50% surfactant mixture of a 2:1 weight ratio of Tween 20 and ethyl alcohol.

Keywords: *Cymbopogon citratus*, antityrosinase, essential oil, microemulsion, plant

1. Introduction

Tyrosinase is an enzyme involved in melanin production *via* an enzymatic oxidative pathway which is of considerable importance in the coloring of skin, hair, eyes, and in some food browning (*1*,*2*). Chemical agents that demonstrate anti-tyrosinase activity have been used in clinical medicine for the treatment of some dermatologic disorders associated with melanin hyperpigmentation (*3*), and are useful in cosmetic preparations and the food industry (*4*,*5*). Melanin production might be responsible for some of the histo-pathological features exclusive to malignant cancer. Therefore, anti-tyrosinase substances may be clinically helpful in dealing with skin cancer. In recent years, more attention has been paid to the use of natural products instead of chemical or synthetic compounds in order to be not only economical but also environmentally friendly as well as safe. Moreover, the exploration of green technology and of low cost raw materials is an important feature for the industry as well as for making improved use of plant resources. Recently, the anti-tyrosinase activity from the methanol and acetone extracts of certain plants has been reported (*6*). However, there is less data from essential oils of natural plants. Therefore, searching for plant essential oils which possesses high anti-tyrosinase activity is of interest. The attempt is to develop a suitable microemulsion from such oils would be beneficial for pharmaceutical and cosmetic applications.

A microemulsion is a thermodynamically stable and clear dispersion composed of two immiscible liquids, usually oil and water. Microemulsions have received increasing attention as drug delivery systems during the past several years because they have many potential characteristics suitable for pharmaceutical and cosmetic applications such as enhanced aqueous solubilization of lipophilic compounds, increased drug permeation rates, good thermodynamic stability, and ease of preparation (*7*,*8*). The immiscible lipophilic and hydrophilic liquids in microemulsions can be assembled into a one clear liquid phase system by using surfactant and cosurfactant (*9*,*10*). In most cases, the lipophilic liquids used for microemulsion are inactive or less biologically active oils. Research on plants have explored the potential of essential oils extracted from plants for anti-fertility (*11*,*12*), anti-antioxidant (*13*,*14*), anti-inflammatory, and antimicrobial activities (*15*-*17*). Recently the anti-tyrosinase activity of rose, carnation, and hyacinth oils has been reported (*18*).

In the present study, several edible essence plants believed by local people in Thailand to support skin whitening were collected. The anti-tyrosinase

**Address correspondence to:*
Dr. Siriporn Okonogi, Department of Pharmaceutical Science, Faculty of Pharmacy, Chiang Mai University, Chiang Mai 50200, Thailand.
e-mail: sirioko@chiangmai.ac.th

activity of the essential oils extracted from these plants was compared. The microemulsion of the oil which possessed the highest activity was developed by using a phase diagram. The effect of oil, water, and surfactant quantity as well as the type of cosurfactant on the characteristics of the microemulsion was examined.

2. Materials and Methods

2.1. *Plant materials and essential oil extraction*

Six edible plant samples; *Cymbopogon citratus*, *Eryngium foetidum*, *Ocimum canum*, *Alpinia galanga*, *Curcuma longa*, and *Curcuma zedoaria* were collected from a local garden located in Chiang Mai, Thailand during June 2010. The plants were authenticated and the voucher specimens were deposited in the Herbarium of the Faculty of Pharmacy, Chiang Mai University, Thailand. The fresh aerial parts of *C. citratus*, *E. foetidum*, and *O. canum* and the fresh rhizomes of *A. galanga*, *C. longa*, and *C. zedoaria* were cut into small pieces and subjected to a hydro-distillation apparatus for 3 h using a Clevenger type apparatus to collect the oil. The essential oils were dried over anhydrous sodium sulfate and kept in light protected containers at 4ºC until further experiments.

2.2. *Chemicals and reagents*

Mushroom tyrosinase and L-dopa were purchased from Fluka Chemical Co. (Japan). Ethyl alcohol, propyl alcohol, and butyl alcohol were obtained from Fisher Chemicals (Loughborough, UK). Dimethylsulfoxide (DMSO) was from Fisher Scientific (Leicestershire, UK). These reagents were of analytical grade. Polyoxyethylene sorbitan monolaurate (Tween 20) of pharmaceutical grade was purchased from Namsiang Co., Ltd. (Bangkok, Thailand). Other chemicals were of the highest grade available.

2.3. *Determination of antityrosinase activity*

Anti-tyrosinase activity of the essential oils was determined using the modified dopachrome method with L-dopa as substrate (*19*). Assays were conducted in a 96-well microtitre plate. Test samples were dissolved in 50% DMSO. Each well contained 40 µL of sample, 80 µL of phosphate buffer solution (PBS) (0.1 M, pH 6.8), 40 µL of tyrosinase (200 units/mL) and 40 µL of L-dopa (2 µM). The microplate reader was read at 450 nm. Each sample was accompanied by a blank that had all the components except L-dopa. Results were compared to a control consisting of 50% DMSO in place of the sample. The anti-tyrosinase activity of the oil samples expressed as percentage tyrosinase inhibition was calculated using the following equation.

$$\% \text{ Inhibition} = 100 \times (Ac - As)/Ac$$

where Ac is the absorbance of control and As is the absorbance of sample.

2.4. *Cytotoxicity tests*

The cytotoxicity of oil samples on normal human cells using peripheral blood mononuclear cells (PBMCs) was determined using a colorimetric technique and the 3-(4,5-dimethylthiazol-2-yl)-2,5-diphenyltetrazolium bromide (MTT) assay. PBMCs were plated in 96-well plates to obtain a cell concentration of 1×10^5 cells/well. Serial dilutions of oils were added to the wells. The wells were incubated in a 37°C, 5% CO_2 and 90% humidity incubator for 48 h. After the corresponding time, 15 µL of MTT at 5 mg/mL was added into each well in the 96-well plate and further incubated for 4 h in a 37°C, 5% CO_2 and 90% humidity incubator. One hundred and seventy microlitres of medium with MTT was removed from every well and 100 µL DMSO was added to each well to extract and solubilize the formazan crystals by incubating for 20 min in a 37°C, 5% CO_2 incubator. Finally, the plate was read at 540 nm using an ELISA Reader. The percentage of cell viability was calculated by the following formula.

$$\% \text{ Cell viability} = 100 \times (Ds - Dc)/Dc$$

where Ds is the OD of sample and Dc is the OD of control.

2.5. *GC-MS analysis*

The essential oil which showed the highest anti-tyrosinase activity was subjected to GC-MS in order to analyze the components existing in the oil. The GC-MS analysis was performed on an Agilent 6890 gas chromatograph coupled to electron impact (EI, 70 eV) using an HP 5973 mass selective detector fitted with a fused silica capillary column (HP-5MS) supplied by HP, Palo Alto, CA, USA (30.0 m × 250 mm, *i.d.* 0.25 mm film thickness). The analytical conditions were; carrier gas: helium (ca. 1.0 mL/min), injector temperature: 260°C, oven temperature: 3 min isothermal at 100°C (No peaks before 100°C after first injection), then at 3ºC/min to 188°C and then at 20°C/min to 280°C (3 min isothermal), and detector temperature: 280°C. The programmed-temperature Kováts retention indices (RI) were obtained by GC-MS analysis of an aliquot of the volatile oil spiked with an *n*-alkane mixture containing each homologue from *n*-C11 to *n*-C27. Identification of the compounds was based on a comparison of their mass spectra database (WILEY&NIST) and spectroscopic data. The percentage amount of each component was calculated based on the total area of all peaks

obtained from the oil. The data obtained were used as a standard for further batches of the oil.

2.6. *Construction of phase diagrams*

The pseudo-ternary phase diagram of *C. citratus* oil was constructed using a water titration method (*20*). Tween 20 was mixed with different cosurfactants (ethyl alcohol, propyl alcohol, or butyl alcohol) at a weight ratio of 2:1 to obtain a surfactant mixture. For each phase diagram, the weight ratios of the oil and the surfactant mixture were varied as ratios of 1:9, 2:8, 3:7, 4:6, 5:5, 6:4, 7:3, 8:2, and 9:1. These mixtures were titrated with water, under moderate agitation at ambient temperature. The phase boundary was determined by observing the changes of the sample appearance going from transparent to turbid. The experiment was done in triplicate. The pseudo-ternary phase diagram was drawn by SigmaPlot for Windows version 10.0. The samples were classified as microemulsions when they appeared as a clear liquid.

2.7. *Preparation and characterization of microemulsions*

Several microemulsion formulas of *C. citratus* oil were developed by mixing the oil with other components presented in the microemulsion region of the most suitable phase diagram obtained with moderate agitation at ambient temperature. The microemulsions obtained were characterized for conductivity and microemulsion type.

2.8. *Conductivity measurement*

The electrical conductivity of the microemulsion was measured using a Cyberscan CON 11: hand-held conductivity meter (Eutech instruments, Singapore) using a conductivity/TDS electrode cell. The experiment was performed at 25 ± 1.0°C by dipping the electrode into the test sample until equilibrium was reached and the reading became stable. The performance was done in triplicate.

2.9. *Microemulsion type determination*

The type of microemulsion was judged by color diffusion using oil soluble sudan red and water soluble methylene blue solutions. If the red diffused faster than the blue, the microemulsion was the w/o type. On the contrary, if the blue diffused faster than red, it was the o/w type.

3. Results and Discussion

3.1. *Antityrosinase activity and safety of the oils*

It is known that tyrosinase, a copper-containing monooxygenase, widely distributed in microorganisms, animals, and plants, is an important enzyme implicated in melanin biosynthesis mainly using two distinct reactions of monophenolase and diphenolase activities (*21*,*22*). The overall activity of this enzyme can cause epidermal hyperpigmentation which leads to various dermatological disorders such as melasma, freckles, age spots, and skin cancer (*23*). Compounds having an anti-tyrosinase activity hence are, so far, the agents of interest in treatment and prevention of those dermatological disorders. The essential oils extracted by hydro-distillation of six different edible plants used in this study demonstrated their activity on inhibition of tyrosinase activity as shown in Figure 1. Among them, the oil of *C. citratus* displayed the strongest anti-tyrosinase activity with an IC_{50} of 0.5 mg/mL followed distantly by *C. longa*, and *A. galanga* oils with an IC_{50} of 3.6 mg/mL as shown in Table 1. Compared to the other plant extracts previously reported (*19*) *e.g. Etlingera littorali*, *E. rubrostriata*, *E. maingayi*, and *E. fulgens*, the essential oil of *C. citratus* was more effective in tyrosinase inhibition than those plants. The essential oils of *C. citratus*, *C. longa*, and *A. galanga* hence were considered to be a group of high activity whereas the other three plant oils of *O. canum*, *E. foetidum*, and *C. zedoaria* in which the IC_{50} was higher were considered to be a low activity group. The three oils of the high potential group then were selected for further tests of cytotoxicity in order to interpret the safety to normal human cells.

The cell viability of human peripheral blood mononuclear cells (PBMCs) could indicate the safety of the oil samples. In general, cell viability greater than 80% after exposure to test samples is recognized as safe for human use (*24*). Figure 2 displays cell viability after contact with different concentration of the oils. The results demonstrate that after 48 h incubation with *C. citratus*, *C. longa*, and *A. galanga* oils, the cell viability was more than 80%. More importantly, it is noted that the cell viability after *C. citratus* oil exposure was constantly near 100% whereas that of *C. longa* and *A. galanga* oils was slightly decreased with higher oil concentration. This result indicates *C. citratus* oil is nontoxic to human cells.

According to the extremely highest anti-tyrosinase activity of *C. citratus* oil as well as its complete safety to human cells, this oil was considered to be the most effective in the inhibition of melanin formation and is suitable for further study. Prior to microemulsion development, the chemical composition of the oil was investigated by GC-MS. The result is demonstrated in Table 2. Twelve volatiles were identified, making up 89.5% of the total composition. The majority of this oil was monoterpene which comprised up to 85.2%. The most abundant constituents were geranial (42.0%) and neral (32.1%). This finding was in accordance with the previous published data on *C. citratus* oils by

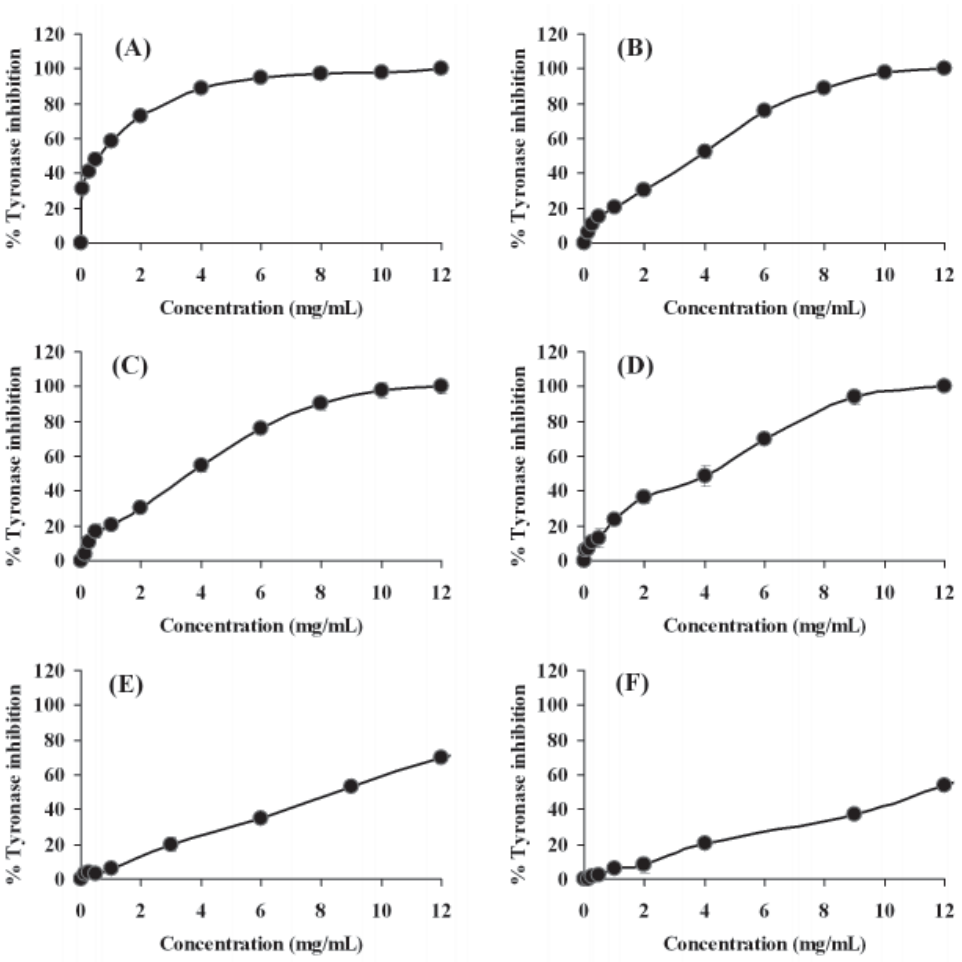

Figure 1. Effect of different oil concentrations of *C. citratus* (A), *C. longa* (B), *A. galanga* (C), *O. canum* (D), *E. foetidum* (E), and *C. zedoaria* (F) on inhibition of tyrosinase activity.

Table 1. The IC_{50} of anti-tyrosinase activity of the essential oils

Scientific name	IC_{50} (mg/mL)
C. citratus	0.5
C. longa	3.6
A. galanga	3.6
O. canum	4.2
E. foetidum	8.2
C. zedoaria	10.2

Blanco *et al*. (*25*) that geranial and neral were the main compounds of this oil. It is known that geranial and neral are isomers of citral. Matsuura *et al*. (*26*) reported that the tyrosinase inhibitory activity of citrus essential oils was relative to the abundance of citral. Our result was similar to this report that geranial and neral were related to this activity. Therefore, it was considered that these two compounds might play an important role in anti-tyrosinase activity.

3.2. *Phase diagram of microemulsion*

The pseudo-ternary phase diagrams with three different cosurfactants (C2-C4 alcohols) are shown in Figure 3. The transparent microemulsion region (ME) is

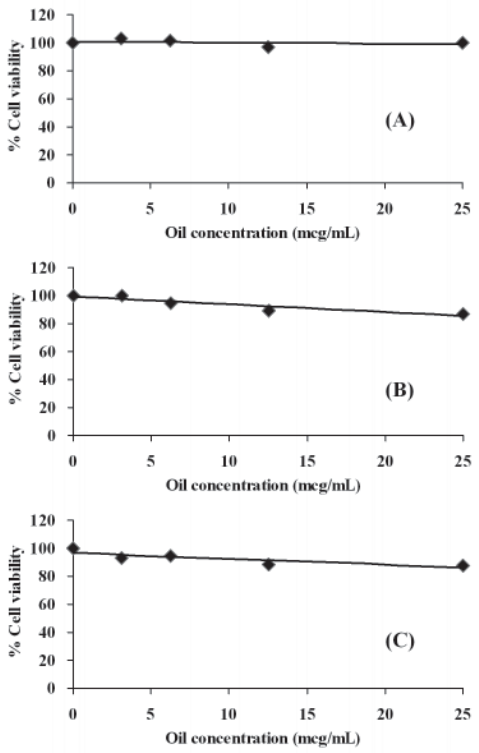

Figure 2. Cytotoxicity of the essential oils of *C. citratus* (A), *C. longa* (B), and *A. galanga* (C), on normal human PBMCs.

presented in the phase diagrams. It is obviously seen that alcohols of C2-C4 had a different effect. This is in contrast to the findings reported by Alany *et al*. (*27*) where no distinct trends were observed in the homologous series of the alcohols. However, the effect of alcohols may be influenced by the oil and surfactant combination used in the pseudoternary system. Among the three alcohols used in the present study, C2 alcohol (ethyl alcohol) showed the largest ME. Ethyl alcohol is safe and widely used in skin products. Moreover, it was reported that ethyl alcohol could act as a skin enhancer (*28*). Hence, ethyl alcohol was considered to be the most suitable cosurfactant for the *C. citratus* oil microemulsion. Therefore, it was selected to be used as a cosurfactant for the further study.

Table 2. Chemical compositions of the essential oil of *C. citratus*

Retention time (min)	Component	Peak area (%)
3.48	*trans*-β-Ocimene	0.58
4.07	*n*-Undecene	1.4
5.32	D-Camphor	0.49
5.75	(+)-Borneol	0.35
7.25	Neral	32.07
7.55	Geraniol	5.21
8.13	Geranial	42.01
11.38	Piperitenone oxide	2.25
11.53	Decaoic acid	0.79
11.72	α-Copaene	1.4
20.66	β-Maaliene	0.94
21.02	α-Cadinol	2.04
	Total	89.53

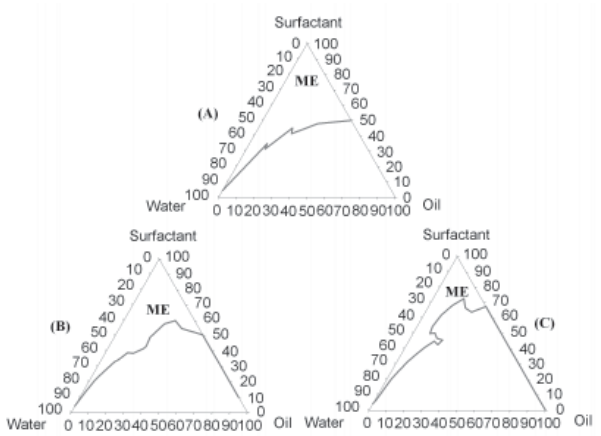

Figure 3. Pseudo-ternary phase diagrams of *C. citratus* oil microemulsions (ME) with different cosurfactants; ethyl alcohol (A), propyl alcohol (B), and butyl alcohol (C).

3.3. *Preparation and characterization of microemulsions*

In this study, three criteria were defined for the selection of microemulsion formulations from the developed phase diagrams; *i*) the percentage of oil should be more than 10%, *ii*) the type of microemulsion should be o/w, and *iii*) the amount of surfactant should be minimized. Because the ME in the pseudo-ternary phase diagram of *C. citratus* oil could be obtained using different amounts of oil, water, and surfactant in the system, eight formula compositions shown in Table 3 were prepared. The results revealed that all microemulsions obtained were clear with pale yellowish color solutions. The conductivity of each formulation was performed. It was found that high conductivity was obtained when the percentage of water was increased or when the oil was decreased. The dye solubility test is an excellent tool for determination of microemulsion type. In this study, the oil soluble red dye was not miscible with the o/w type but completely miscible with the w/o type whereas the water soluble blue dye demonstrated complete miscibility with microemulsions of the o/w type but not with the w/o type. The results showed that the o/w type could be obtained from the high conductivity microemulsion whereas in low conductivity microemulsions, the w/o type was observed. The result also indicated that when the conductivity of the system was above 40 μS/cm, the type of *C. citratus* oil microemulsion was reversed from w/o to o/w. Therefore, this conductivity value was considered to be a critical point of the microemulsion type. This value is slightly lower than previously reported by Yuan, *et al*. (*29*). However, this finding was in agreement with other authors that increasing the water fraction affected higher conductivity and o/w microemulsions were obtained (*30*). The present results

Table 3. The conductivity and emulsion type of various formulas of *C. citratus* oil microemulsions

Formulation	Composition (w/w)			Conductivity (μS)	Dye solubility test*
	Oil	Surfactant mixture	Water		
ME-1	10	50	40	98.47 ± 0.15	A
ME-2	10	60	30	68.17 ± 0.06	A
ME-3	10	70	20	45.33 ± 0.06	A
ME-4	20	50	30	63.50 ± 0.10	A
ME-5	20	60	20	41.37 ± 0.15	A
ME-6	30	50	20	32.73 ± 0.06	B
ME-7	30	60	10	26.30 ± 0.00	B
ME-8	40	50	10	19.08 ± 0.04	B

* A, Miscible with water soluble dye = o/w type; B, Miscible with oil soluble dye = w/o type.

demonstrate that the increase in percentage of oil could lead the microemulsion type to be w/o. The results from Table 3 exhibited that the highest percentage of oil that could produce a o/w type microemulsion could be obtained from formula ME-4 and ME-5 with an oil content of 20%. However, ME-4 contained less surfactant that ME-5. Therefore, formula ME-4 was considered to be the most desirable microemulsion of *C. citratus* oil.

4. Conclusion

The essential oil of *C. citratus* demonstrated the highest anti-tyrosinase activity among six edible plant oils. The GC-MS indicated that geranial and neral are the major compounds in the oil. The safety data suggested that *C. citratus* oil can be a promising plant oil effective and worthy for development of a microemulsion for anti-tyrosinase activity. The development of the *C. citratus* oil microemulsion indicated that ethyl alcohol was the best cosurfactant for the system using Tween 20 as a principle surfactant. The amount of oil and water in the formula played an important role on microemulsion conductivity and type. The most desirable formula for *C. citratus* oil microemulsion was composed of 20% oil, 30% water, and 50% surfactant mixture of a 2:1 weight ratio of Tween 20 and ethyl alcohol.

Acknowledgement

The authors are grateful for the financial support from the Thailand Research Fund (TRF) through grant number IUG 5080012. We also thank the Graduate school, Chiang Mai University for their support.

References

1. Azhar-Ul-Haq, Malik A, Khan MT, Anwar-Ul-Haq, Khan SB, Ahmad A, Choudhary MI. Tyrosinase inhibitory lignans from the methanol extract of the roots of *Vitex negundo* Linn. and their structure-activity relationship. Phytomedicine. 2006; 13:255-260.
2. Song KK, Huang H, Han P, Zhang CL, Shi Y, Chen QX. Inhibitory effects of *cis*- and *trans*-isomers of 3,5-dihydroxystilbene on the activity of mushroom tyrosinase. Biochem Biophys Res Commun. 2006; 342:1147-1151.
3. Okombi S, Rival D, Bonnet S, Mariotte AM, Perrier E, Boumendjel A. Analogues of *N*-hydroxy cinnamoylphenalkyl amides as inhibitors of human melanocyte-tyrosinase. Bioorg Med Chem Lett. 2006; 16:2252-2255.
4. Sugimoto K, Nomura K, Nishimura T, Kiso T, Sugimoto K, Kuriki T. Syntheses of alpha-arbutin-alpha-glycosides and their inhibitory effects on human tyrosinase. J Biosci Bioeng. 2005; 99:272-276.
5. Wang KH, Lin RD, Hsu FL, Huang YH, Chang HC, Huang CY, Lee MH. Cosmetic applications of selected traditional Chinese herbal medicines. J Ethnopharmacol. 2006; 106:353-359.
6. Momtaz S, Mapunya BM, Houghton PJ, Edgerly C, Hussein A, Naidoo S, Lall N. Tyrosinase inhibition by extracts and constituents of *Sideroxylon inerme* L. stem bark,used in South Africa for skin lightening. J Ethnopharmacol. 2008; 119: 507-512.
7. Lawrence MJ, Rees GD. Microemulsion-based media as novel drug delivery systems. Adv Drug Deliv Rev. 2000; 45:89-121.
8. Sintov AC, Botner S. Transdermal drug delivery using microemulsion and aqueous systems: Influence of skin storage conditions on the *in vitro* permeability of diclofenac from aqueous vehicle systems. Int J Pharm. 2006; 311:55-62.
9. Kawakami K, Yoshikawa T, Moroto Y, Kanaoka E, Takahashi K, Nishihara Y, Masuda K. Microemulsion formulation for enhanced absorption of poorly soluble drugs. I. Prescription design. J Control Release. 2002; 81:65-74.
10. Flanagan J, Kortegaard K, Pinder DN, Rades T, Singh H. Solubilisation of soybean oil in microemulsions using various surfactants. Food Hydrocolloids. 2006; 20:253-260.
11. Biswas K, Chattopadhyay I, Banerjee RK, Bandyopadhyay U. Biological activities and medicinal properties of neem (*Azadirachta indica*). Curr Sci. 2002; 82:1336-1345.
12. Prakash O, Kasana VK, Pant AK, Zafar A, Hore SK, Mathela CS. Phytochemical composition of essential oil from seeds of *Zingiber roseum* Rosc. and its antispasmodic activity in rat duodenum. J Ethnopharmacol. 2006; 106:344-347.
13. Politeo O, Jukic M, Milos M. Chemical composition and antioxidant capacity of free volatile aglycones from basil (*Ocimum basilicum* L.) compared with its essential oil. Food Chem. 2007; 101:379-385.
14. Miguel G, Simoes M, Figueiredo AC, Barroso JG, Pedro LG, Carvalho L. Composition and antioxidant activities of the essential oils of *Thymus caespititius*, *Thymus camphoratus* and *Thymus mastichina*. Food Chem. 2004; 86:183-188.
15. Kelen M, Tepe B. Chemical composition, antioxidant and antimicrobial properties of the essential oils of three *Salvia* species from Turkish flora. Biores Technol. 2008; 99:4096-4104.
16. Burt S. Essential oils: Their antibacterial properties and potential applications in foods – a review. Int J Food Microbiol. 2004; 94:223-253.
17. Chang ST, Chen PF, Chang SC. Antibacterial activity of leaf essential oils and their constituents from *Cinnamomum osmophloeum*. J Ethnopharmacol. 2001; 77:123-127.
18. Zhu YJ, Zhou HT, Hu YH, Tang JY, Su MX, Guo YJ, Chen QX, Liu B. Antityrosinase and antimicrobial activities of 2-phenylethanol, 2-phenylacetaldehyde and 2-phenylacetic acid. Food Chem. 2011; 124:298-302.
19. Chan EWC, Lim YY, Wong LF, Lianto FS, Wong SK, Lim KK, Joe CE, Lim TY. Antioxidant and tyrosinase inhibition properties of leaves and rhizomes of ginger species. Food Chem. 2008; 109:477-483.
20. Pons R, Carrera I, Caelles J, Rouch J, Panizza P. Formation and properties of miniemulsions formed by microemulsions dilution. Adv Colloid Interface Sci. 2003; 106:129-146.
21. Hsu CK, Chang CT, Lu HY, Chung YC. Inhibitory effects of the water extracts of *Lavendula sp*. on mushroom

tyrosinase activity. Food Chem. 2007; 105:1099-1105.
22. Seo SY, Sharma VK, Sharma N. Mushroom tyrosinase: Recent prospects. J Agr Food Chem. 2003; 51:2837-2853.
23. Kim YJ, Uyama H. Tyrosinase inhibitors from natural and synthetic sources: Structure, inhibition mechanism and perspective for the future. Cell Mol Life Sci. 2005; 62:1707-1723.
24. Yeap SK, Alitheen NB, Ali AM, Omar AR, Raha AR, Suraini AA, Muhajir AH. Effect of Rhaphidophora korthalsii methanol extract on human peripheral blood mononuclear cell (PBMC) proliferation and cytolytic activity toward HepG2. J Ethnopharmacol. 2007; 114:406-411.
25. Blanco MM, Costa CA, Freire AO, Santos JG Jr, Costa M. Neurobehavioral effect of essential oil of *Cymbopogon citratus* in mice. Phytomedicine. 2009; 16:265-270.
26. Matsuura R, Ukeda H, Sawamura M. Tyrosinase inhibitory activity of citrus essential oils. J Agr Food Chem. 2006; 54:2309-2313.
27. Alany RG, Rades T, Agatonovic-Kustrin S, Davies NM, Tucker IG. Effects of alcohols and diols on the phase behavior of quaternary systems. Int J Pharm. 2000; 196:141-145.
28. El Maghraby GM. Transdermal delivery of hydrocortisone from eucalyptus oil microemulsion: Effect of cosurfactants. Int J Pharm. 2008; 355:285-292.
29. Yuan Y, Li SM, Mo FK, Zhong DF. Investigation of microemulsion system for transdermal delivery of meloxicam. Int J Pharm. 2006; 321:117-123.
30. Zhu W, Yu A, Wang W, Dong R, Wu J, Zhai G. Formulation design of microemulsion for dermal delivery of penciclovir. Int J Pharm. 2008; 360:184-190.

(Received August 16, 2011; Revised October 13, 2011; Accepted October 14, 2011)

Original Article

DOI: 10.5582/ddt.2011.v5.5.253

Initial characterization of D-cycloserine for future formulation development for anxiety disorders

Gagan Kaushal[1,*], Ronaldo Ramirez[1], Demelash Alambo[1], Wacharah Taupradist[1], Krunal Choksi[1], Cristian Sirbu[2]

[1] *School of Pharmacy, University of Charleston, Charleston, WV, USA;*
[2] *Department of Behavioral Medicine and Psychiatry, School of Medicine, West Virginia University, Charleston Division, Charleston, WV, USA.*

ABSTRACT: The purpose of this study is to characterize D-cycloserine (DCS) physico-chemical properties to facilitate future formulation development of DCS for anxiety disorders. A stability-indicating HPLC assay method for the quantitation of DCS was developed and calibrated to be used for this study. The partition coefficient was determined and compared with the predicted value. The solution stability of DCS was studied under various pH (2-11.5) and ionic strengths of 10 and 20 mM at physiological temperature of 37°C. The 250 mg capsule was compounded to the nominal strength of 50 mg used for anxiety disorders. These capsules were then put under stability. The *in vitro* dissolution was also carried out at 37°C as per the United States Pharmacopeia (USP) guidelines. The partition coefficient value (Kp) determined for the DCS was log Kp = –2.89 ± 0.06 (*n* = 6). The pH-solution stability profile shows that DCS has maximum stability under alkaline conditions. The maximum rate of degradation was seen at pH of 4.7. The mean percent recovery of DCS from the capsules compounded to strength of 50 mg was 100.3 ± 1.4. The stability study of the reformulated capsules concluded that reformulated DCS is stable for at least one year at room temperature. The *in vitro* dissolution illustrates that all the DCS is released from the capsules in 10 min. The present characterization of DCS study will serve as guidance for the future directions regarding the reformulation of DCS in order to be used in anxiety disorders.

Keywords: D-Cycloserine, HPLC, stability, pH-solution stability, anxiety, formulation, physicochemical properties

**Address correspondence to:*
Dr. Gagan Kaushal, School of Pharmacy, University of Charleston, Charleston, WV 25304, USA.
e-mail: gagankaushal@ucwv.edu

1. Introduction

D-Cycloserine (DCS), an FDA approved drug under the name Seromycin® (D-cycloserine capsules, USP, 250 mg), (*R*)-4-amino-1,2-oxazolidin-3-one, is a broad-spectrum antibiotic that is produced by a strain of *Streptomyces orchidaceus* and has also been synthesized (Figure 1). It is used as a second line treatment for tuberculosis. Besides of that, *in vitro* studies have demonstrated that DCS has a high affinity, high efficacy partial agonist with moderate specificity for strychnine-insensitive excitatory (GLY-B) glycine site of the *N*-methyl-D-aspartate (NMDA) receptor (*1,2*). Based on its action on the NMDA receptors, recently this drug has been used on numerous clinical trials as an enhancer of exposure therapy for the treatment of anxiety disorders (*3-8*). DCS has been shown to facilitate exposure treatment and its consequential extinction learning and fear reduction in animal and human studies. Studies of acrophobia (fear of heights; (*4*)), social phobia/social anxiety disorder (*3*), and obsessive-compulsive disorder (*9,10*) have shown more rapid extinction learning and fear reduction with DCS when compared to placebo.

DCS first entered the market in 1952 and since the commercial introduction of DCS; very few studies have examined the physicochemical properties of this drug (*11,12*). Some of its physicochemical properties are listed in Table 1. In order to be used as an enhancer of exposure therapy for the treatment of anxiety disorders, the possibility of using this drug in different formulations, other than capsules, as well as using alternate routes of administration needs to be explored to maximize efficacy.

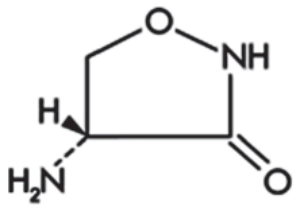

Figure 1. The structural formula of D-cycloserine.

Table 1. Physicochemical properties of D-cycloserine

Physicochemical parameter	DCS values (*16*)	ACD/PhysChem predicted values
Aqueous solubility	> 1 mg/mL	1,000 mg/mL
Partition coefficient	–1.631	–2.99
Molecular weight	102.09	102.09
Melting point	147°C	–
pH of saturated aqueous solution	5.5-6.5	–

Very few studies have explored these possibilities. The application of DCS through the nose mucosa for delivery to the brain was done by Musumeci *et al*. (*13*). This drug is very hydrophilic in character and cannot easily pass through the blood-brain barrier. Thus the nasal delivery gives the advantage of delivering this drug to the CNS and eliminates the need for systemic delivery. In their study (*13*), DCS liposomes were formulated for nasal delivery. The stability of the final formulation at different temperature (25, 37, and 60°C) and pH (5.0, 7.4, and 9.0) was studied by these researchers. In another recently published study by the same group (*14*), the feasibility of using DCS loaded w/o nanocapsules for intranasal delivery was explored as well.

DCS needs to be well characterized with the present technology before any new formulation can be developed for this compound. It is very important to know its stability under different conditions. These studies were done back in 1950s and 60s and investigated the stability of DCS at different pH values in aqueous solutions (*12,15,16*). The studies found that DCS is stable under alkaline conditions and is easily degraded under the acidic conditions. The conditions used for these studies and the analogues that resulted after degradation is inconsistent. No study so far has used a stability-indicating HPLC method to monitor the degradation peaks. The degradation peaks can be monitored easily by using an HPLC method and can help better understand the process of degradation. Knowing these conditions would be very important to further develop any formulation of DCS. Thus one of our objectives of this investigation is to study the effect of pH, ionic strength, and temperature on the stability of DCS using a stability indicating HPLC method.

An important challenge in studies examining DCS efficacy as an enhancer of exposure therapy for anxiety disorders is identifying the doses that are associated with the highest therapeutic efficacy. DCS is commercially available as a 250 mg capsule. However on examining the eight clinical trial studies that use DCS in patients with anxiety disorders, a dose of 50 mg is commonly used. In order to give these doses to the patients, the 250 mg capsule is reformulated to 50 mg capsules. It is very important to make sure that no degradation has taken place and the correct strength of DCS is being administered to the patient. Thus, in the present study, we have investigated the stability of 50 mg compounded DCS capsules and also analyzed the *in vitro* dissolution of these capsules.

2. Materials and Methods

2.1. *Materials*

D-Cycloserine was obtained from Research Products International Corp. (Mt. Prospect, IL, USA) and was used without further purification. All chemicals, buffer reagents, and solvents used were of analytical grade and were purchased from Fisher Chemicals (Fair Lawn, NJ, USA). HPLC grade water and acetonitrile were also purchased from Fisher Chemicals (Fair Lawn, NJ, USA) and used throughout this study.

Lactose and gelatin capsules size#3 used for the compounding in the present study were purchased from Professional Compounding Centers of America (PCCA, 9901 South Wilcrest Drive, Houston, TX, USA) and are approved for human consumption. The DCS capsules (Seromycin®, 250 mg) used for compounding was procured from our local pharmacy and was purchased by the pharmacy from The Chao Center (Purdue Research Park, 3070 Kent Avenue, West Lafayette, IN, USA).

2.2. *HPLC method for DCS analysis*

For the analysis of DCS in unknown samples, a stability-indicating HPLC method for the separation and the detection of DCS in aqueous media was developed. All the chromatographic studies were performed on a Dionex Ultimate 3000 HPLC system connected with an absorbance detector. The separations were performed on Atlantis T3 C18 cartridge column (250 × 4.6 mm I.D., Waters Associates, Milford, MA, USA) with the column particle diameter of 5 µm. Column effluents were monitored at the wavelength of 220 nm for a run time of 5.0 min at the temperature of 30°C. For the mobile phase, 90% of 10 mM sodium phosphate buffer (pH 7.5) and 10% acetonitrile was used. The mobile phase was filtered and degassed before use. The flow rate was 0.75 mL/min with the injection volume of 10 µL.

2.3. *DCS standard curve*

The calibration of HPLC system was performed by constructing a standard curve using seven known concentrations of DCS. In order to prepare the standard curve, fixed amounts (25, 50, 100, 250, 500, 750, and 1,000 µg/mL) of standard DCS were respectively added to the HPLC grade water and these samples were analysed by using the standardized HPLC conditions.

Three quality control samples (30, 150 and 700 µg/mL) were processed and each of these samples was analyzed three times (inter-day variation) on three different days (intra-days variation). These were labeled as LQC (30 µg/mL), MQC (50 µg/mL), and HQC (700 µg/mL). The accuracy was calculated at each concentration as the ratio of the measured concentration to the nominal concentration multiplied by 100%.

The limit of quantitation (LOQ) of the method was defined as the lowest concentration that could be quantitatively determined with an acceptable precision and accuracy. The acceptable limits were defined as accuracy of 80-120% and precision of ≤ 20%.

2.4. *Stability-indicating assay and validation*

The suitability of the present HPLC conditions to be used as a stability-indicating method was tested by forced degradation of DCS. The forced degradation of all the samples was performed at an initial drug concentration of 500 µg/mL and was done under acidic and alkaline conditions. Acid hydrolysis was performed in a solution of pH of 1.5 adjusted with 1 M HCl and alkaline condition was carried out at pH of 12.5 adjusted with 1 M NaOH. Each of these two extreme pH solutions was prepared in triplicate. All the solutions were heated at 90°C for at least 4 h and the samples were withdrawn every hour. In order to see the effect of light, a standard concentration was also prepared and was stored at room temperature under normal fluorescent light. Each sample was analysed by HPLC using the standard conditions as explained above.

2.5. *Determination of partition coefficient*

The partition coefficient of DCS was determined in octanol against water. Water saturated with octanol was prepared by equilibrating 5 mL each of octanol and water by gentle stirring for 24 h using wrist action shaker (Model 75, Burrell Scientific, Pittsburgh, PA, USA) at room temperature. This solvent mixture was allowed to settle for 2 h and then 5 mg of DCS was added to this mixture in a 50 mL tube. The tube was again shaken using wrist action shaker for 24 h and was then left at room temperature for at least 2 h. A sample of 500 µL was taken from both the organic and aqueous phase for HPLC assay. The partition coefficients were then calculated as the ratio of the tested compound concentration in organic to that in the aqueous phase. The same procedure was followed by replacing the water phase with phosphate buffer saline (PBS, pH 7.4).

2.6. *pH-solution stability*

The stability study was designed as per a previous study done by Claudius *et al.* (*17*) on vancomycin with some modifications. DCS solution stability was analyzed under various pH (2.0-11.5) and ionic strength (10-20 mM) conditions at physiological temperature of 37°C. The buffers used for this study were as follows: 0.01 N HCl (pH 2.0), acetate (pH 4.7), phosphate (pH 7.0), Tris-HCl (pH 8.5), and phosphate (pH 11.5). The ionic strength was held constant at each buffer concentration by adjusting with sodium chloride. In addition, the stability was also analyzed in simulated gastric (SGF) and intestinal (SIF) fluids.

DCS samples were prepared in triplicate at a concentration of 500 µg/mL by dissolving it in the desired buffer in 25-mL type I clear glass vials (Wheaton Glass, Wheaton, IL, USA). The vials were then sealed with Teflon-coated butadiene stoppers and further covered with Parafilm® to minimize evaporation. Each of the vials was further wrapped with aluminum foil in order to protect from the light. Samples were stored in a static oven at 37°C and 1-mL samples were withdrawn, filtered and analyzed at 0, 1, 7, 15, 22, and 30 days, respectively.

2.7. *Reformulation of 50 mg DCS capsules*

Seromycin® (D-cycloserine) is available as a 250 mg capsule and was compounded to the nominal strength of 50 mg per capsule using standard compounding techniques following the USP (Chapter <1075>) and GMP guidelines. The capsules were manually filled using ProFill 100 Capsule Filling Machine (Capsugel, 535 North Emerald Road, Greenwood, SC, USA), which can fill 100 capsules at one time. At least six capsules were withdrawn from a batch of 100 capsules and were tested for weight variation test as per the USP guidelines (Chapter <905>) on uniformity of dosage units. For the assay analysis, three capsules were randomly withdrawn from the batch of compounded capsules and were assayed for the active content by the stability indicating HPLC procedure as outlined above.

2.8. *In vitro dissolution of DCS capsules*

In vitro dissolution is one of the most important tools that should be carried out in order to predict the *in vivo* performance of any dosage form. The *in vitro* dissolution was carried out at 37°C using Distek Dissolution System 2100C (Distek, Inc., North Brunswick, NJ, USA) as per the USP 32 guidelines. The dissolution media used for the studies was phosphate buffer (pH 6.8) and was prepared as per the USP guidelines. The USP dissolution Apparatus I set at speed of 100 rpm with 900 mL of buffer was used for this study. Both, 50 and 250 mg capsules of DCS were used for the dissolution study.

Samples (10 mL) of dissolution medium were removed at regular time intervals for up to 30 min. An equal volume of dissolution medium at 37°C was added to maintain a constant volume. The samples were prepared and the drug concentration was quantified by the standardized HPLC method outlined above. Six capsules were used for this study to make the data statistically significant and this experiment was repeated on three different days.

2.9. *Data analysis*

Statistical analysis was performed using Student's *t*-test or Two Way ANOVA. $p < 0.05$ was indicative of a significant difference.

3. Results

3.1. *Standard curve and method validation*

The chromatogram of DCS standards shows a peak at retention time of 3.5 min (Figure 2). A blank sample was also injected to the HPLC system and no peak was observed from this sample. As shown in Figure 3, a good linearity was exhibited in the concentration range (25-750 μg/mL) by using the presently developed HPLC method. The average coefficient of determination of 0.99 was observed for the standard curve. The slopes of the curves illustrated an excellent agreement with coefficient of variability.

The % R.S.D. values for intra-day precision study were < 1.0% and for inter-day study were < 2.0%, confirming that the method was sufficiently precise. An acceptable precision and accuracy was acquired by this method for all the standards and quality controls based on the recommended criteria (*18*). The percentage recovery of DCS using the present HPLC method was also calculated from the peak areas obtained. As shown from the data in Table 2, an admirable recovery was obtained at each of the added concentration. In accordance to the official requirements the limit of quantitation (LOQ) for the present method was 30 μg/mL.

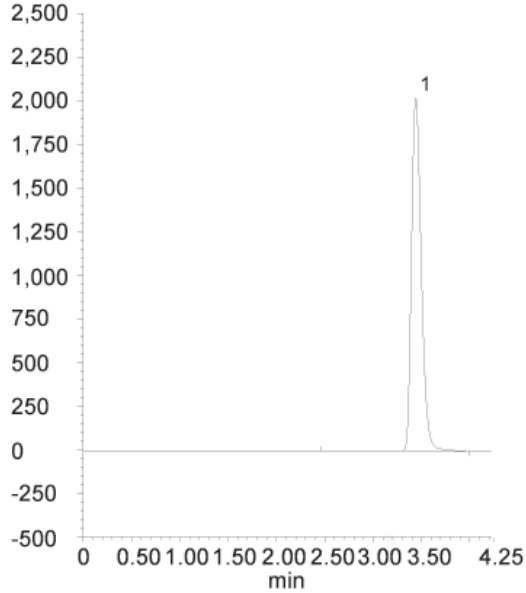

Figure 2. A representative HPLC chromatogram of D-cycloserine.

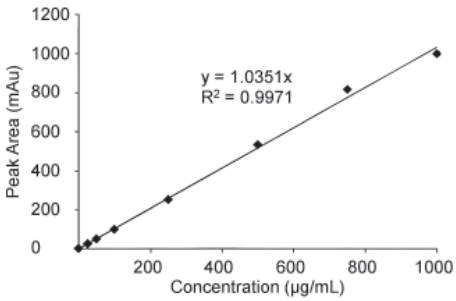

Figure 3. A standard curve for the HPLC assay of D-cycloserine.

3.2. *Stability-indicating HPLC method characterization*

One of our major goals was to develop a stability-indicating method for the detection of DCS. As soon as the DCS was added to a low pH solution, a significant degradation was observed. As per Figure 4A, a degradation peak was seen at the retention time of 3.39 min and there was a significant decrease in the DCS peak after adding DCS to low pH (1.5) solution

Table 2. D-Cycloserine HPLC assay precision and accuracy (*n* = 9)

Concentration added (μg/mL)	Concentration obtained (mU/mL)	CV* (%)	RE# (%)	Recovery (%)
30	0.336	6.24	6.6	106.7
150	3.24	2.76	2.8	102.3
700	9.59	0.57	1.6	101.5

* Coefficient of Variation. # Relative Error.

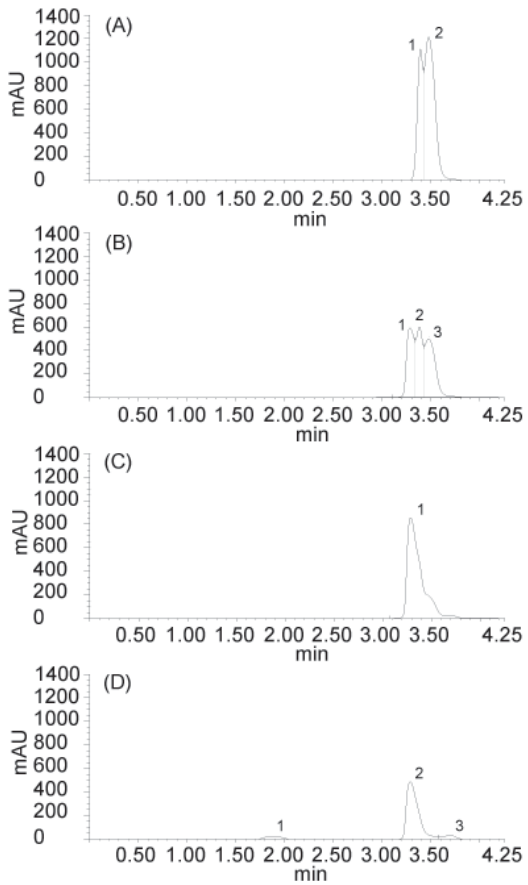

Figure 4. Chromatograms of D-cycloserine subjected to accelerated degradation at low pH of 1.5 after heating at 90°C for (A) 0 h; (B) 1 h; (C) 2 h; and (D) 4 h. The samples were analyzed by HPLC described above.

of water. As compared to the standard, the peak area of DCS decreased to around 60%, thus there was at least 40% degradation of DCS at this pH. After heating this solution at 90°C at low pH for 1 h, one more degradation product was seen on HPLC analysis (Figure 4B). In addition to the already observed degradation product 1 (deg1), observed at 3.38 min, another degradation product (deg2) was also seen at the retention time of 3.28 min. As seen in Figure 4C, after 2 h at 90°C, no peak due to deg1 was seen and only one peak of deg2 product was seen and the peak area of this product was more than double as compared to the peak area observed at 1 h (increased from around 50 mAU*min to around 140 mAU*min). After heating for 4 h, the deg2 peak decreased to half as compared to the peak area observed at 2 h (from peak area of around 140 mAU*min to around 70 mAU*min) as displayed in Figure 4D.

Under alkaline conditions, upon heating the DCS solution at 90°C, no significant change (*t*-test, $p > 0.05$) in peak area was observed for up to 3 h. Under these conditions, a reduction in peak area of DCS to around 86% was seen after 4 h. This peak further decreased to around 80% after 2 days and then to around 58% after 5 days. Standard samples were also prepared in distilled water and were subjected to high temperature of 90°C. No significant degradation (*t*-test, $p > 0.05$) was seen until 3 h. After 24 h, the peak decreased to around 60% and then further decreased to 46% after 2 days.

The DCS was observed to be light-sensitive as well because there was a decrease to around 88% of the initial concentration after 24 h when DCS was exposed to normal fluorescent light. From day one onwards, the decrease in DCS amount shows first-order degradation rate (data not shown). Thus all the DCS samples for our future studies were protected from light.

3.3. *Partition coefficient*

In our study, the partition coefficient value (Kp) determined for the DCS was logKp = –2.89 ± 0.06 ($n = 6$) for octanol against water. The log Kp value when PBS was used as an aqueous phase was –2.94 ± 0.06 ($n = 6$). LogKp and other physicochemical constants were predicted by using ACD/PhysChem software (ACD/Labs, ver. 12.01, Advanced Chemistry Development, Inc., Toronto, ON, Canada, 2010) and the predicted values are reported in Table 1. The logKp value calculated by our studies is very close to this value. The logKp value is not very well reported in the literature and very few studies that do report this value do not cite a reference to substantiate the study carried out to determine this value. To date this is the only study where an actual analysis is done to measure the partition coefficient value and compare it with the predicted value.

3.4. *pH-solution stability*

As per the pH-solution stability profiles at different pH values (Figure 5), DCS shows extensive degradation at acidic pH values of 2.0 and 4.7. At both these pH values, the degradation was buffer ionic concentration dependent and there was a significant increase (*t*-test, $p < 0.05$) with the increase in buffer ionic concentration. At the neutral pH of 7, the degradation was not as rapid as observed at the acidic pH values. The DCS degraded to around 10% of the initial concentration in one week. No significant effect (*t*-test, $p > 0.05$) of buffer ionic concentration on the degradation of DCS was seen at the neutral pH. At slightly basic pH of 8.5, DCS shows a better stability and the effect was buffer concentration dependent as well. DCS shows significantly higher (*t*-test, $p < 0.05$) degradation at lower buffer concentration of 10 mM as compared to 20 mM. The minimum degradation of DCS was observed at the highly basic pH of 11.5. At this pH, no significant change (*t*-test, $p > 0.05$) in DCS concentration was observed over a period of 30 days and this effect was seen at both the buffer concentrations. These studies were carried out at an ambient temperature of 37°C. In our forced degradation study carried out at 90°C, the highly basic solution of DCS (pH 12.5) shows maximum stability under these adverse conditions as well.

3.5. *Reformulation of 50 mg DCS capsules*

The reformulated DCS capsules were stored under the standard conditions of room temperature (between 22 and 25°C) and three capsules samples were withdrawn

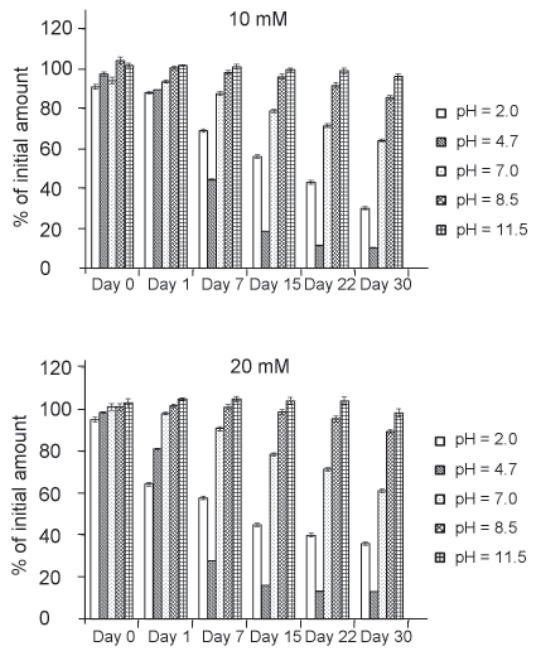

Figure 5. D-Cycloserine pH-stability profiles at 10 mM and 20 mM.

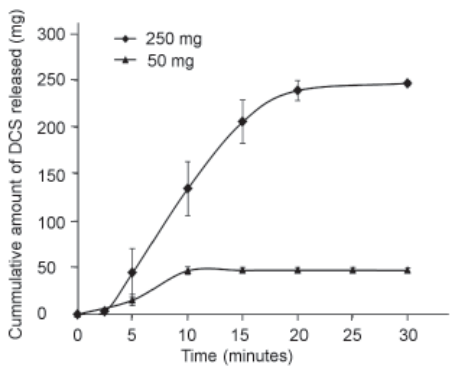

Figure 6. *In vitro* release profile of D-cycloserine from 250 and 50 mg capsules (*n* = 6).

for analysis at 0 day, 7 days, 15 days, 30 days and after every month until 12 months after this.

The weight variation test confirms to the limits as set by the USP. The percent recovery of DCS from the capsules was 100.3 ± 1.4 using this method. The stability of reformulated capsules has been done until 1 year and they contain at least 90% of the initial amount of DCS and thus are stable for at least 1 year at room temperature.

Our *in vitro* dissolution results show that all the DCS is released within 10 min from a 50 mg capsule (Figure 6). From a 250 mg capsule it takes at least 20 min for all the DCS to be completely released from the capsule.

4. Discussion

Cycloserine is degraded to serine and hydroxylamine and is relatively stable to alkali. Based on previous degradation studies, mild acid hydrolysis results in D-serine and hydroxylamine, while on prolonged hydrolysis DL-serine and hydroxylamine are formed (*15*). These were the first studies to report the hydrolysis of DCS. Prior to this, other researchers did carry out the degradation of DCS under different conditions (*15*). All these studies did observe the high stability of DCS under alkaline conditions as compared to the acidic conditions, but still the conditions that were used and the analogues that resulted were inconsistent. No study so far has used a stability-indicating HPLC method to monitor the degradation peaks.

The parent drug stability test guideline Q1A (R2) issued by International Conference on Harmonization (ICH) suggest that stress studies should be carried out on a drug to ascertain its inherent stability characteristics (*19*). A proper identification of degradation products would hence support the suitability of the proposed analytical procedures. It also requires that analytical test procedures for stability samples should be stability-indicating and be fully validated. In order to analyze the concentration of DCS, a stability-indicating HPLC method was validated and

Table 3. Degradation rate constants of D-cycloserine at 37°C

Buffer	pH	Order of reaction	Observed rate constant (day^{-1})	r^2
10 mM	2	First	1.9345	0.98
	4	Second	k_1 = 0.1601 k_2 = 7.567	0.99
	7	First	1.0334	0.99
	8.5	First	0.4989	0.96
	11.5	First	0.1793	0.94
20 mM	2	First	0.6508	0.93
	4	Second	k_1 = 0.1876 k_2 = 8.037	0.94
	7	First	1.3049	0.99
	8.5	First	0.401	0.91
	11.5	First	0.1987	0.95
–	SGF	First	1.2237	0.98
	SIF	First	1.6321	0.98

used for the present study. The present HPLC method meets all the acceptance criteria and was sensitive and reproducible enough for the acceptable study of DCS in unknown samples. As reported by Trissel (*20*), the failure to recognize the degradation products is the most common point that leads to erroneous reporting of the data on the stability studies. The present HPLC method does identify DCS and its degradation products based on the chromatograms of forced degradation of DCS. Thus, we can say that the present method is sufficiently specific to the drug and can simultaneously analyze DCS and its degradation products in a sample.

A drug's partition coefficient dictates the ease with which the drug reaches its intended target in the body, the potency of therapeutic response and also the transit time of the drug in the body. Thus the partition coefficient value can have a direct impact on both pharmacodynamics and pharmacokinetics of the drug. It is due to this fact that for any drug molecule, it is imperative to know this value.

DCS has good water solubility (as shown in Table 1) and based on its logKp value it can be concluded that this drug is mainly hydrophilic in character. Owing to the hydrophobic nature of the skin and its role as a barrier for keeping unwanted substances out of the body, it would be challenging to deliver a hydrophilic compound like DCS through topical route. Thus before any topical delivery system can be developed for DCS, it is very important to consider the use of an active delivery system to breach the skin barrier or other epithelial barriers, thereby allowing the drug to be absorbed in therapeutic amounts.

The degradation rate of DCS is adequately described by a pseudo first-order kinetic model for all stability samples except for pH 4. First order degradation rate constants for all the samples are included in Table 3 and have been estimated from the slopes of their corresponding log-linear plots. Extensive degradation was seen at pH value of 4 and fits into more complex second-order equation. The correlation coefficient for

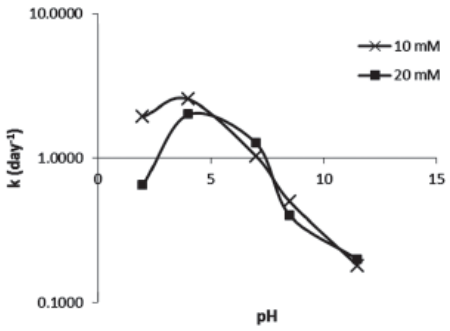

Figure 7. pH-rate profiles of D-cycloserine at 10 mM and 20 mM based on first order degradation rates.

second-order at this pH was observed to be 0.99 and 0.94 at buffer concentrations of 10 and 20 mM, respectively.

From this data, the pH of maximum stability appears to be alkaline pH of around 11.5. There was no ionic catalysis observed in the samples from buffer concentrations of 10 to 20 mM based on analysis of variance (ANOVA) at pH values of 7, 8.5, and 11.5. A probability level of $p = 0.05$ or greater indicates that no significant difference exists between the degradation rate constants estimated at 10 and 20 mM buffer concentrations. At pH of 2.0, a higher rate of degradation was observed at higher ionic strength of 20 mM as compared to 10 mM. From the plot of log K_{obs} versus pH (Figure 7), it is very clear that the reaction is primarily catalyzed by H^+ ion. DCS shows very minimal or no degradation at high pH and thus is not catalyzed by OH^- ion.

The dose of 50 mg is being used on all the clinical trials for anxiety disorders. In order to give a dose of 50 mg to the patients, the 250 mg capsule is reformulated to a 50 mg capsule. Currently, there are no pharmaceutical studies investigating the reformulation of DCS to a nominal strength. Thus, it is very important to monitor the stability of these reformulated capsules. Based on our results, these capsules do show appreciable stability at room temperature for 1 year. The *in vitro* dissolution illustrates that all the DCS is released from the capsules in 10 min. From 50 mg reformulated capsules there would be a significant loss of DCS before it can reach systemic circulation mainly because of the acidic pH in the stomach. This loss should be taken into consideration when 50 mg capsules are used through oral route. Also there is an issue of timing of administration of the current oral formulation. Using the capsules the systemic level of DCS fluctuates, which creates particular problems with the timing of administration. In some studies the DCS is administered before the session (from 30 min to 2 h), while in other studies DCS is administered after the session. Thus a formulation of DCS needs to be developed which can sustain the amount of DCS to a desired level for appreciable period of time, eliminating the conundrum of timing.

5. Conclusion

A stability-indicating method was developed, which separates all the degradation products formed. Based on the partition coefficient value –2.89, it can be established that DCS is primarily hydrophilic in character. The pH-solution stability profile shows that DCS shows maximum degradation at pH value of 4.7 and was very stable under highly alkaline conditions. The degradation was observed to be independent of ionic strength of buffer, except for pH of 2.0. The *in vitro* dissolution of these 50 mg strength DCS capsules illustrated that all the DCS is released from the capsules in 10 min. Significant degradation of DCS was observed at the acidic pH; accordingly we can conclude that there will be a significant loss of the orally administered DCS before it can reach the systemic circulation. Future directions' regarding the reformulation of this drug to maximize its efficacy should be explored.

Acknowledgements

This project was supported by NIH Grant 5P20RR016477 to the West Virginia IDeA Network for Biomedical Research Excellence. We would also like to acknowledge Charleston Area Medical Center Health Education and Research Institute and West Virginia University School of Medicine Charleston Division for providing support and partial funding on this project.

References

1. Henderson G, Johnson JW, Ascher P. Competitive antagonists and partial agonists at the glycine modulatory site of the mouse *N*-methyl-D-aspartate receptor. J Physiol. 1990; 430:189-212.
2. Monahan JB, Handelmann GE, Hood WF, Cordi AA. D-cycloserine, a positive modulator of the *N*-methyl-D-aspartate receptor, enhances performance of learning tasks in rats. Pharmacol Biochem Behav. 1989; 34:649-653.
3. Hofmann SG, Meuret AE, Smits JA, Simon NM, Pollack MH, Eisenmenger K, Shiekh M, Otto MW. Augmentation of exposure therapy with D-cycloserine for social anxiety disorder. Arch Gen Psychiatry. 2006; 63:298-304.
4. Ressler KJ, Rothbaum BO, Tannenbaum L, Anderson P, Graap K, Zimand E, Hodges L, Davis M. Cognitive enhancers as adjuncts to psychotherapy: Use of D-cycloserine in phobic individuals to facilitate extinction of fear. Arch Gen Psychiatry. 2004; 61:1136-1144.
5. Guastella AJ, Richardson R, Lovibond PF, Rapee RM, Gaston JE, Mitchell P, Dadds MR. A randomized controlled trial of D-cycloserine enhancement of exposure therapy for social anxiety disorder. Biol Psychiatry. 2008; 63:544-549.
6. Otto MW, Tolin DF, Simon NM, Pearlson GD, Basden S, Meunier SA, Hofmann SG, Eisenmenger K, Krystal JH, Pollack MH. Efficacy of d-cycloserine for enhancing

response to cognitive-behavior therapy for panic disorder. Biol psychiatry. 2010; 67:365-370.
7. Heresco-Levy U, Kremer I, Javitt DC, Goichman R, Reshef A, Blanaru M, Cohen T. Pilot-controlled trial of D-cycloserine for the treatment of post-traumatic stress disorder. Int J Neuropsychopharmacol. 2002; 5:301-307.
8. Guastella AJ, Dadds MR, Lovibond PF, Mitchell P, Richardson R. A randomized controlled trial of the effect of D-cycloserine on exposure therapy for spider fear. J Psychiatr Res. 2007; 41:466-471.
9. Chasson GS, Buhlmann U, Tolin DF, Rao SR, Reese HE, Rowley T, Welsh KS, Wilhelm S. Need for speed: Evaluating slopes of OCD recovery in behavior therapy enhanced with D-cycloserine. Behav Res Ther. 2010; 48:675-679.
10. Kushner MG, Kim SW, Donahue C, Thuras P, Adson D, Kotlyar M, McCabe J, Peterson J, Foa EB. D-Cycloserine augmented exposure therapy for obsessive-compulsive disorder. Biol Psychiatry. 2007; 62:835-838.
11. Cycloserine. Tuberculosis (Edinb). 2008; 88:100-101.
12. Iakhontova LF, Bruns BP, Kartseva VD, Kobzieva SN, Perevozskaia NA. Physico-chemical and sorption properties of D-cycloserine. Antibiotiki. 1969; 14:205-210.
13. Musumeci T, Ventura CA, Giannone I, Pignatello R, Puglisi G. Development of a liposome formulation for D-cycloserine local delivery. J Liposome Res. 2008; 18:211-224.
14. Musumeci T, Ventura CA, Carbone C, Pignatello R, Puglisi G. Effects of external phase on D-cycloserine loaded W/O nanocapsules prepared by the interfacial polymerization method. Eur J Med Chem. 2011; 46:2828-2834.
15. Malspeis L, Gold D. Stability of cycloserine in buffered aqueous solutions. J Pharm Sci. 1964; 53:1173-1180.
16. Kartseva VD, Iakhontova LF, Isaeva NL, Bruns BP. On the stability of crystalline D-cycloserine. Antibiotiki. 1967; 12:772-775.
17. Claudius JS, Neau SH, Kenny MT, Dulworth JK. The antimicrobial activity of vancomycin in the presence and absence of sodium carboxymethyl starch. J Pharm Pharmacol. 1999; 51:1333-1337.
18. Karnes HT, March C. Precision, accuracy, and data acceptance criteria in biopharmaceutical analysis. Pharm Res. 1993; 10:1420-1426.
19. International Conference on Harmonization. Stability Data Package for Registration Applications in Climatic Zones III and IV; Stability Testing of New Drug Substances and Products; availability. Notice. US Fed Reg. 2003; 68:65717-65718.
20. Trissel LA. Avoiding common flaws in stability and compatibility studies of injectable drugs. Am J Hosp Pharm. 1983; 40:1159-1160.

(*Received September 24, 2011; Revised October 5, 2011; Accepted October 11, 2011****)***

DD&T
Drug Discoveries & Therapeutics

Guide for Authors

1. Scope of Articles

Drug Discoveries & Therapeutics welcomes contributions in all fields of pharmaceutical and therapeutic research such as medicinal chemistry, pharmacology, pharmaceutical analysis, pharmaceutics, pharmaceutical administration, and experimental and clinical studies of effects, mechanisms, or uses of various treatments. Studies in drug-related fields such as biology, biochemistry, physiology, microbiology, and immunology are also within the scope of this journal.

2. Submission Types

Original Articles should be well-documented, novel, and significant to the field as a whole. An Original Article should be arranged into the following sections: Title page, Abstract, Introduction, Materials and Methods, Results, Discussion, Acknowledgments, and References. Original articles should not exceed 5,000 words in length (excluding references) and should be limited to a maximum of 50 references. Articles may contain a maximum of 10 figures and/or tables.

Brief Reports definitively documenting either experimental results or informative clinical observations will be considered for publication in this category. Brief Reports are not intended for publication of incomplete or preliminary findings. Brief Reports should not exceed 3,000 words in length (excluding references) and should be limited to a maximum of 4 figures and/or tables and 30 references. A Brief Report contains the same sections as an Original Article, but the Results and Discussion sections should be combined.

Reviews should present a full and up-to-date account of recent developments within an area of research. Normally, reviews should not exceed 8,000 words in length (excluding references) and should be limited to a maximum of 100 references. Mini reviews are also accepted.

Policy Forum articles discuss research and policy issues in areas related to life science such as public health, the medical care system, and social science and may address governmental issues at district, national, and international levels of discourse. Policy Forum articles should not exceed 2,000 words in length (excluding references).

Case Reports should be detailed reports of the symptoms, signs, diagnosis, treatment, and follow-up of an individual patient. Case reports may contain a demographic profile of the patient but usually describe an unusual or novel occurrence. Unreported or unusual side effects or adverse interactions involving medications will also be considered. Case Reports should not exceed 3,000 words in length (excluding references).

News articles should report the latest events in health sciences and medical research from around the world. News should not exceed 500 words in length.

Letters should present considered opinions in response to articles published in Drug Discoveries & Therapeutics in the last 6 months or issues of general interest. Letters should not exceed 800 words in length and may contain a maximum of 10 references.

3. Editorial Policies

Ethics: Drug Discoveries & Therapeutics requires that authors of reports of investigations in humans or animals indicate that those studies were formally approved by a relevant ethics committee or review board.

Conflict of Interest: All authors are required to disclose any actual or potential conflict of interest including financial interests or relationships with other people or organizations that might raise questions of bias in the work reported. If no conflict of interest exists for each author, please state "There is no conflict of interest to disclose".

Submission Declaration: When a manuscript is considered for submission to Drug Discoveries & Therapeutics, the authors should confirm that 1) no part of this manuscript is currently under consideration for publication elsewhere; 2) this manuscript does not contain the same information in whole or in part as manuscripts that have been published, accepted, or are under review elsewhere, except in the form of an abstract, a letter to the editor, or part of a published lecture or academic thesis; 3) authorization for publication has been obtained from the authors' employer or institution; and 4) all contributing authors have agreed to submit this manuscript.

Cover Letter: The manuscript must be accompanied by a cover letter signed by the corresponding author on behalf of all authors. The letter should indicate the basic findings of the work and their significance. The letter should also include a statement affirming that all authors concur with the submission and that the material submitted for publication has not been published previously or is not under consideration for publication elsewhere. The cover letter should be submitted in PDF format. For example of Cover Letter, please visit http://www.ddtjournal.com/downcentre.php (Download Centre).

Copyright: A signed JOURNAL PUBLISHING AGREEMENT (JPA) must be provided by post, fax, or as a scanned file before acceptance of the article. Only forms with a hand-written signature are accepted. This copyright will ensure the widest possible dissemination of information. A form facilitating transfer of copyright can be downloaded by clicking the appropriate link and can be returned to the e-mail address or fax number noted on the form (Please visit Download Centre). Please note that your manuscript will not proceed to the next step in publication until the JPA form is received. In addition, if excerpts from other copyrighted works are included, the author(s) must obtain written permission from the copyright owners and credit the source(s) in the article.

Suggested Reviewers: A list of up to 3 reviewers who are qualified to assess the scientific merit of the study is welcomed. Reviewer information including names, affiliations, addresses, and e-mail should be provided at the same time the manuscript is submitted online. Please do not suggest reviewers with known conflicts of interest, including participants or anyone with a stake in the proposed research; anyone from the same institution; former students, advisors, or research collaborators (within the last three years); or close personal contacts. Please note that the Editor-in-Chief may accept one or more of the proposed reviewers or may request a review by other qualified persons.

Language Editing: Manuscripts prepared by authors whose native language is not English should have their work proofread by a native English speaker before submission. If not, this might delay the publication of your manuscript in Drug Discoveries & Therapeutics.

The Editing Support Organization can provide English proofreading, Japanese-English translation, and Chinese-English translation services to authors who want to publish in Drug Discoveries & Therapeutics and need assistance before submitting a manuscript. Authors can visit this organization directly at http://www.iacmhr.com/iac-eso/support.php?lang=en. IAC-ESO was established to facilitate manuscript preparation by researchers whose native language is not English and to help edit works intended for international academic journals.

4. Manuscript Preparation

Manuscripts should be written in clear, grammatically correct English and submitted as a Microsoft Word file in a single-column format. Manuscripts must be paginated and typed in 12-point Times New Roman font with 24-point line spacing. Please do not embed figures in the text. Abbreviations should be used as little as possible and should be explained at first mention unless the term is a well-known abbreviation (*e.g.* DNA). Single words should not be abbreviated.

Title page: The title page must include 1) the title of the paper (Please note the title should be short, informative, and contain the major key words); 2) full name(s) and affiliation(s) of the author(s), 3) abbreviated names of the author(s), 4) full name, mailing address, telephone/fax numbers, and e-mail address of the corresponding author; and 5) conflicts of interest (if you have an actual or potential conflict of interest to disclose, it must be included as a footnote on the title page of the manuscript; if no conflict of interest exists for each author, please state "There is no conflict of interest to disclose"). Please visit Download Centre and refer to the title page of the manuscript sample.

Abstract: A one-paragraph abstract consisting of no more than 250 words must be included. The abstract should briefly state the purpose of the study, methods, main findings, and conclusions. Abbreviations must be kept to a minimum and non-standard abbreviations explained in brackets at first mention. References should be avoided in the abstract. Key words or phrases that do not occur in the title should be included in the Abstract page.

Introduction: The introduction should be a concise statement of the basis for the study and its scientific context.

Materials and Methods: The description should be brief but with sufficient detail to enable others to reproduce the experiments. Procedures that have been published previously should not be described in detail but appropriate references should simply be cited. Only new and significant modifications of previously published procedures require complete description. Names of products and manufacturers with their locations (city and state/country) should be given and sources of animals and cell lines should always be indicated. All clinical investigations must have been conducted in accordance with Declaration of Helsinki principles. All human and animal studies must have been approved by the appropriate institutional review board(s) and a specific declaration of approval must be made within this section.

Results: The description of the experimental results should be succinct but in sufficient detail to allow the experiments to be analyzed and interpreted by an independent reader. If necessary, subheadings may be used for an orderly presentation. All figures and tables must be referred to in the text.

Discussion: The data should be interpreted concisely without repeating material already presented in the Results section. Speculation is permissible, but it must be well-founded, and discussion of the wider implications of the findings is encouraged. Conclusions derived from the study should be included in this section.

Acknowledgments: All funding sources should be credited in the Acknowledgments section. In addition, people who contributed to the work but who do not meet the criteria for authors should be listed along with their contributions.

References: References should be numbered in the order in which they appear in the text. Citing of unpublished results, personal communications, conference abstracts, and theses in the reference list is not recommended but these sources may be mentioned in the text. In the reference list, cite the names of all authors when there are fifteen or fewer authors; if there are sixteen or more authors, list the first three followed by *et al*. Names of journals should be abbreviated in the style used in PubMed. Authors are responsible for the accuracy of the references. Examples are given below:

Example 1 (Sample journal reference):
Nakata M, Tang W. Japan-China Joint Medical Workshop on Drug Discoveries and Therapeutics 2008: The need of Asian pharmaceutical researchers' cooperation. Drug Discov Ther. 2008; 2:262-263.

Example 2 (Sample journal reference with more than 15 authors):
Darby S, Hill D, Auvinen A, *et al*. Radon in homes and risk of lung cancer: Collaborative analysis of individual data from 13 European case-control studies. BMJ. 2005; 330:223.

Example 3 (Sample book reference):
Shalev AY. Post-traumatic stress disorder: diagnosis, history and life course. In: Post-traumatic Stress Disorder, Diagnosis, Management and Treatment (Nutt DJ, Davidson JR, Zohar J, eds.). Martin Dunitz, London, UK, 2000; pp. 1-15.

Example 4 (Sample web page reference):
World Health Organization. The World Health Report 2008 – primary health care: Now more than ever. *http://www.who.int/whr/2008/whr08_en.pdf* (accessed September 23, 2010).

Tables: All tables should be prepared in Microsoft Word or Excel and should be arranged at the end of the manuscript after the References section. Please note that tables should not in image format. All tables should have a concise title and should be numbered consecutively with Arabic numerals. If necessary, additional information should be given below the table.

Figure Legend: The figure legend should be typed on a separate page of the main manuscript and should include a short title and explanation. The legend should be concise but comprehensive and should be understood without referring to the text. Symbols used in figures must be explained.

Figure Preparation: All figures should be clear and cited in numerical order in the text. Figures must fit a one- or two-column format on the journal page: 8.3 cm (3.3 in.) wide for a single column, 17.3 cm (6.8 in.) wide for a double column; maximum height: 24.0 cm (9.5 in.). Please make sure that artwork files are in an acceptable format (TIFF or JPEG) at minimum resolution (600 dpi for illustrations, graphs, and annotated artwork, and 300 dpi for micrographs and photographs). Please provide all figures as separate files. Please note that low-resolution images are one of the leading causes of article resubmission and schedule delays. All color figures will be reproduced in full color in the online edition of the journal at no cost to authors.

Units and Symbols: Units and symbols conforming to the International System of Units (SI) should be used for physicochemical quantities. Solidus notation (*e.g.* mg/kg, mg/mL, mol/mm^2/min) should be used. Please refer to the SI Guide www.bipm.org/en/si/ for standard units.

Supplemental data: Supplemental data might be useful for supporting and enhancing your scientific research and Drug Discoveries & Therapeutics accepts the submission of these materials which will be only published online alongside the electronic version of your article. Supplemental files (figures, tables, and other text materials) should be prepared according to the above guidelines, numbered in Arabic numerals (*e.g.*, Figure S1, Figure S2, and Table S1, Table S2) and referred to in the text. All figures and tables should have titles and legends. All figure legends, tables and supplemental text materials should be placed at the end of the paper. Please note all of these supplemental data should be provided at the time of initial submission and note that the editors reserve the right to limit the size and length of Supplemental Data.

5. Submission Checklist

The Submission Checklist will be useful during the final checking of a manuscript prior to sending it to Drug Discoveries & Therapeutics for review. Please visit Download Centre and download the Submission Checklist file.

6. Online submission

Manuscripts should be submitted to Drug Discoveries & Therapeutics online at http://www.ddtjournal.com. The manuscript file should be smaller than 5 MB in size. If for any reason you are unable to submit a file online, please contact the Editorial Office by e-mail at office@ddtjournal.com

7. Accepted manuscripts

Proofs: Galley proofs in PDF format will be sent to the corresponding author *via* e-mail. Corrections must be returned to the editor (proof-editing@ddtjournal.com) within 3 working days.

Offprints: Authors will be provided with electronic offprints of their article. Paper offprints can be ordered at prices quoted on the order form that accompanies the proofs.

Page Charge: A page charge of $140 will be assessed for each printed page of an accepted manuscript. The charge for printing color figures is $340 for each page. Under exceptional circumstances, the author(s) may apply to the editorial office for a waiver of the publication charges at the time of submission.

(Revised October 2011)

Editorial and Head Office:

Pearl City Koishikawa 603
2-4-5 Kasuga, Bunkyo-ku
Tokyo 112-0003
Japan
Tel: +81-3-5840-9697
Fax: +81-3-5840-9698
E-mail: office@ddtjournal.com

DD&T
Drug Discoveries & Therapeutics

JOURNAL PUBLISHING AGREEMENT (JPA)

Manuscript No:

Title:

Corresponding author:

The International Advancement Center for Medicine & Health Research Co., Ltd. (IACMHR Co., Ltd.) is pleased to accept the above article for publication in Drug Discoveries & Therapeutics. The International Research and Cooperation Association for Bio & Socio-Sciences Advancement (IRCA-BSSA) reserves all rights to the published article. Your written acceptance of this JOURNAL PUBLISHING AGREEMENT is required before the article can be published. Please read this form carefully and sign it if you agree to its terms. The signed JOURNAL PUBLISHING AGREEMENT should be sent to the Drug Discoveries & Therapeutics office (Pearl City Koishikawa 603, 2-4-5 Kasuga, Bunkyo-ku, Tokyo 112-0003, Japan; E-mail: office@ddtjournal.com; Tel: +81-3-5840-9697; Fax: +81-3-5840-9698).

1. Authorship Criteria

As the corresponding author, I certify on behalf of all of the authors that:

1) The article is an original work and does not involve fraud, fabrication, or plagiarism.
2) The article has not been published previously and is not currently under consideration for publication elsewhere. If accepted by Drug Discoveries & Therapeutics, the article will not be submitted for publication to any other journal.
3) The article contains no libelous or other unlawful statements and does not contain any materials that infringes upon individual privacy or proprietary rights or any statutory copyright.
4) I have obtained written permission from copyright owners for any excerpts from copyrighted works that are included and have credited the sources in my article.
5) All authors have made significant contributions to the study including the conception and design of this work, the analysis of the data, and the writing of the manuscript.
6) All authors have reviewed this manuscript and take responsibility for its content and approve its publication.
7) I have informed all of the authors of the terms of this publishing agreement and I am signing on their behalf as their agent.

2. Copyright Transfer Agreement

I hereby assign and transfer to IACMHR Co., Ltd. all exclusive rights of copyright ownership to the above work in the journal Drug Discoveries & Therapeutics, including but not limited to the right 1) to publish, republish, derivate, distribute, transmit, sell, and otherwise use the work and other related material worldwide, in whole or in part, in all languages, in electronic, printed, or any other forms of media now known or hereafter developed and the right 2) to authorize or license third parties to do any of the above.

I understand that these exclusive rights will become the property of IACMHR Co., Ltd., from the date the article is accepted for publication in the journal Drug Discoveries & Therapeutics. I also understand that IACMHR Co., Ltd. as a copyright owner has sole authority to license and permit reproductions of the article.

I understand that except for copyright, other proprietary rights related to the Work (*e.g.* patent or other rights to any process or procedure) shall be retained by the authors. To reproduce any text, figures, tables, or illustrations from this Work in future works of their own, the authors must obtain written permission from IACMHR Co., Ltd.; such permission cannot be unreasonably withheld by IACMHR Co., Ltd.

3. Conflict of Interest Disclosure

I confirm that all funding sources supporting the work and all institutions or people who contributed to the work but who do not meet the criteria for authors are acknowledged. I also confirm that all commercial affiliations, stock ownership, equity interests, or patent-licensing arrangements that could be considered to pose a financial conflict of interest in connection with the article have been disclosed.

Corresponding Author's Name (Signature):

Date: